

Table of Contents

1. Mismatch discrimination.....	3
2. Molecular modeling	3
3. Characterization of oligonucleotides.....	6
4. Evidence of a bimolecular association between ON13 and ON14	6
5. Synthesis of cytosine phosphoramidite building block.....	7
6. Synthesis of 7'-O-p-nitrobenzoyl-7',5'-bc-T	13
7. NMR spectra	15
8. NOESY spectra	52
9. HMBC spectra.....	53
10. Crystal-Structure Determination.	53
11. References	59

1. Mismatch discrimination

Table S1. T_m values from UV-melting curves (260 nm) of **ON1** and **DNA1** in duplex with complementary DNA incorporating one mismatch.

Entry	Duplex	X=A	X=T	X=G	X=C
ON1	5'-d(GGA TGT TCT CGA)-3'		50.3	41.0	45.2
DNA	5'-d(TCG XGA ACA TCC)-3'			37.3	
DNA1	5'-d(GGA TGT TCT CGA)-3'		49.1	38.3	40.5
DNA	5'-d(TCG XGA ACA TCC)-3'			36.7	

Experimental conditions: total strand conc. 2 μM in 10 mM NaH₂PO₄, 150 mM NaCl, pH 7.0

2. Molecular modeling

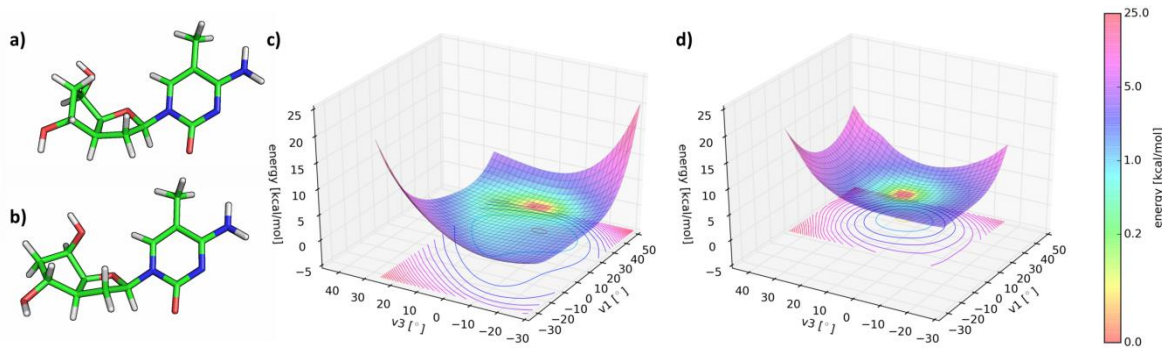


Figure S1: The two minimum energy conformers of 7',5'-bc-⁵-MeC nucleosides a): C6'-endo and b): C6'-exo. Potential energy surfaces of c): the C6'-endo conformer and d): the C6'-exo conformer.

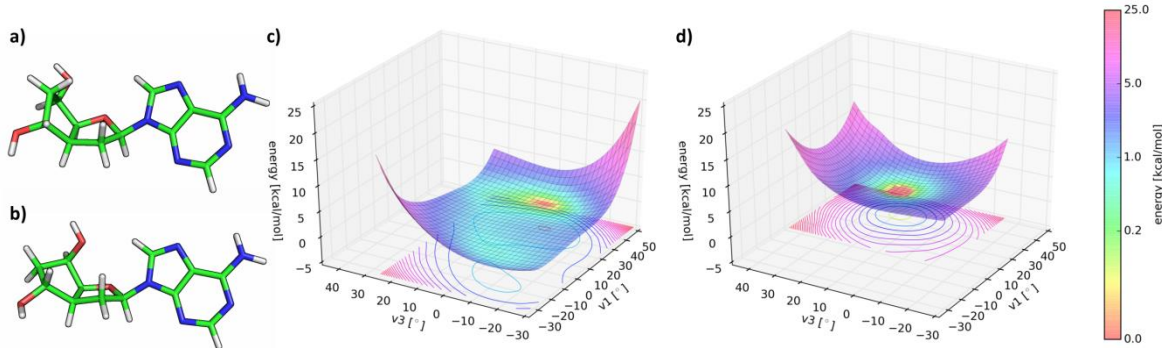


Figure S2: The two minimum energy conformers of 7',5'-bc-A nucleosides a): C6'-endo and b): C6'-exo. Potential energy surfaces of c): the C6'-endo conformer and d): the C6'-exo conformer

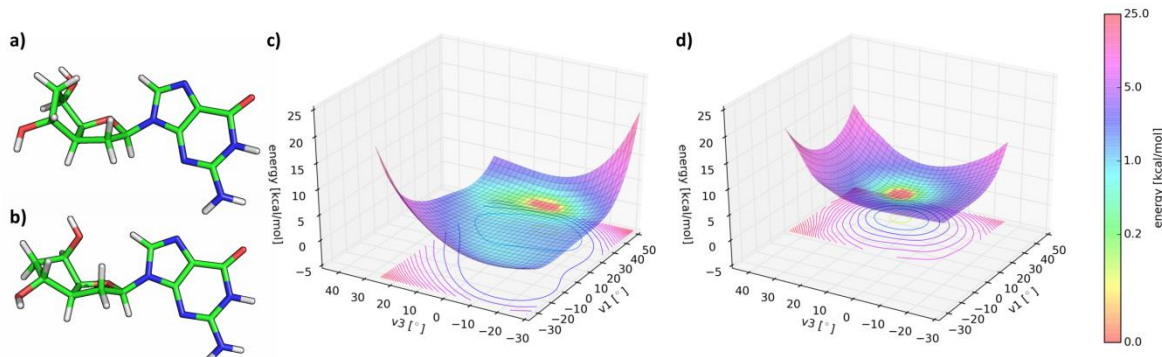


Figure S3: The two minimum energy conformers of 7',5'-bc-G nucleosides a): C6'-endo and b): C6'-exo. Potential energy surfaces of c): the C6'-endo conformer and d): the C6'-exo conformer

Table S2. Energy of formation in the gas phase and aqueous phase of the four 7',5'-bc-DNA nucleosides. Values are in kcal/mol.

Nucleoside	C6'-endo conformer		C6'-exo conformer	
	Gas phase	Aqueous phase	Gas phase	Aqueous phase
7',5'-bc-T	-594230.17	-594256.03	-594231.56	-594255.98
7',5'-bc- ^{5-Me} C	-581770.53	-581802.00	-581771.17	-581801.54
7',5'-bc-A	-602395.55	-602424.63	-602396.93	-602424.62
7',5'-bc-G	-649378.33	-649417.69	-649379.88	-649417.43

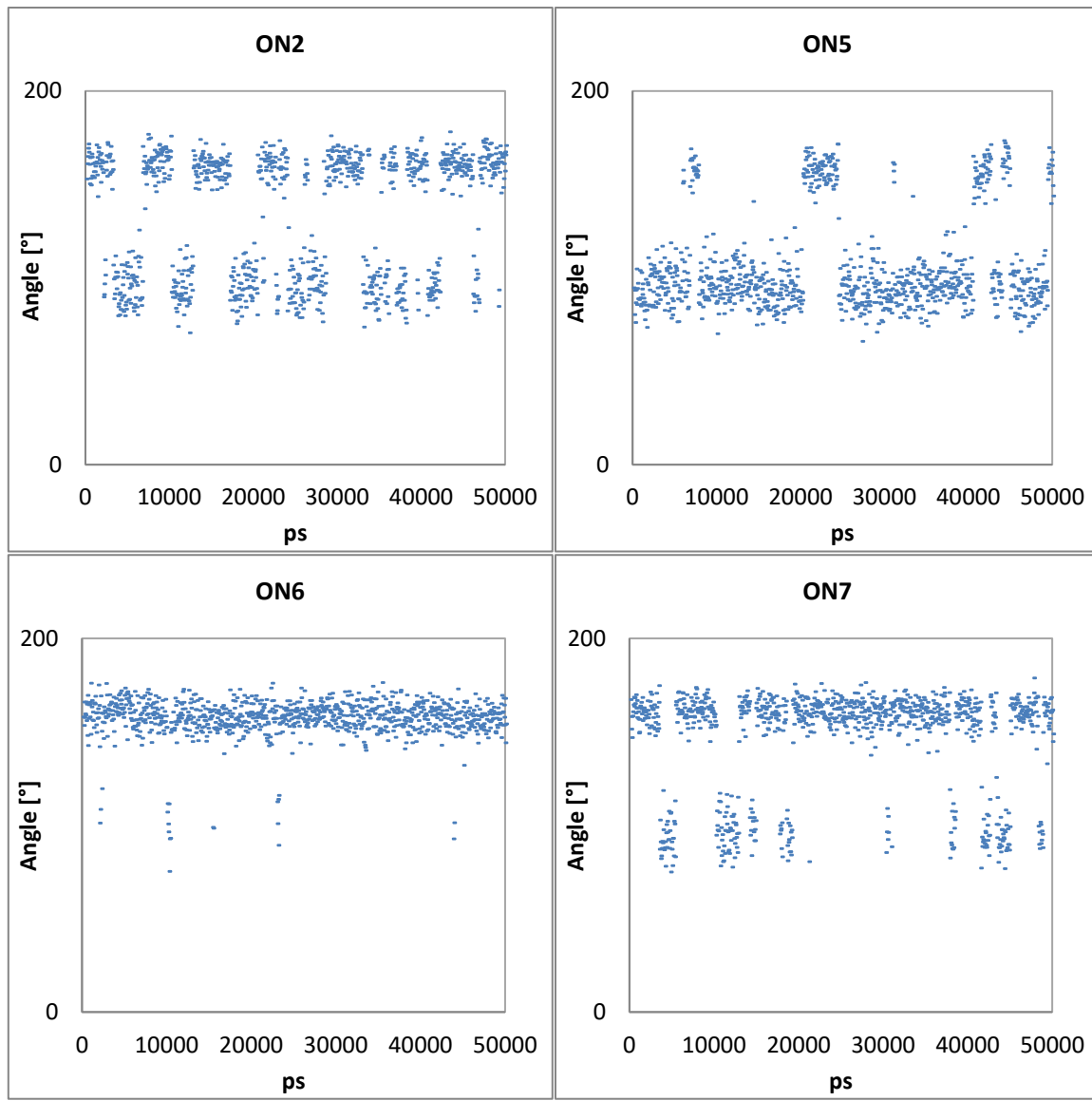


Figure S4: Orientation of the γ angle for the 7',5'-bc-DNA residue in **ON2**, **ON5**, **ON6** and **ON7** during the simulation. An angle below 130° indicate C6'-exo conformation and an angle above 130° indicate a C6'-endo conformation.

3. Characterization of oligonucleotides

Table S3. List of oligonucleotides and results of the characterization.

Entry	Sequence ^[a]	HPLC Gradient ^[b]	Retention time [min]	Purity [%]	Exact mass	Experimental mass
ON1	5'-d(GGATGTT t CGA)-3' B: 15 → 55%		12.15	96.2	3700.67	3701.7
ON2	5'-d(GG a TGTTCTCGA)-3' B: 15 → 55%		12.25	95.4	3700.67	3701.7
ON3	5'-d(GGATG t tCTCGA)-3' B: 15 → 55%		11.85	90.2	3726.68	3727.7
ON4	5'-d(GGATGTT c TCGA)-3' B: 15 → 55%		12.52	96.1	3714.68	3715.7
ON5	5'-d(GGATGTT C T GA)-3' B: 15 → 55%		12.91	93.2	3714.68	3715.7
ON6	5'-d(GG a TGTTCTCGA)-3' B: 15 → 55%		12.63	90.3	3700.67	3701.7
ON7	5'-d(GGAT g TGTTCTCGA)-3' B: 15 → 55%		12.79	96.7	3700.67	3701.7
ON8	5'-d(GGATGTT c TCGA)-3' B: 15 → 55%		12.67	98.4	3700.67	3701.7
ON9	5'-d(GGATGTT C T GA)-3' B: 15 → 55%		12.75	99.2	3700.67	3701.7
ON10	5'-d(GGATGTT T C GA)-3' B: 15 → 55%		12.82	99.3	3726.68	3727.7
ON11	5'-d(GC A tttttACCG)-3' B: 15 → 55%		11.88	98.1	3739.71	3740.7
ON12	5'-d(ttttc c t c t) -7' B: 7 → 32%		13.77	90.4	2905.65	2906.6
ON13	5'-d(ggatgtt c t c ga) -7' B: 15 → 35%		15.00	95.4	4014.87	4015.9
ON14	5'-d(tcgaga ac atcc) -7' B: 15 → 35%		13.43	95.0	3980.91	3981.9
ON15	5'-d(cetaca aa agatc) -7' B: 15 → 35%		14.98	94.8	3980.91	3981.9

^[a]A,G,T,C denote natural 2'-deoxynucleosides; **a,t,g,c** corresponds to modified nucleosides, **c** stands for the modified 5-methylcytosine nucleoside.

^[b] Mobile phase “A”: 25 mM Trizma in H₂O, pH 8.0; Mobile phase “B”: 25 mM Trizma, 1.25 M NaCl in H₂O, pH 8.0; Analyses were performed by using a linear gradient of B in A, over 20 min, with a flow of 1 ml/min.

4. Evidence of a bimolecular association between ON13 and ON14

To confirm the bimolecular association between **ON13** and **ON14**, the spectroscopic properties of the homo 7',5'-bc-DNA duplex were compared with its constituting separated single strands. Unlike the UV-melting curve of the **ON13**•**ON14** duplex, the UV-melting curves of the single strands do not display a sigmoidal melting behavior (Figure S5, left). Furthermore, the CD-spectra of the single strands do not reproduce the features of the homo 7',5'-bc-DNA duplex (Figure S5, right). This data unambiguously confirms the formation of a complex between **ON13** and **ON14**.

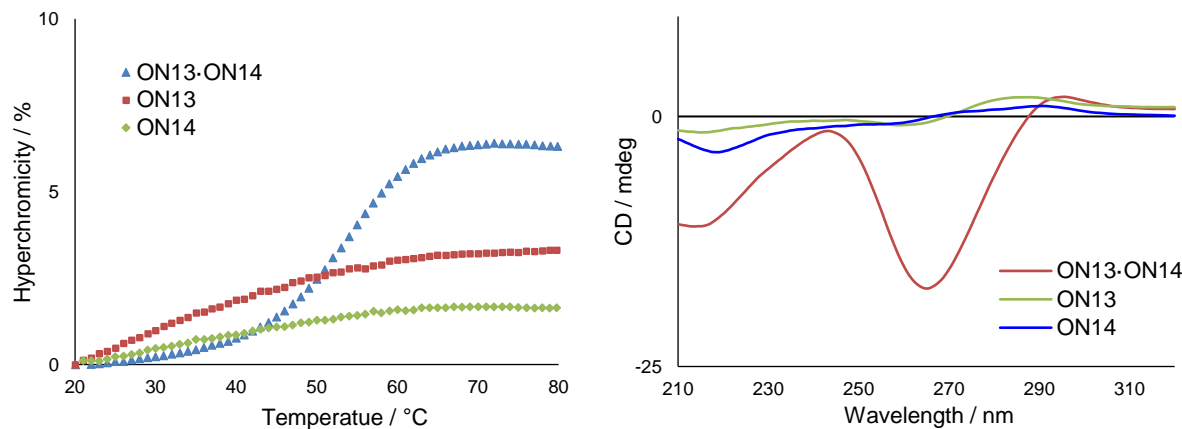
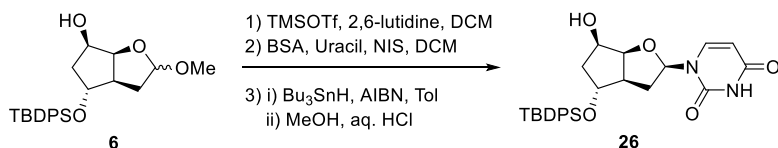


Figure S5: (Left) UV-melting curves (260 nm) of the homo 7',5'-bc-DNA duplex (**ON13-ON14**) in comparison with the corresponding separated single strands. Experimental conditions: total strand conc. 2 μ M in 10 mM NaH₂PO₄, 150 mM NaCl, pH 7.0; (Right) CD-spectra of the homo 7',5'-bc-DNA duplex (**ON13-ON14**) in comparison with the corresponding separated single strands. Experimental conditions: total strand conc. 2 μ M in 10 mM NaH₂PO₄, 150 mM NaCl, pH 7.0, 10°C.

5. Synthesis of cytosine phosphoramidite building block

(3'S,5'R,7'R)-1-{7'-[*tert*-butyldiphenylsilyl]oxy}-2',3'-Dideoxy-3',5'-ethano- β -D-ribofuranosyl uracil (26) :

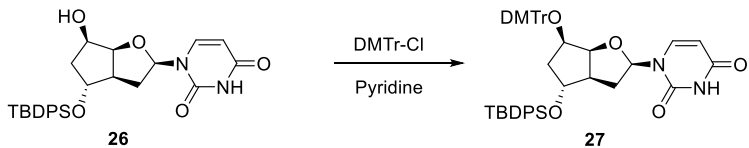


To a solution of the sugar **6** (669 mg, 1.62 mmol) in dry DCM (13 mL) was added 2,6-lutidine (0.94 mL, 8.10 mmol) at 0°C. After stirring for 20 min at 0°C, TMSOTf (0.89 mL, 4.86 mmol) was added dropwise and then the solution was allowed to warm to rt and was stirred for an additional 3 h. The reaction was then quenched by addition of satd NaHCO₃ (20 mL). The organic phase was separated and aqueous phase was further extracted with DCM (2 X 20 mL). The combined organic phases were dried over MgSO₄, filtered and evaporated. The crude product was dissolved in dry DCM (12 mL) and then uracil (545 mg, 4.86 mmol) and BSA (1.8 mL, 7.29 mmol) were added at rt. After stirring for 60 min at rt, the resulting fine suspension was cool down to 0°C and N-iodosuccinimide (578 mg, 2.52 mmol) was added. After stirring for 30 min at 0°C and for 4 h at rt, the reaction mixture was diluted with

EtOAc (50 mL) and subsequently washed with a 10% aq solution of Na₂S₂O₃ (30 mL) and satd NaHCO₃ (30 mL). Aqueous phases were combined and extracted with DCM (2 X 20 mL). The combined organic phases were dried over MgSO₄, filtered and evaporated. The crude product was dissolved in dry toluene (15 mL) and then Bu₃SnH (0.65 mL, 2.43 mmol) and azoisobutyronitrile (AIBN, 13 mg, 0.081 mmol) were added at rt. After heating at 95°C for 2 h, the mixture was cool down to rt and MeOH (7 mL) and HCl (1M in water, 1.6 mL, 1.6 mmol) were added. The solution was further stirred for 15 min and was then diluted with satd NaHCO₃ (50 mL) and extracted with DCM (3 X 50 mL). The combined organic phases were dried over MgSO₄, filtered and evaporated. The crude product was purified by CC (EtOAc/hexane 4:1) to yield **26** (490 mg, 61% over three steps) as a white foam.

Data for **26**: R_f = 0.15 (EtOAc/hexane 2:1); ¹H NMR (300 MHz, CDCl₃) δ 9.95 (br, 1H, H-N(3)), 7.69 (d, J = 6.4 Hz, 4H, H-arom), 7.54 – 7.39 (m, 7H, H-C(6), H-arom), 5.98 (dd, J = 9.3, 5.6 Hz, 1H, H-C(1')), 5.71 (d, J = 8.1 Hz, 1H, H-C(5)), 4.51 (dd, J = 13.7, 6.3 Hz, 2H, H-C(4'), H-C(5')), 4.14 (br, 1H, H-C(7')), 3.25 (br, 1H, OH), 2.74 (dd, J = 17.1, 8.7 Hz, 1H, H-C(3')), 2.26 – 1.87 (m, 3H, H-C(2'), H-C(6')), 1.49 – 1.19 (m, 1H, H-C(2')), 1.12 (s, 9H, (CH₃)₃-C-Si); ¹³C NMR (75 MHz, CDCl₃) δ 163.65 (C(4)), 150.46 (C(2)), 139.85 (C(6)), 135.69, 135.66 (CH-arom), 133.71, 133.42 (C-arom), 129.98, 129.93, 127.85, 127.81 (CH-arom), 102.84 (C(5)), 86.17 (C(1')), 81.83 (C(4')), 76.94 (C(7')), 72.45 (C(5')), 50.09 (C(3')), 40.93 (C(6')), 35.83 (C(2')), 26.91 (CH₃)₃-C-Si), 19.03 (CH₃)₃-C-Si); ESI⁺-HRMS *m/z* calcd for C₂₇H₃₂O₅N₂NaSi ([M + Na]⁺) 515.1973, found 515.1963.

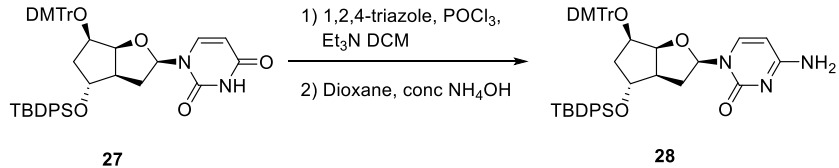
(3'S,5'R,7'R)-1-{7'-[(tert*-butyldiphenylsilyl)oxy]-2',3'-Dideoxy-3',5'-ethano-5'-O-[(4,4'-dimethoxytriphenyl)methyl]-β-D-ribofuranosyl} uracil (27) :*



To a solution of nucleoside **26** (438 mg, 0.889 mmol) in dry pyridine (7 mL) was added DMTr-Cl (1.20 g, 3.55 mmol) at rt. The solution was stirred for 1 day at rt and then was diluted with satd NaHCO₃ (30 mL) and extracted with DCM (3 X 40 mL). The combined organic phases were dried over MgSO₄, filtered and evaporated. The crude product was purified by CC (1.5% MeOH in DCM, +0.5 % Et₃N) to yield **27** (601 mg, 80%) as a yellow foam.

Data for **27**: $R_f = 0.48$ (EtOAc/hexane 2:1); ^1H NMR (300 MHz, CDCl_3) δ 9.26 (br, 1H, H-N(3)), 7.84 (d, $J = 8.1$ Hz, 1H, H-C(6)), 7.40 – 7.08 (m, 19H, H-arom), 6.69 (dd, $J = 8.8, 4.9$ Hz, 4H, H-arom), 5.70 (dd, $J = 7.8, 5.8$ Hz, 1H, H-C(1')), 5.49 (dd, $J = 8.1, 1.5$ Hz, 1H, H-C(5)), 4.24 – 4.11 (m, 1H, H-C(5')), 4.05 – 3.95 (m, 1H, H-C(4')), 3.65 (d, $J = 1.7$ Hz, 6H, MeO), 3.62 (d, $J = 3.0$ Hz, 1H, H-C(7')), 2.41 (dd, $J = 17.2, 8.5$ Hz, 1H, H-C(3')), 2.24 (ddd, $J = 13.5, 10.2, 5.7$ Hz, 1H, H-C(2')), 1.39 – 1.24 (m, 1H, H-C(6')), 1.04 (dd, $J = 13.1, 5.7$ Hz, 1H, H-C(6')), 0.89 (dt, $J = 13.8, 8.3$ Hz, 1H, H-C(2')), 0.81 (s, 9H, $(\text{CH}_3)_3\text{-C-Si}$); ^{13}C NMR (75 MHz, CDCl_3) δ 163.58 (C(4)), 158.66 (MeO-C-arom), 150.38 (C(2)), 145.61 (C-arom), 139.92 (C(6)), 136.71, 136.56(C-arom), 135.61, 135.55 (CH-arom), 133.55, 133.41 (C-arom), 130.30, 129.92, 129.84, 128.16, 127.90, 127.74, 127.67, 126.90, 113.19, 113.15 (CH-arom), 102.12 (C(5)), 87.41 ($\text{C}(\text{Ph})_3$), 86.80 (C(1')), 82.32 (C4')), 75.54 (C(7')), 74.41 (C(5')), 55.23 (MeO-DMTr), 50.05 (C(3')), 38.49 (C(6')), 37.53 (C(2')), 26.81 ($\text{CH}_3)_3\text{-C-Si}$), 18.99 ($\text{CH}_3)_3\text{-C-Si}$); ESI $^+$ -HRMS m/z calcd for $\text{C}_{48}\text{H}_{50}\text{O}_7\text{N}_2\text{NaSi}$ ($[\text{M} + \text{Na}]^+$) 817.3279, found 817.3286.

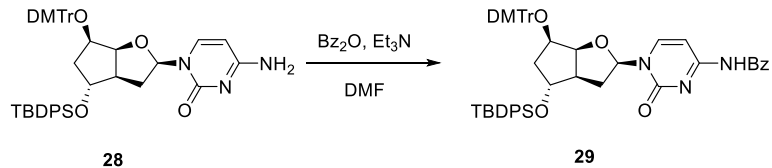
(3'S,5'R,7'R)-1-{7'-[*(tert*-butyldiphenylsilyl)oxy]-2',3'-Dideoxy-3',5'-ethano-5'-O-[(4,4'-dimethoxytriphenyl)methyl]- β -D-ribofuranosyl} cytosine (28) :



To a suspension of 1,2,4-triazole (1.83g, 26.5 mmol) in dry MeCN (70 mL), at 0°C, were added POCl_3 (0.57 mL, 6.05 mmol) followed by Et_3N (4.2 mL, 30.2 mmol). The suspension was stirred for 30 min at 0°C and then a solution of the nucleoside **27** (601 mg, 0.756 mmol) in dry MeCN (4 mL) was added at 0°C. After for 4 h of stirring at rt, the reaction was quenched with addition of satd NaHCO_3 (20 mL), MeCN removed under reduced pressure and the resulting mixture diluted with satd NaHCO_3 (30 mL) and extracted with DCM (3 X 60 mL). The combined organic phases were dried over MgSO_4 , filtered and evaporated. The crude product was then dissolved in a mixture of 1,4-dioxane (18 mL) and concd NH_4OH (18 mL). After stirring for 3 h at rt, the mixture was reduced to half of the volume in vacuo, diluted with satd NaHCO_3 (30 mL) and extracted with DCM (3 X 30 mL). The combined organic phases were dried over MgSO_4 , filtered and evaporated. The crude product was purified by CC (5% MeOH in DCM, +0.5 % Et_3N) to yield **28** (520 mg, 87%) as a white foam.

Data for **28**: $R_f = 0.41$ (10% MeOH in DCM); ^1H NMR (300 MHz, CDCl_3) δ 7.96 (d, $J = 7.4$ Hz, 1H, H-C(6)), 7.45 (d, $J = 7.4$ Hz, 2H, H-arom), 7.38 – 7.08 (m, 17H, H-arom), 6.73 (dd, $J = 8.7, 4.7$ Hz, 4H, H-arom), 5.73 (t, $J = 8.6$ Hz, 2H, H-C(5), H-C(1')), 4.32 – 4.16 (m, 1H, H-C(5')), 4.03 (t, $J = 5.6$ Hz, 1H, H-C(4')), 3.66 (d, $J = 0.9$ Hz, 6H, MeO), 3.61 (d, $J = 2.9$ Hz, 1H, H-C(7')), 2.50 – 2.33 (m, 2H, H-C(2'), H-C(3')), 1.47 – 1.28 (m, 1H, H-C(6')), 1.03 (dd, $J = 12.9, 5.6$ Hz, 1H, H-C(6')), 0.92 – 0.75 (m, 10H, H-C(2'), $(\text{CH}_3)_3\text{-C-Si}$); ^{13}C NMR (75 MHz, CDCl_3) δ 165.78 (C(4)), 158.59 (MeO-C-arom), 155.94 (C(2)), 145.88 (C-arom), 140.68 (C(6)), 136.93, 136.78 (C-arom), 135.59, 135.53 (CH-arom), 133.60, 133.54 (C-arom), 130.31, 129.86, 129.77, 128.15, 127.88, 127.71, 127.64, 126.79, 113.18, 113.14 (CH-arom), 94.53 (C(5)), 87.55 ($\text{C}(\text{Ph})_3$), 87.22 (C(1')), 82.23 (C(4')), 75.76 (C(7')), 74.68 (C(5')), 55.21 (MeO-DMTr), 50.18 (C(3')), 38.25 (C(6')), 38.08 (C(2')), 26.83 ($\text{CH}_3)_3\text{-C-Si}$), 19.00 ($\text{CH}_3)_3\text{-C-Si}$); ESI⁺-HRMS m/z calcd for $\text{C}_{48}\text{H}_{52}\text{O}_6\text{N}_3\text{Si}$ ([M + H]⁺) 794.3620, found 794.3649.

(3'S,5'R,7'R)- N4-Benzoyl-1-{7'-[*tert*-butyldiphenylsilyl]oxy}-2',3'-Dideoxy-3',5'-ethano-5'-O-[(4,4'-dimethoxytriphenyl)methyl]- β -D-ribofuranosyl cytosine (29) :

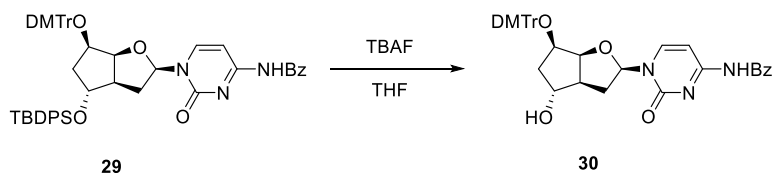


To a solution of nucleoside **28** (519 mg, 0.653 mmol) in dry DMF (15 mL) were added Et_3N (110 μL , 0.784 mmol) followed by Bz_2O (370 mg, 1.633 mmol) at rt and the solution was stirred overnight. Then the solution was quenched by careful addition of satd NaHCO_3 (60 mL) and extracted with DCM (3 X 70 mL). The combined organic phases were dried over MgSO_4 , filtered and evaporated. The crude product was purified by CC (hexane/EtOAc 2:3, +0.5 % Et_3N) to yield **29** (580 mg, 99%) as a white foam.

Data for **29**: $R_f = 0.51$ (EtOAc); ^1H NMR (300 MHz, CDCl_3) δ 8.61 (d, $J = 7.4$ Hz, 1H, H-C(6)), 7.81 (d, $J = 7.5$ Hz, 2H, H-arom), 7.49 – 7.13 (m, 24H, H-arom, H-C(5)), 6.77 (dd, $J = 8.5, 4.4$ Hz, 4H, H-arom), 5.73 (t, $J = 6.4$ Hz, 1H, H-C(1')), 4.39 – 4.20 (m, 1H, H-C(5')), 4.05 (t, $J = 6.1$ Hz, 1H, H-C(4')), 3.70 (s, 6H, MeO), 3.63 (d, $J = 2.3$ Hz, 1H, H-C(7')), 2.72 – 2.55 (m, 1H, H-C(2')), 2.48 (dd, $J = 16.0, 8.4$ Hz, 1H, H-C(3')), 1.42 – 1.29 (m, 1H, H-C(6')), 1.19 – 1.11 (m, 1H, H-C(6')), 1.07 – 0.96 (m, 1H, H-C(2')), 0.85 (s, 9H, $(\text{CH}_3)_3\text{-C-Si}$). ^{13}C NMR (75 MHz, CDCl_3) δ 166.64 (CONH), 162.25 (C(4)), 158.70 (MeO-C-arom), 154.84 (C(2)), 145.71 (C-arom), 144.84 (C(6)), 136.74, 136.67 (C-arom), 135.59, 135.51 (CH-arom),

133.52, 133.42, 133.24 (C-arom), 133.11, 130.30, 129.92, 129.85, 129.02, 128.12, 127.97, 127.76, 127.68, 127.61, 126.94, 113.25, 113.22(CH-arom), 96.22 (C(5)), 89.07 (*C*(Ph)₃), 87.53 (C(1')), 83.46 (C(4')), 75.59 (C(7')), 74.71 (C(5')), 55.24 (*MeO*-DMTr), 50.35 (C(3')), 38.61 (C(6')), 38.15 (C(2')), 26.82 (CH₃)₃-C-Si), 19.00 (CH₃)₃-C-Si). ESI⁺-HRMS *m/z* calcd for C₅₅H₅₆O₇N₃Si ([M + H]⁺) 898.3882, found 898.3898.

(3'S,5'R,7'R)- N4-Benzoyl-1-{2',3'-Dideoxy-3',5'-ethano-7'-hydroxy-5'-O-[(4,4'-dimethoxytriphenyl)methyl]-β-D-ribofuranosyl} cytosine (30) :

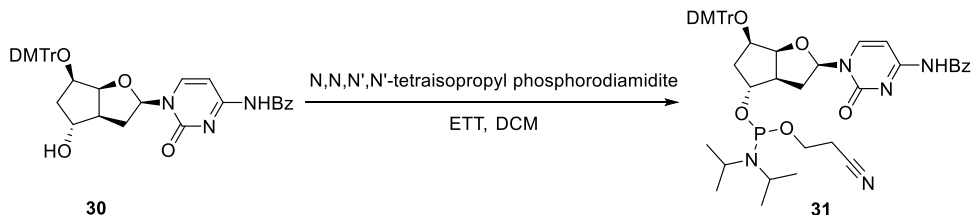


To a solution of **29** (580 mg, 0.648 mmol) in dry THF (14 mL) was added TBAF (1M in THF, 3.25 mL, 3.25 mmol) at rt. The solution was stirred for 1 day and then was diluted with satd NaHCO₃ (50 mL) and extracted with DCM (3 X 40 mL). The combined organic phases were dried over MgSO₄, filtered and evaporated. The crude product was purified by CC (3% MeOH in DCM, +0.5 % Et₃N) to yield **30** (366 mg, 85%) as a white foam.

Data for **30**: *R*_f = 0.31 (5% MeOH in DCM); ¹H NMR (300 MHz, CDCl₃) δ 8.90 (br, 1H, NH), 8.73 (d, *J* = 7.5 Hz, 1H, H-C(6)), 7.82 (d, *J* = 7.3 Hz, 2H, H-arom), 7.55 – 7.31 (m, 10H, H-arom, H-C(5)), 7.28 – 7.09 (m, 3H, H-arom), 6.76 (dd, *J* = 8.8, 1.7 Hz, 4H, H-arom), 5.73 (t, *J* = 6.3 Hz, 1H, H-C(1')), 4.28 – 4.13 (m, 1H, H-C(5')), 3.83 (t, *J* = 6.0 Hz, 1H, H-C(4')), 3.75 (d, *J* = 3.6 Hz, 1H, H-C(7')), 3.70 (s, 6H, *MeO*), 2.86 (d, *J* = 14.7 Hz, 1H, H-C-(2')), 2.54 (dd, *J* = 17.4, 7.4 Hz, 1H, H-C(3')), 1.68 – 1.55 (m, 1H, H-C(6')), 1.45 – 1.13 (m, 3H, H-C(2'), H-C(6'), OH); ¹³C NMR (75 MHz, CDCl₃) δ 166.63 (CONH), 162.34 (C(4)), 158.65 (*MeO*-C-arom), 155.00 (C(2)), 145.62 (C-arom), 145.11 (C(6)), 136.72, 136.64, 133.16 (C-arom), 130.25, 129.02, 128.12, 127.93, 127.61, 126.95, 113.20 (CH-arom), 96.24 (C(5)), 89.20 (*C*(Ph)₃), 87.48 (C(1')), 83.40 (C(4')), 74.50, (C(5')) 73.90 (C(7')), 55.25 (*MeO*-DMTr), 50.05 (C(3')), 38.90 (C(6')), 38.40 (C(2')); ESI⁺-HRMS *m/z* calcd for C₃₉H₃₈O₇N₃ ([M + H]⁺) 660.2704, found 660.2707.

(3'S,5'R,7'R)-N4-Benzoyl-1-{7'-O-[(2-cyanoethoxy)-diisopropylaminophosphoryl]-2',3'-Dideoxy-3',5'-ethano-5'-O-[(4,4'-dimethoxytriphenyl)methyl]-β-D-ribofuranosyl} cytosine

(31) :

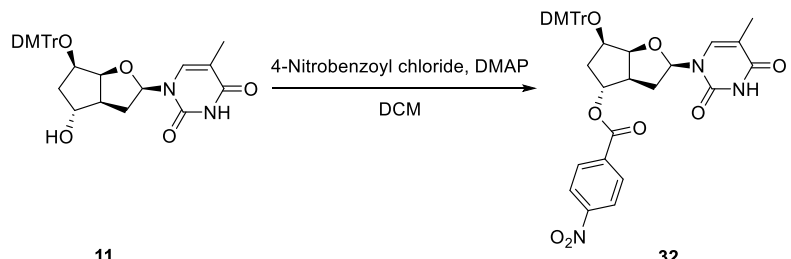


To a solution of the nucleoside **30** (67 mg, 0.101 mmol) and 5-(ethylthio)-1H-tetrazole (22 mg, 0.17 mmol) in dry DCM (3 mL) was added dropwise 2-cyanoethyl N,N,N',N'-tetraisopropylphosphordiamidite (65 µL, 0.20 mmol) at rt. After stirring for 40 min, the reaction mixture was diluted with DCM (20 mL) and washed with satd NaHCO₃ (2 X 15 mL) and satd NaCl (15 mL). Aqueous phases were combined and extracted with DCM (20 mL). The combined organic phases were dried over MgSO₄, filtered and evaporated. The crude product was purified by CC (EtOAc, +0.5 % Et₃N) to yield **31** (75 mg, mixture of two isomers, 86%) as a white foam.

Data for **31**: *R*_f = 0.67 (4% MeOH in DCM); ¹H NMR (300 MHz, CDCl₃) δ 8.88 (s, 1H, NH), 8.79 (d, *J* = 7.5 Hz, 1H, H-C(6)), 7.93 (d, *J* = 7.5 Hz, 2H, H-arom), 7.67 – 7.40 (m, 10H, H-arom, H-C(5)), 7.39 – 7.22 (m, 3H, H-arom), 6.93 – 6.79 (m, 4H, H-arom), 5.97 – 5.77 (m, 1H, H-C(1')), 4.22 (dt, *J* = 14.5, 5.6 Hz, 1H, H-(5')), 3.98 – 3.84 (m, 2H, H-C(4'), H-C(7')), 3.82 (s, 6H, MeO), 3.66 (ddd, *J* = 16.8, 13.5, 6.7 Hz, 2H, OCH₂CH₂CN), 3.53 – 3.37 (m, 2H, (Me₂CH)₂N), 3.14 – 2.93 (m, 1H, H-C(2')), 2.84 – 2.66 (m, 1H, H-C(3')), 2.53 (dt, *J* = 12.4, 6.3 Hz, 2H, OCH₂CH₂CN), 1.83 – 1.56 (m, 2H, H-C(6')), 1.46 (td, *J* = 14.1, 7.0 Hz, 1H, H-C(2')), 1.18 – 0.97 (m, 12H, (Me₂CH)₂N); ¹³C NMR (75 MHz, CDCl₃) δ 166.70 (CONH), 162.32, 162.28 (C(4)), 158.68 (MeO-C-arom), 154.93 (C(2)), 145.53 (C-arom), 144.95, 144.89 (C(6)), 136.69, 136.63, 136.56, 136.52, 133.24 (C-arom), 133.10, 130.24, 130.20, 129.01, 128.10, 127.94, 127.60, 126.96 (CH-arom), 117.53 (OCH₂CH₂CN), 113.20 (CH-arom), 96.24 (C(5)), 89.15, 89.10 (C(Ph)₃), 87.55, 87.54 (C(1')), 83.11, 83.04 (C(4')), 75.93, 75.37 (*J*_{C,P} = 16.7, 15.5 Hz, C(7')), 74.48 (C(5')), 58.25, 57.99 (*J*_{C,P} = 17.9, 18.1 Hz OCH₂CH₂CN), 55.27, 55.24 (MeO-DMTr), 49.27, 49.03 (*J*_{C,P} = 3.1, 4.8 Hz, C(3')), 43.15, 42.98 ((Me₂CH)₂N), 38.89, 38.80 (C(2')), 37.44, 37.24 (*J*_{C,P} = 5.2, 3.2 Hz, C(6')), 24.58, 24.54, 24.48, 24.45, 24.35 (5s, Me₂CH)₂N), 20.33, 20.24 (*J*_{C,P} = 5.8, 5.7 Hz, OCH₂CH₂CN); ³¹P NMR (121 MHz, CDCl₃) δ 147.19, 146.94; ESI⁺-HRMS *m/z* calcd for C₄₈H₅₅O₈N₅P ([M + H]⁺) 860.3783, found 860.3791.

6. Synthesis of 7'-O-p-nitrobenzoyl-7',5'-bc-T

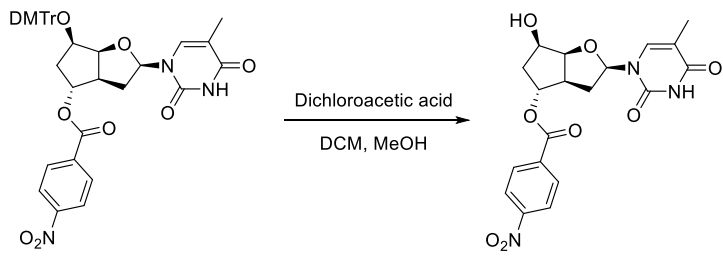
(3'S,5'R,7'R)-1-{2',3'-Dideoxy-3',5'-ethano-7'-O-(4-nitrobenzoate)-5'-O-[(4,4'-dimethoxytriphenyl)methyl]-β-D-ribofuranosyl} thymine (32) :



To a solution of nucleoside **11** (100 mg, 0.175 mmol) and 4-dimethylaminopyridine (26 mg, 0.21 mmol) in dry DCM (8 mL) was added 4-nitrobenzoyl chloride (59 mg, 0.315 mmol) at rt. After stirring for 6 h, the reaction was quenched by addition of satd NaHCO₃ (5 mL). The mixture was then diluted with satd NaHCO₃ (15 mL) and extracted with DCM (3 X 15 mL). The combined organic phases were dried over MgSO₄, filtered and evaporated. The crude product was purified by CC (2.5% MeOH in DCM, +0.5 % Et₃N) to yield **32** (98 mg, 78%) as a white foam, containing traces of Et₃N.

Data for **32**: R_f = 0.42 (5% MeOH in DCM); ¹H NMR (300 MHz, CDCl₃) δ 8.26 (t, J = 7.3 Hz, 3H, H-arom, HN(3)), 8.00 (d, J = 8.9 Hz, 2H, H-arom), 7.72 (d, J = 1.0 Hz, 1H, H-C(6)), 7.55 (d, J = 6.9 Hz, 2H, H-arom), 7.44 (dd, J = 8.8, 6.6 Hz, 4H, H-arom), 7.35 – 7.18 (m, 3H, H-arom), 6.83 (dd, J = 9.0, 2.6 Hz, 4H, H-arom), 6.01 (dd, J = 8.2, 5.2 Hz, 1H, H-C(1')), 4.96 (d, J = 3.3 Hz, 1H, H-C(7')), 4.33 – 4.24 (m, 1H, H-C(4')), 4.24 – 4.13 (m, 1H, H-C(5')), 3.78 (d, J = 0.9 Hz, 6H, MeO), 2.92 – 2.72 (m, 2H, H-C(3'), H-C(2')), 1.81 (d, J = 0.6 Hz, 3H, Me-C(5)), 1.79 – 1.62 (m, 2H, H-C(6')); ¹³C NMR (75 MHz, CDCl₃) δ 164.05, 163.84 (C(4), CO₂R), 158.81 (MeO-C-arom), 150.64, 150.52 (O₂N-C-arom, C(2)), 145.29, 136.43, 136.34 (C-arom), 135.18 (C(6)), 130.62, 130.20, 130.17, 128.16, 128.01, 127.15, 123.58, 113.30, 113.27 (C-arom), 111.17 (C(5)), 87.53 (C(Ph)₃), 86.29 (C(1')), 81.59 (C(4')), 78.65 (C(7')), 74.16 (C(5')), 55.26 (MeO-DMTr), 47.07 (C(3')), 37.35 (C(2')), 35.71 (C(6')), 12.51 (Me-C(5)); ESI⁺-HRMS m/z calcd for C₄₀H₃₇O₁₀N₃Na ([M + Na]⁺) 742.2371, found 742.2375.

(3'S,5'R,7'R)-1-{2',3'-Dideoxy-3',5'-ethano-7'-O-(4-nitrobenzoate)- β -D-ribofuranosyl} thymine (33):

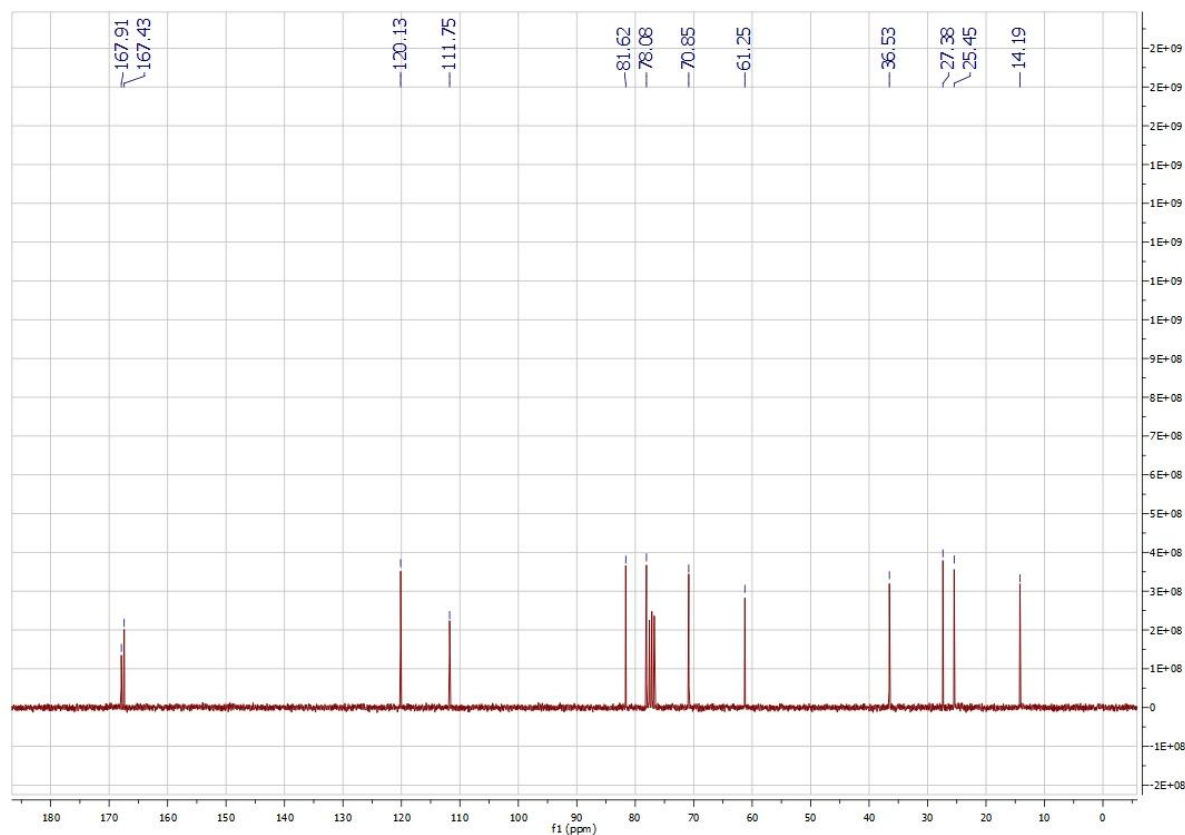
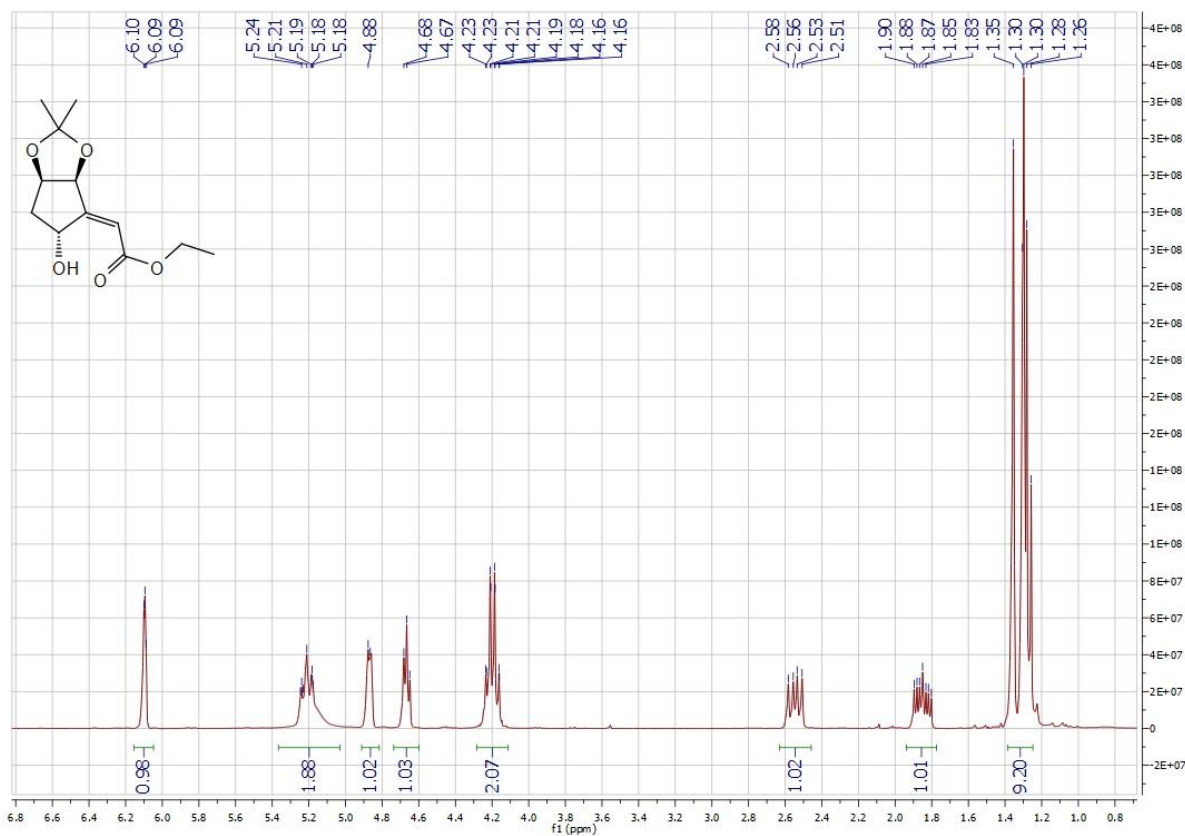


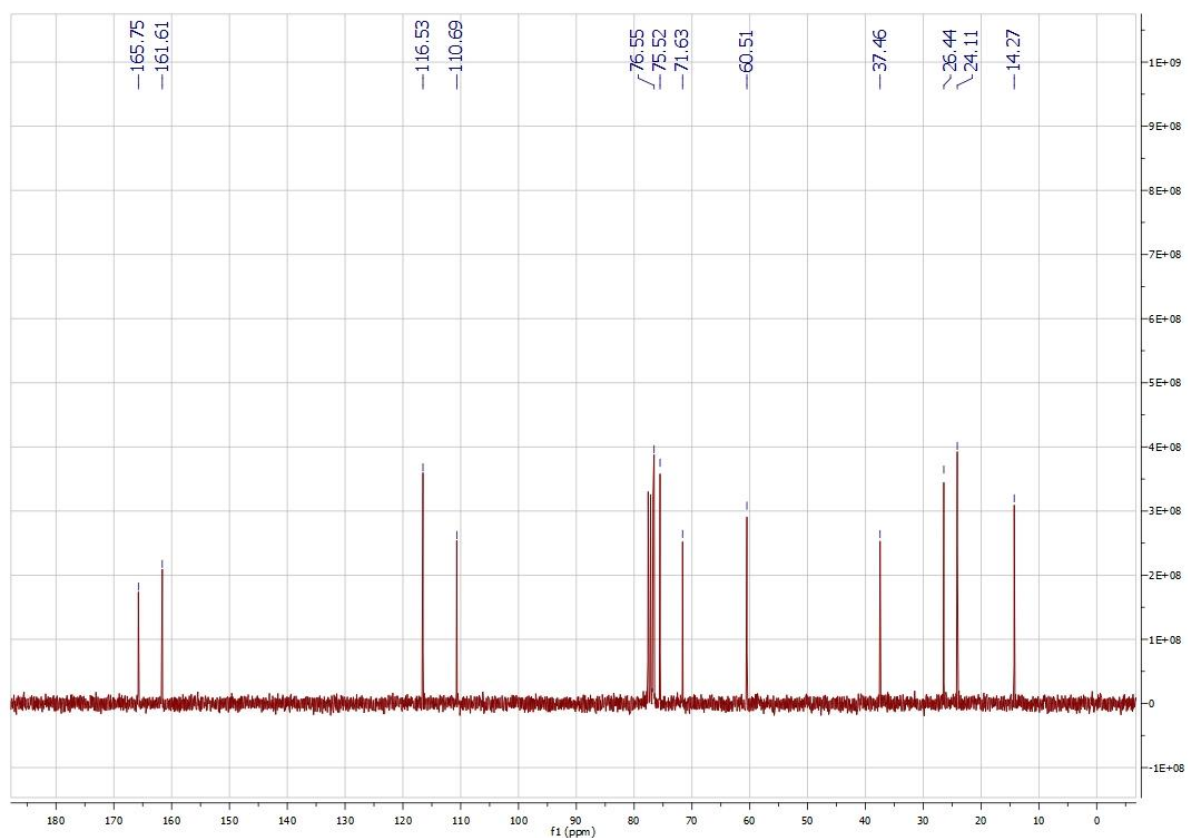
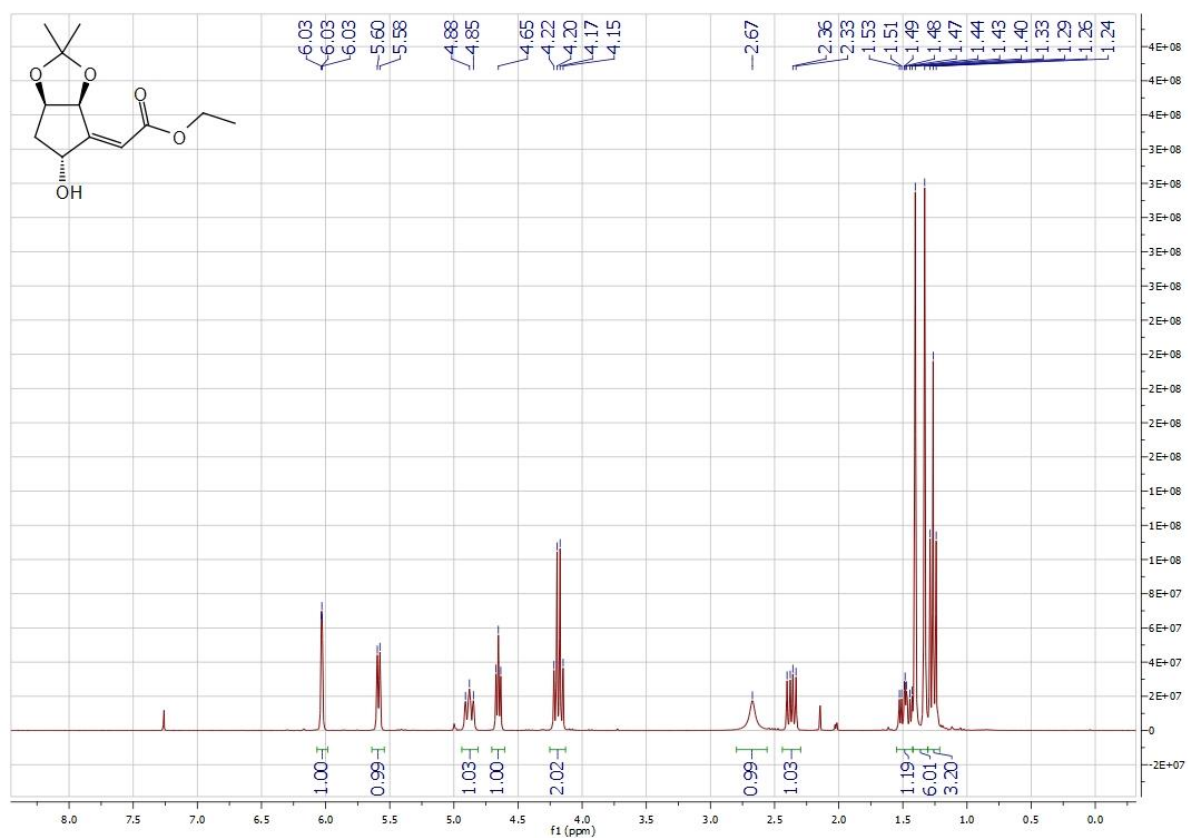
To a solution of **32** (60 mg, 0.083 mmol) in a mixture of dry DCM (1 mL) and MeOH (0.4 mL), was added dropwise dichloroacetic acid (0.2 mL) at rt. After stirring for 3 h, the mixture was then diluted with satd NaHCO₃ (15 mL) and extracted with DCM (3 X 10 mL). The combined organic phases were dried over MgSO₄, filtered and evaporated. The crude product was purified by CC (5% MeOH in DCM) to yield **33** (29 mg, 84%) as a white foam. Crystals suitable for X-ray analysis were obtained by recrystallization in a mixture of H₂O/MeOH.

Data for **33**: R_f = 0.18 (5% MeOH in DCM); ¹H NMR (400 MHz, DMSO) δ 11.33 (s, 1H, H-N(3)), 8.34 (d, J = 8.8 Hz, 2H, H-arom), 8.27 – 8.13 (m, 2H, H-arom), 7.78 (s, 1H, H-C(6)), 5.96 (dd, J = 9.3, 5.6 Hz, 1H, H-C(1')), 5.18 (t, J = 3.8 Hz, 1H, H-C(7')), 5.12 (d, J = 6.0 Hz, 1H, OH), 4.33 (dd, J = 7.3, 4.7 Hz, 1H, H-C(4')), 4.27 (td, J = 10.5, 5.5 Hz, 1H, H-C(5')), 2.90 (dd, J = 17.2, 8.5 Hz, 1H, H-C(3')), 2.58 – 2.46 (m, 1H, H-C(2')), 2.30 (ddd, J = 13.8, 8.8, 5.3 Hz, 1H, H-C(6')), 2.03 (dd, J = 9.6, 4.2 Hz, 1H, H-C(6')); 1H NMR (400 MHz, DMSO) δ 164.33, 164.23 (C(4), CO₂R), 150.91, 150.75 (O₂N-C-arom, C(2)), 136.79 (C-arom), 135.69 (C(6)), 131.20, 124.32 (CH-arom), 109.89 (C(5)), 85.31 (C(1')), 81.48 (C(4')), 80.07 (C(7')), 71.72 (C(5')), 47.18 (C(3')), 37.77 (C(6')), 35.48 (C(2')); ESI⁺-HRMS *m/z* calcd for C₁₉H₂₀O₈N₃ ([M + H]⁺) 418.1245, found 418.1242.

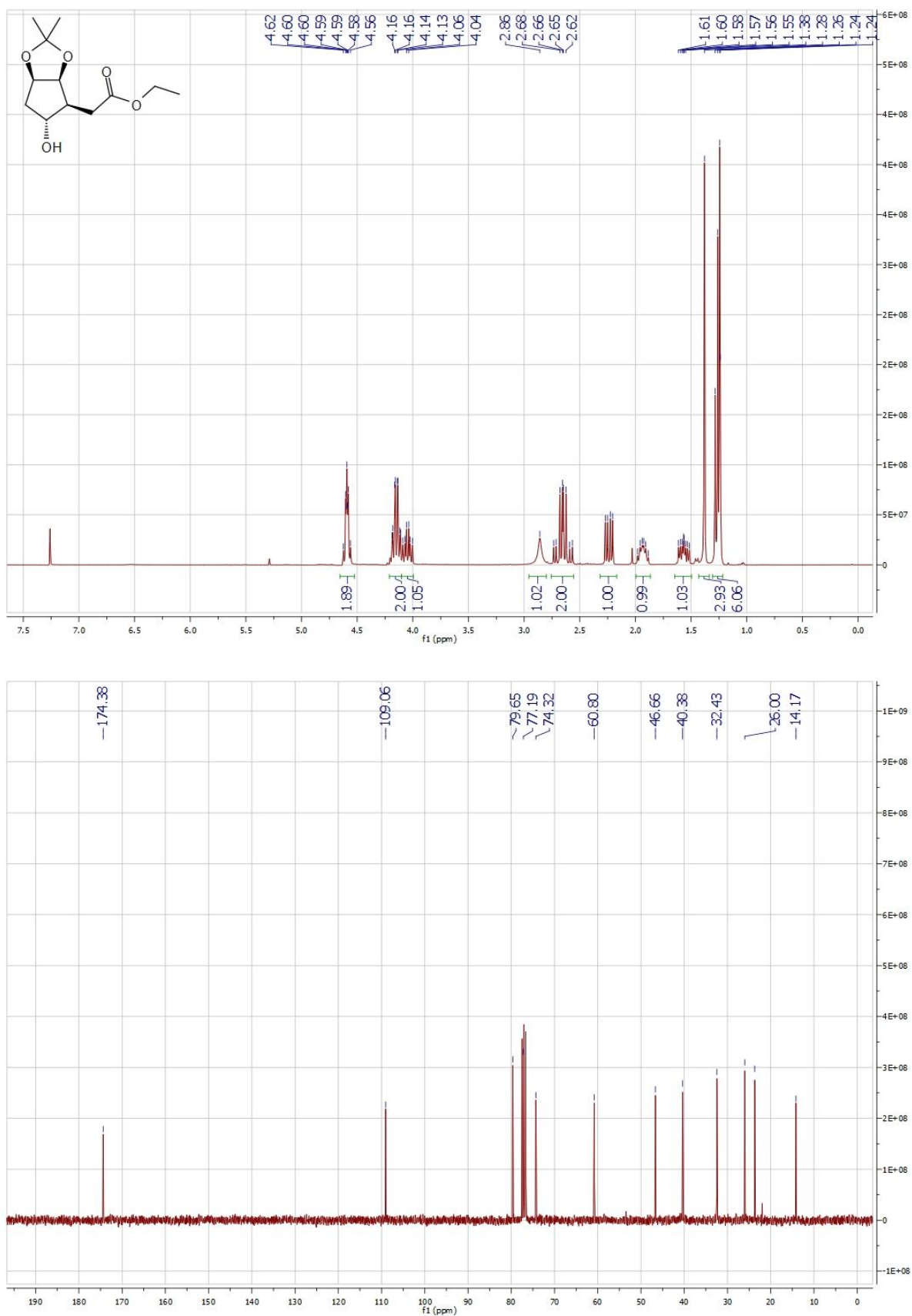
7. NMR spectra

Ethyl (E and Z, 1'R,5'S,7'R)-(7'-hydroxy-3',3'-dimethyl-2',4'-dioxabicyclo[3.3.0]oct-6'-ylidene)acetate (2a/b) :

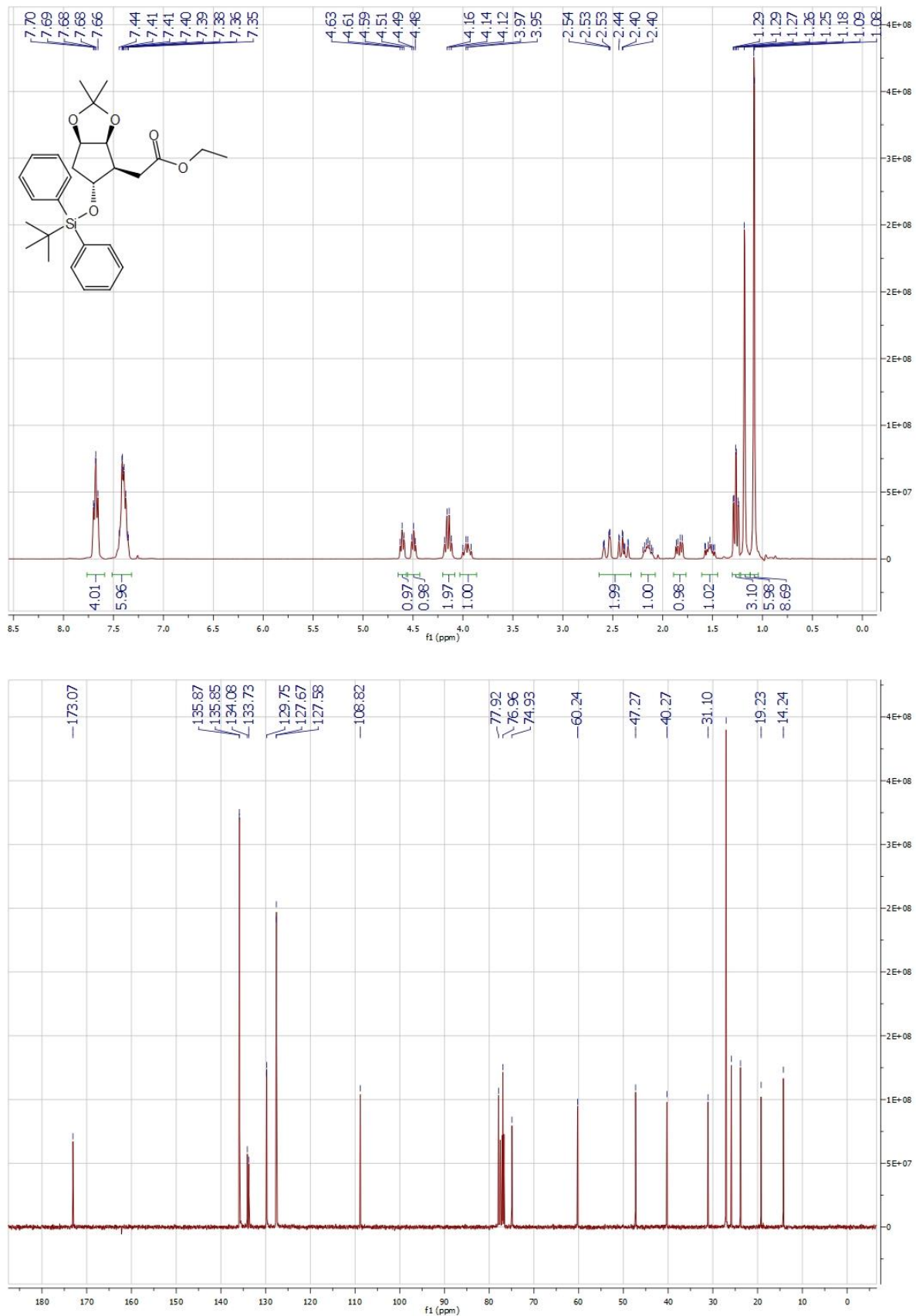




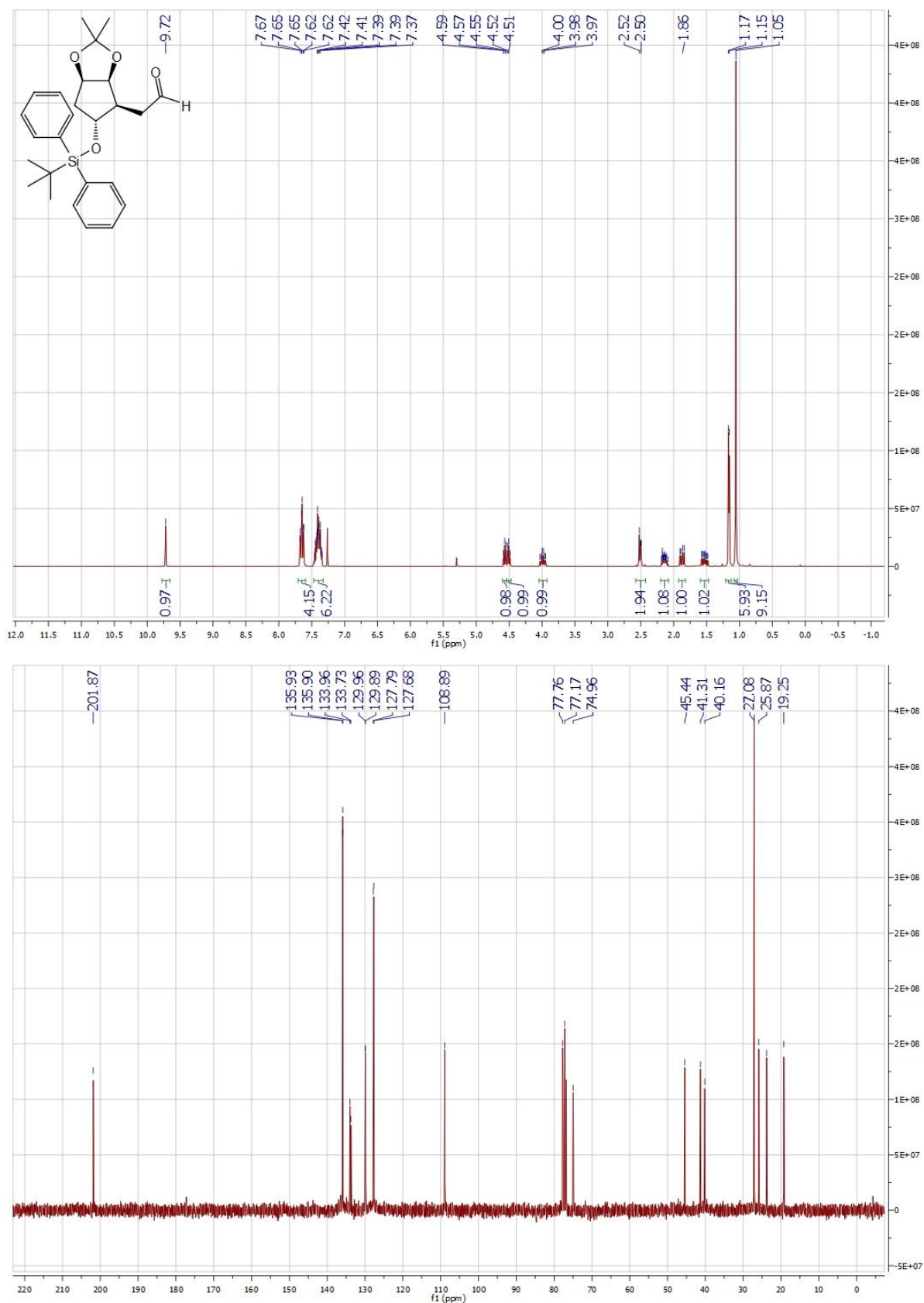
Ethyl (1'R,5'S,6'S,7'R)-(7'-hydroxy-3',3'-dimethyl-2',4'-dioxabicyclo[3.3.0]oct-6'-yl)acetate (3) :



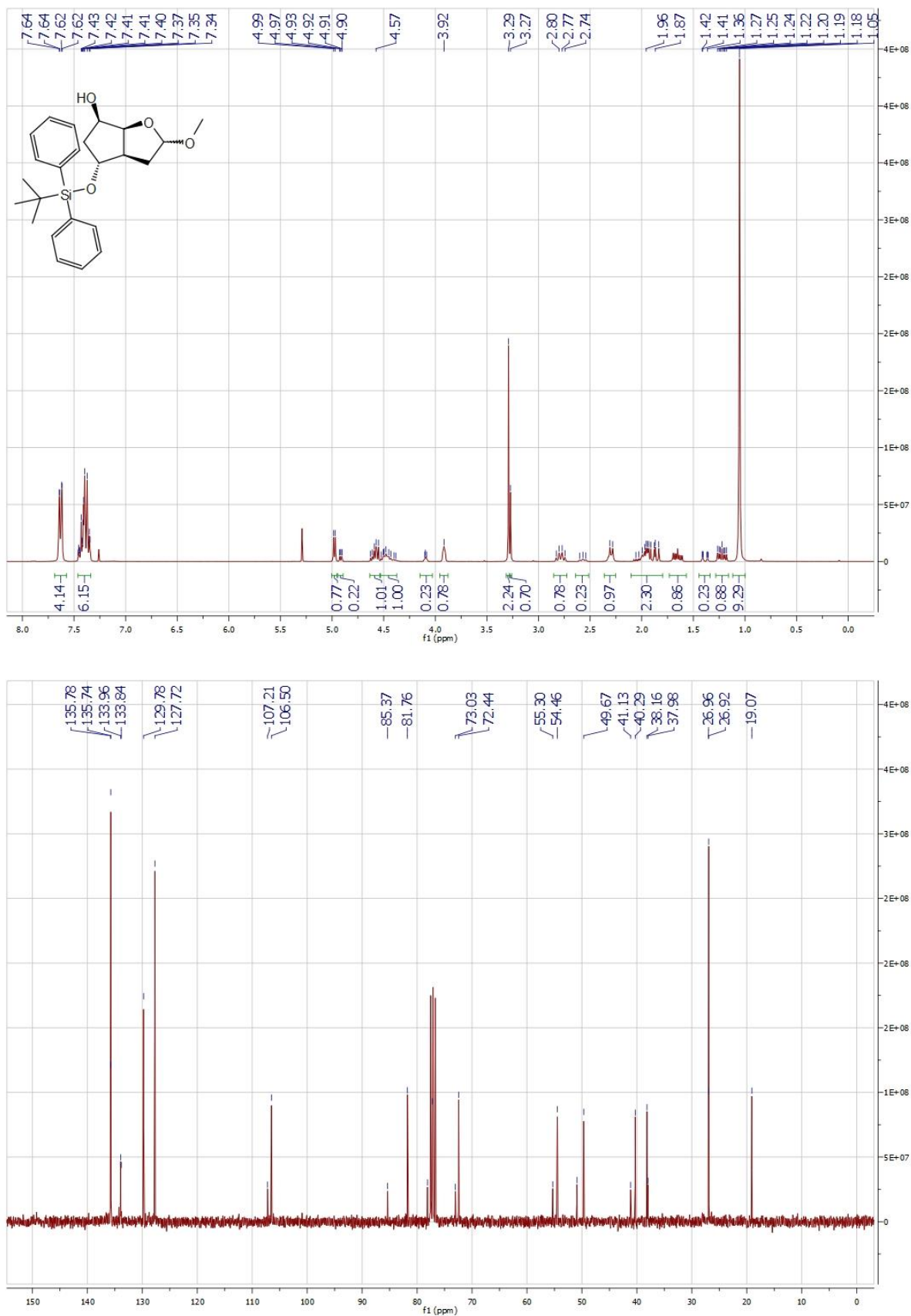
Ethyl (1'R,5'S,6'S,7'R)-(7'-(tert-butyldiphenylsilyl)oxy)-3',3'-dimethyl-2',4'-dioxabicyclo[3.3.0]oct-6'-yl)acetate (4) :



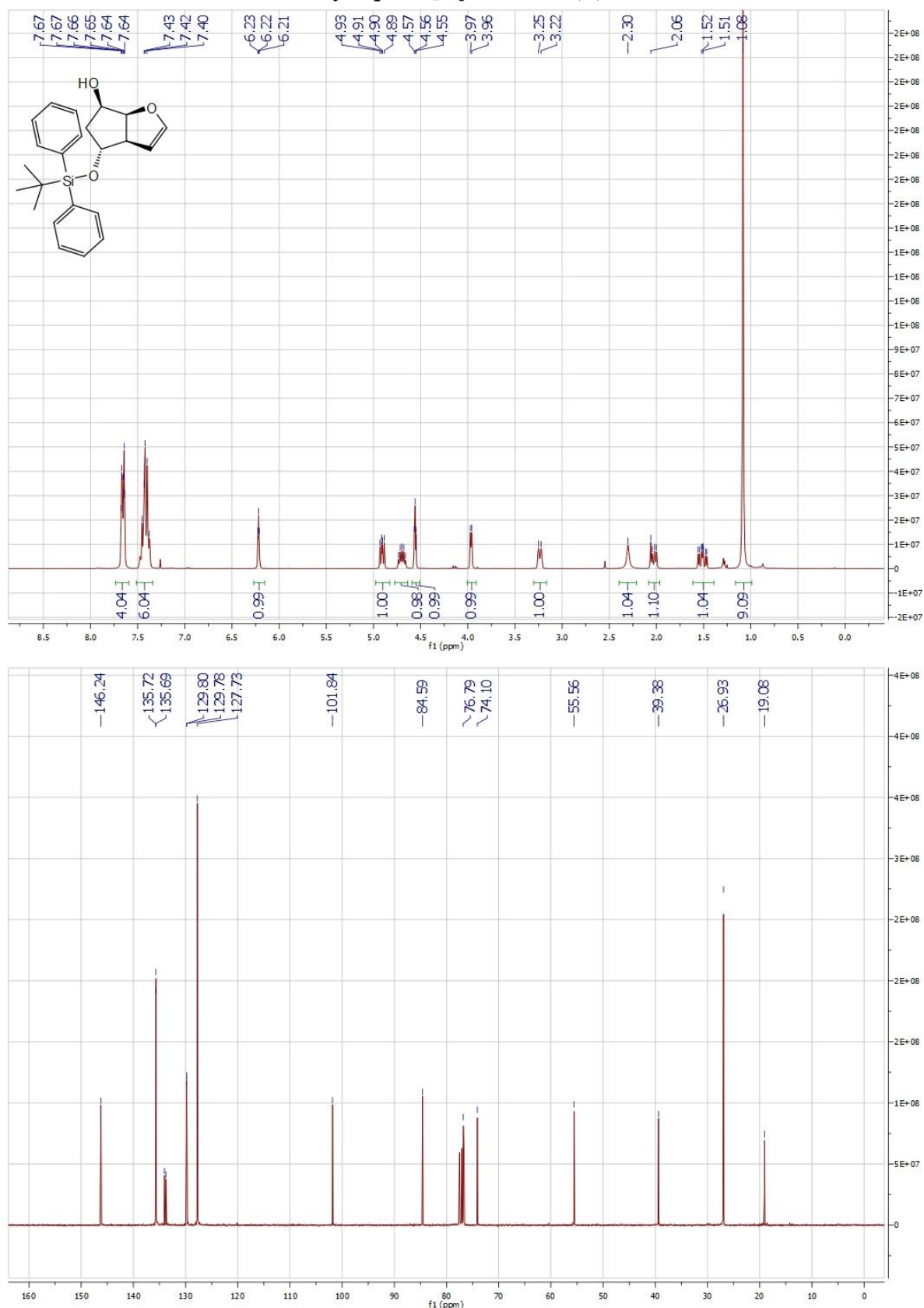
(1'R,5'S,6'S,7'R)-(7'-(tert-butyldiphenylsilyl)oxy)-3',3'-dimethyl-2',4'-dioxabicyclo[3.3.0]oct-6'-yl)acetaldehyde (5) :



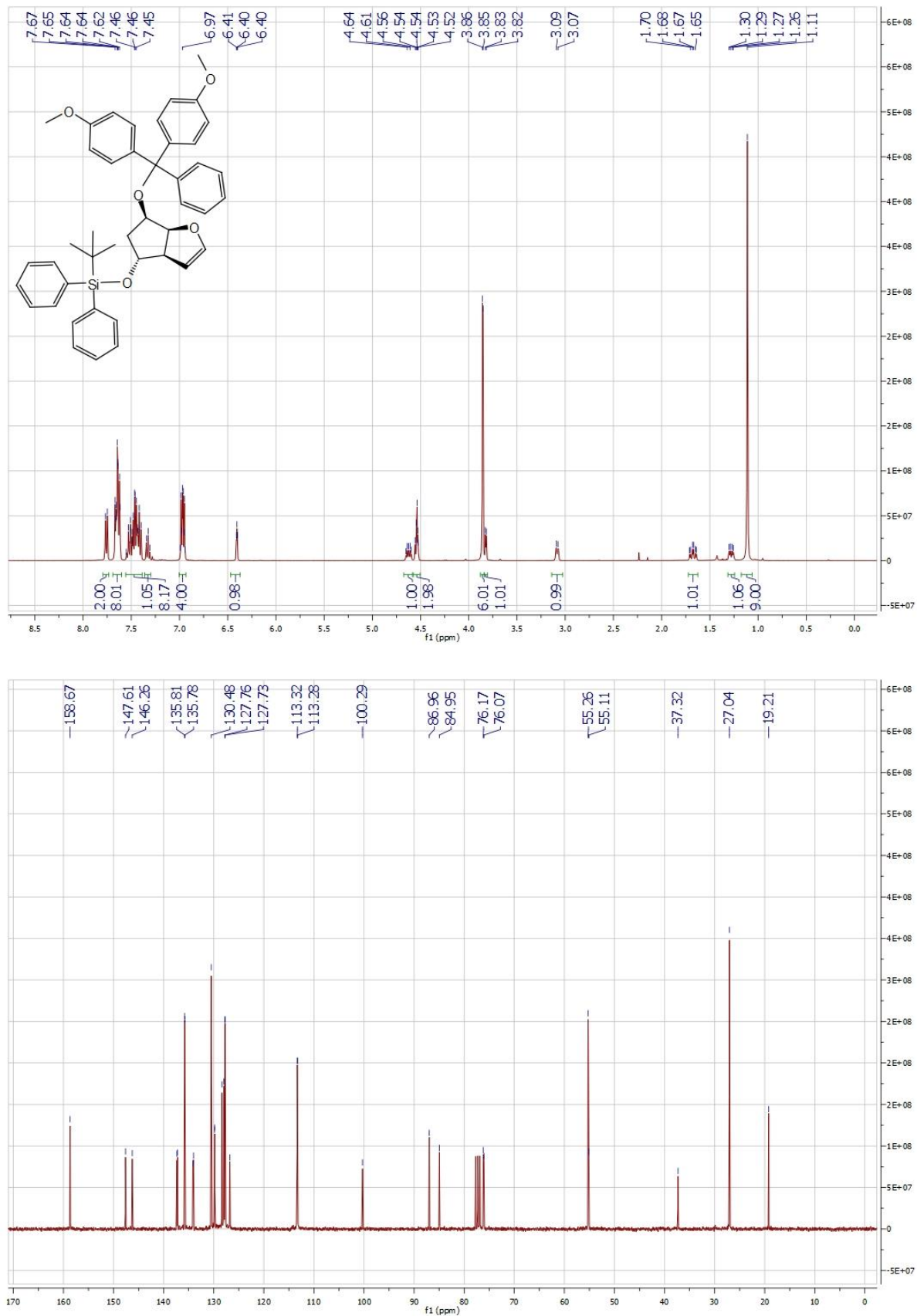
(3a*R*,4*R*,6*R*,6a*S*)-4-((*tert*-butyldiphenylsilyl)oxy)-2-methoxyhexahydro-2*H*-cyclopenta[*b*]furan-6-ol (6**) :**



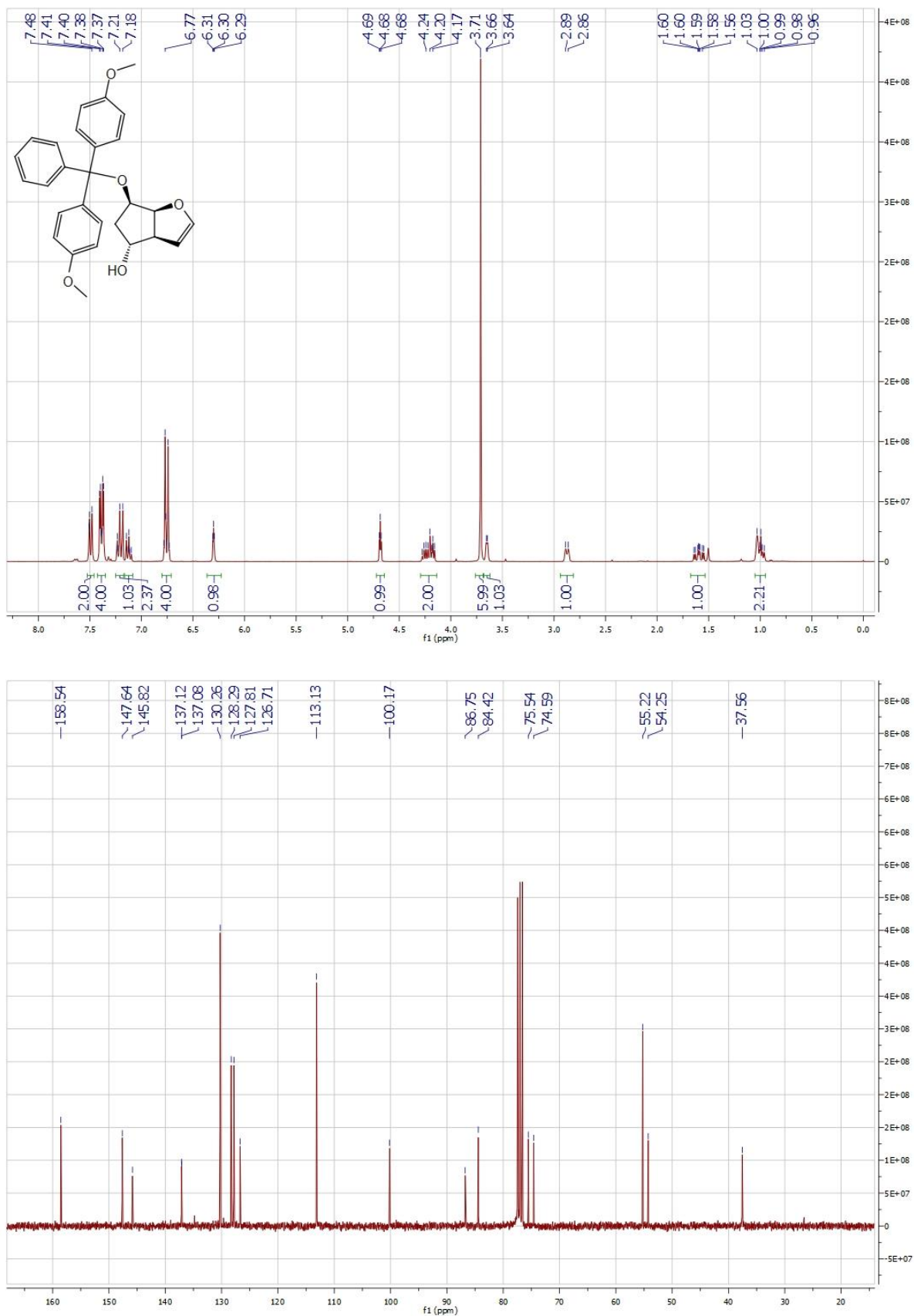
(3a*R*,4*R*,6*R*,6a*S*)-4-((tert-butyldiphenylsilyl)oxy)-3*a*,5,6,6*a*-tetrahydro-4*H*-cyclopenta[*b*]furan-6-ol (8) :



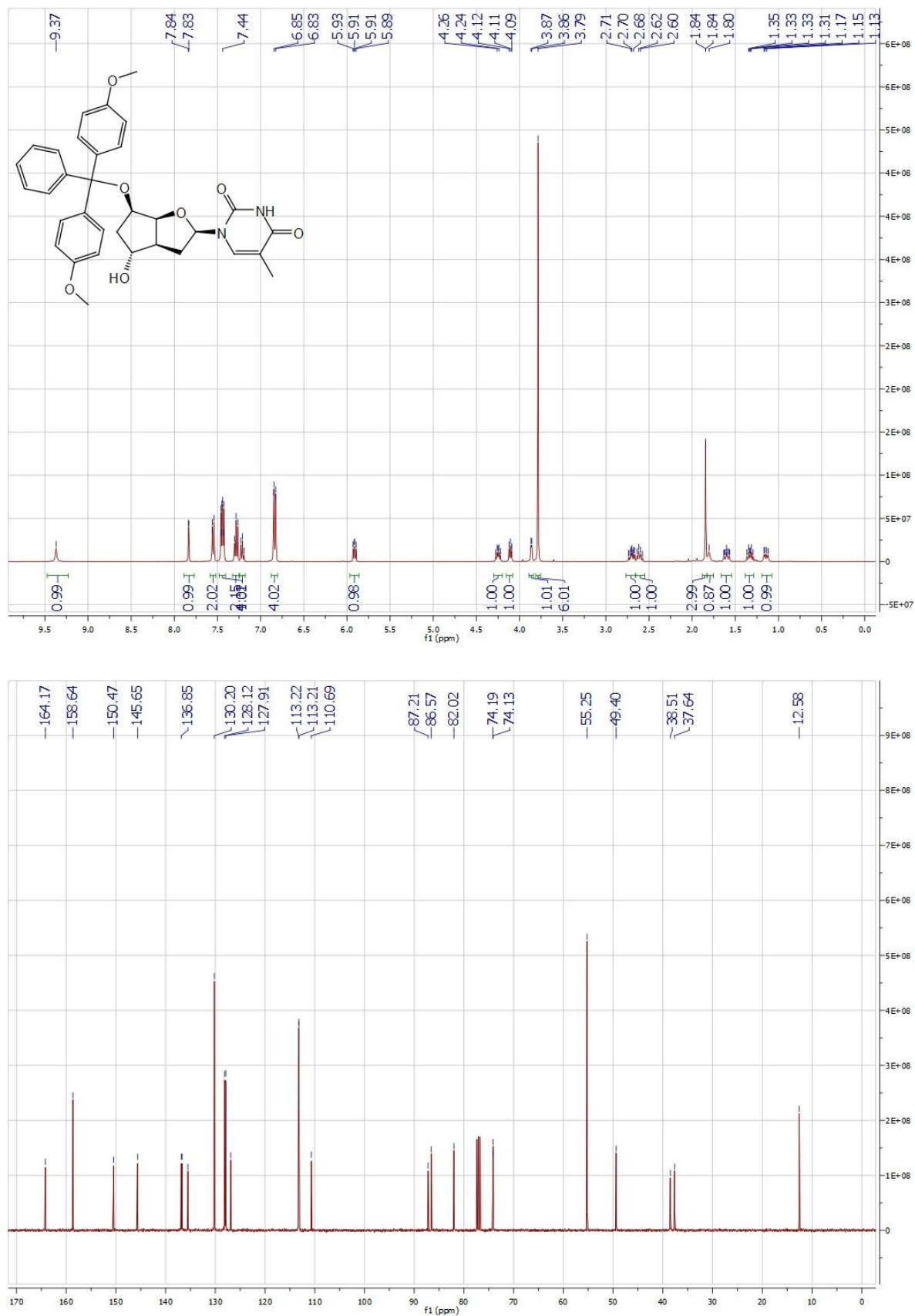
((3aR,4R,6R,6aS)-6-(bis(4-methoxyphenyl)(phenyl)methoxy)-3a,5,6,6a-tetrahydro-4H-cyclopenta[b]furan-4-yl)oxy)(tert-butyl)diphenylsilane (9) :



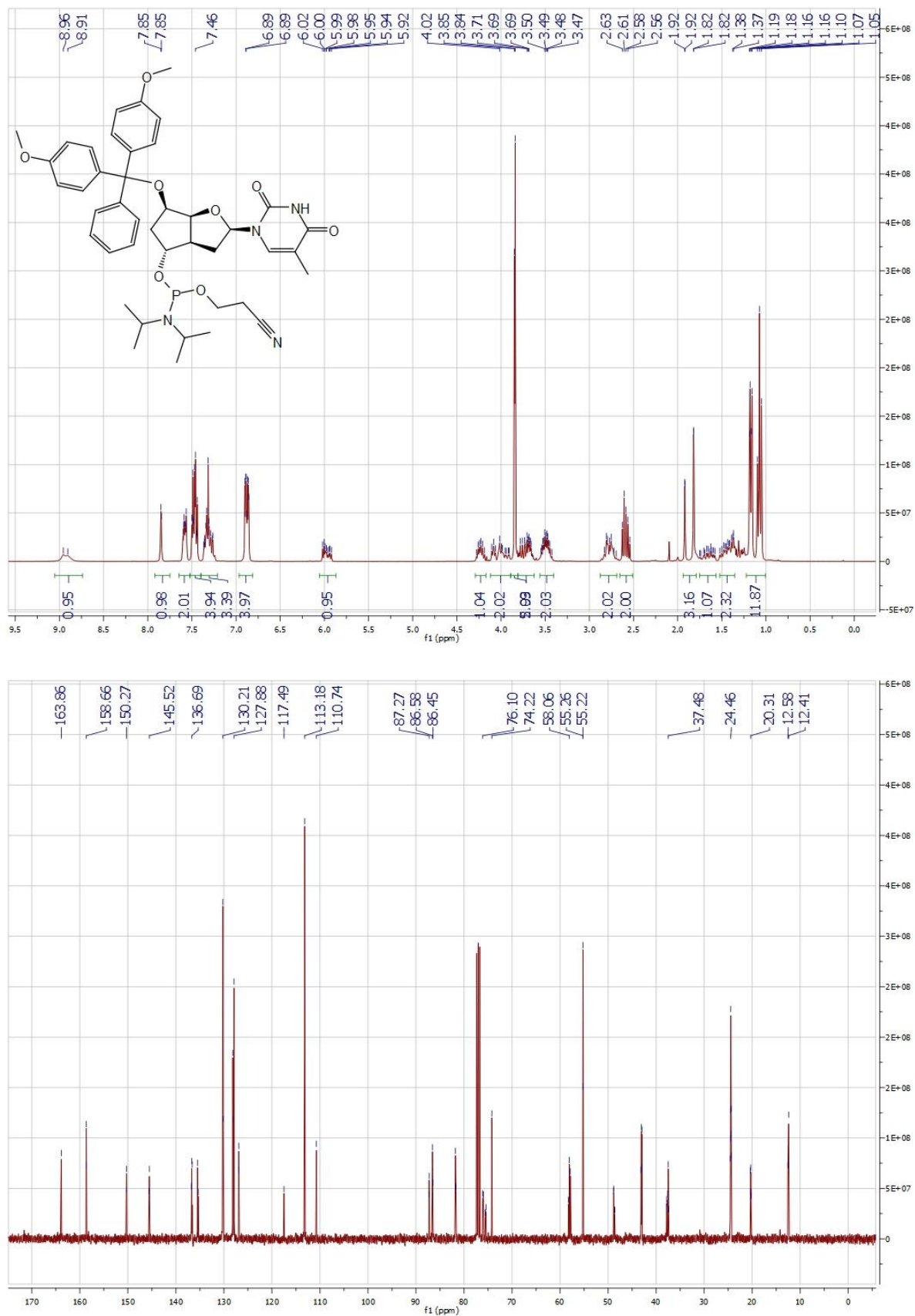
(3a*S*,4*R*,6*R*,6a*S*)-6-(bis(4-methoxyphenyl)(phenyl)methoxy)-3*a*,5,6,6*a*-tetrahydro-4*H*-cyclopenta[*b*]furan-4-ol (10) :

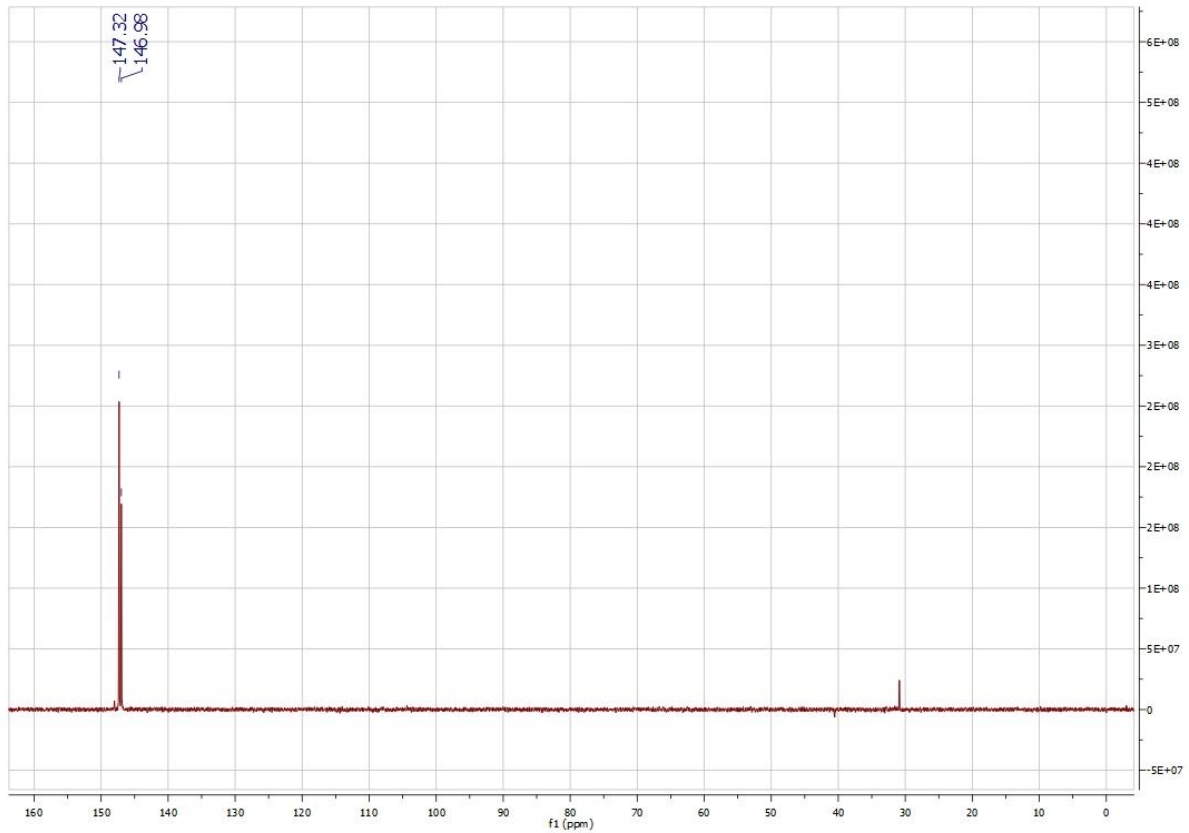


(3'S,5'R,7'R)-1-{2',3'-Dideoxy-3',5'-ethano-7'-hydroxy-5'-O-[(4,4'*-dimethoxytriphenyl)methyl]- β -D-ribofuranosyl} thymine (11) :*

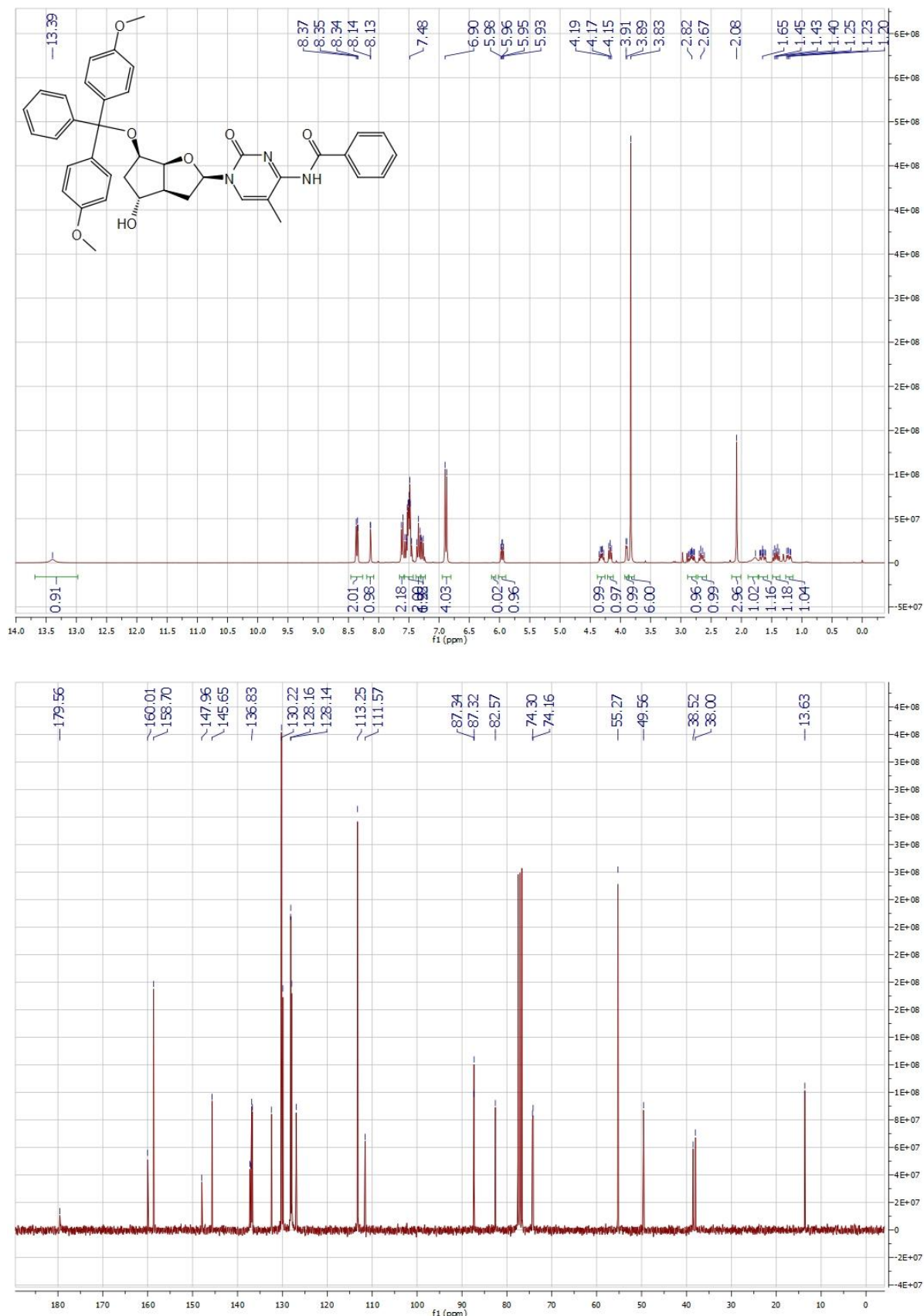


(3'R,5'R,7'R)-1-{7'-O-[(2-cyanoethoxy)-diisopropylaminophosphanyl]-2',3'-Dideoxy-3',5'-ethano-5'-O-[(4,4'-dimethoxytriphenyl)methyl]- β -D-ribofuranosyl} thymine (12) :

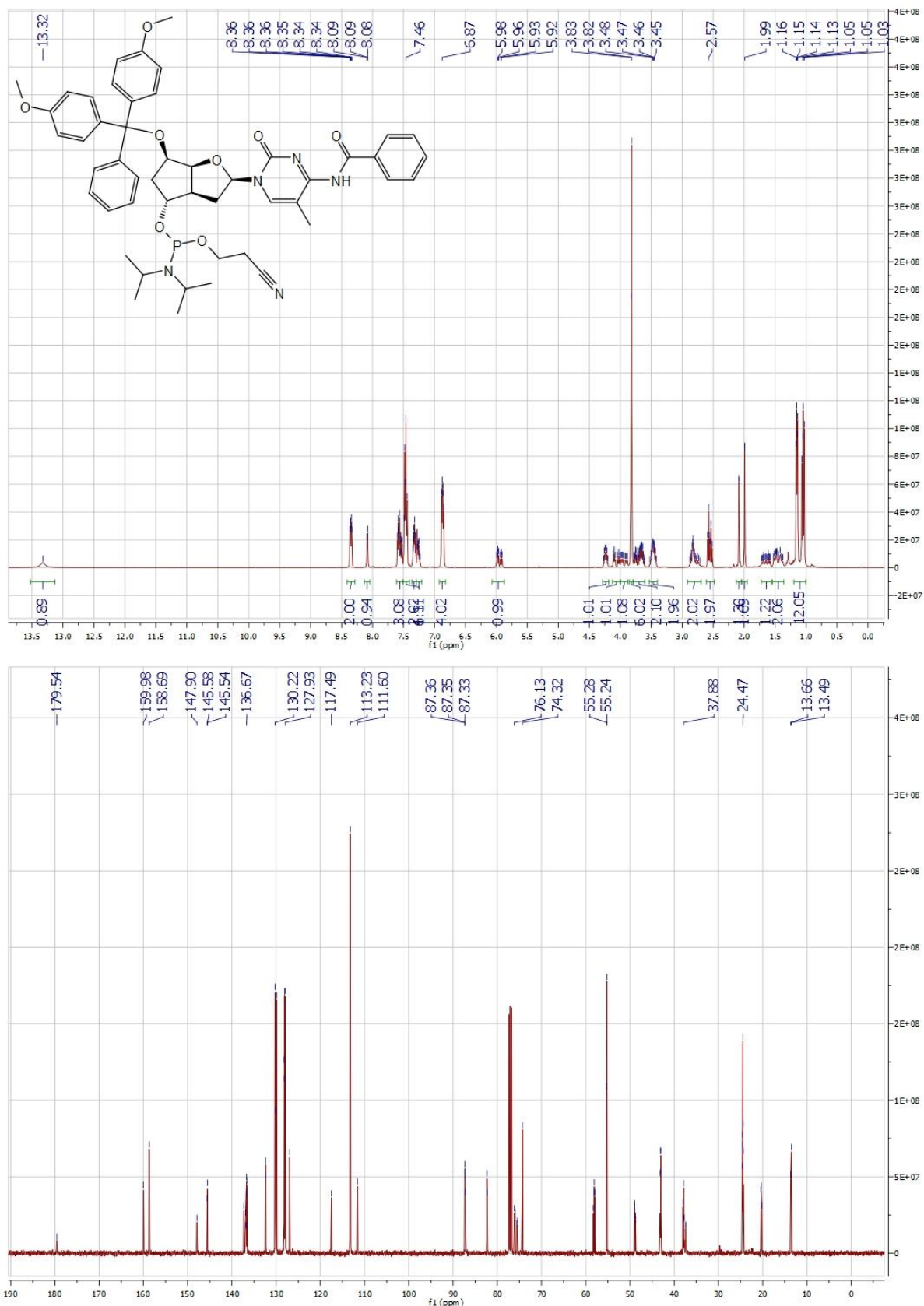


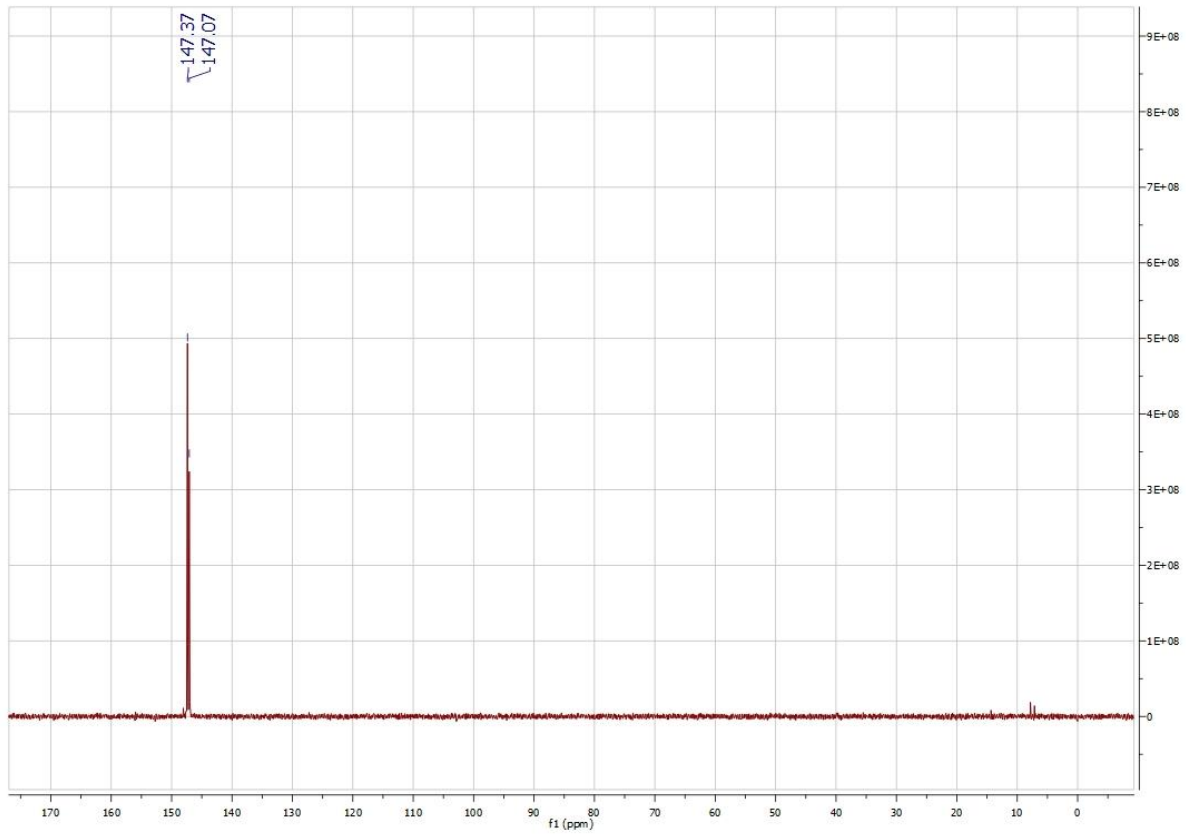


(3'S,5'R,7'R)-N4-Benzoyl-1-{2',3'-Dideoxy-3',5'-ethano-7'-hydroxy-5'-O-[(4,4'-dimethoxytriphenyl)methyl]- β -D-ribofuranosyl}-5-methylcytosine (13) :

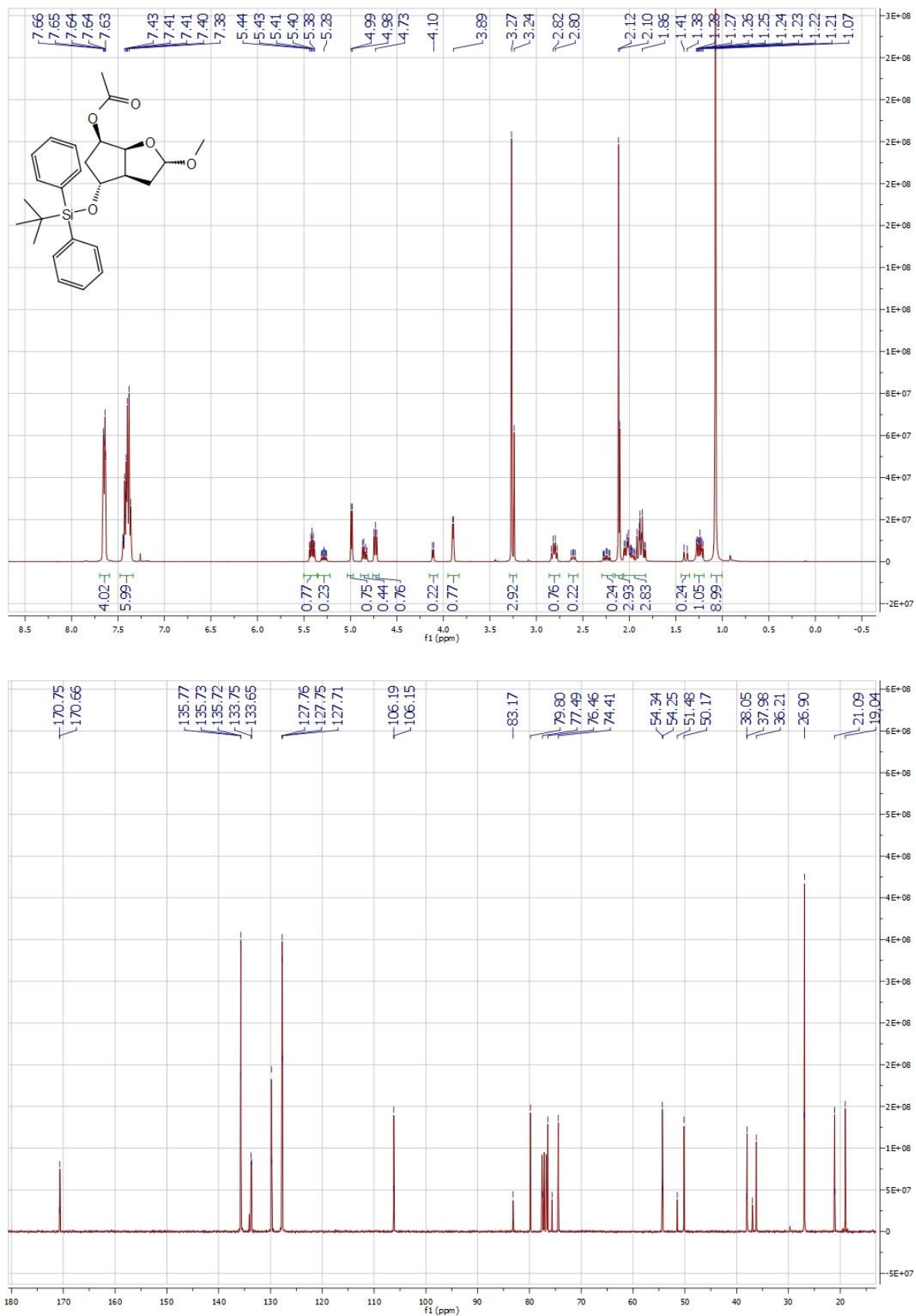


(3'R,5'R,7'R)-N4-Benzoyl-1-{7'-O-[(2-cyanoethoxy)-diisopropylaminophosphanyl]-2',3'-Dideoxy-3',5'-ethano-5'-O-[(4,4'-dimethoxytriphenyl)methyl]- β -D-ribofuranosyl}-5-methylcytosine (14) :

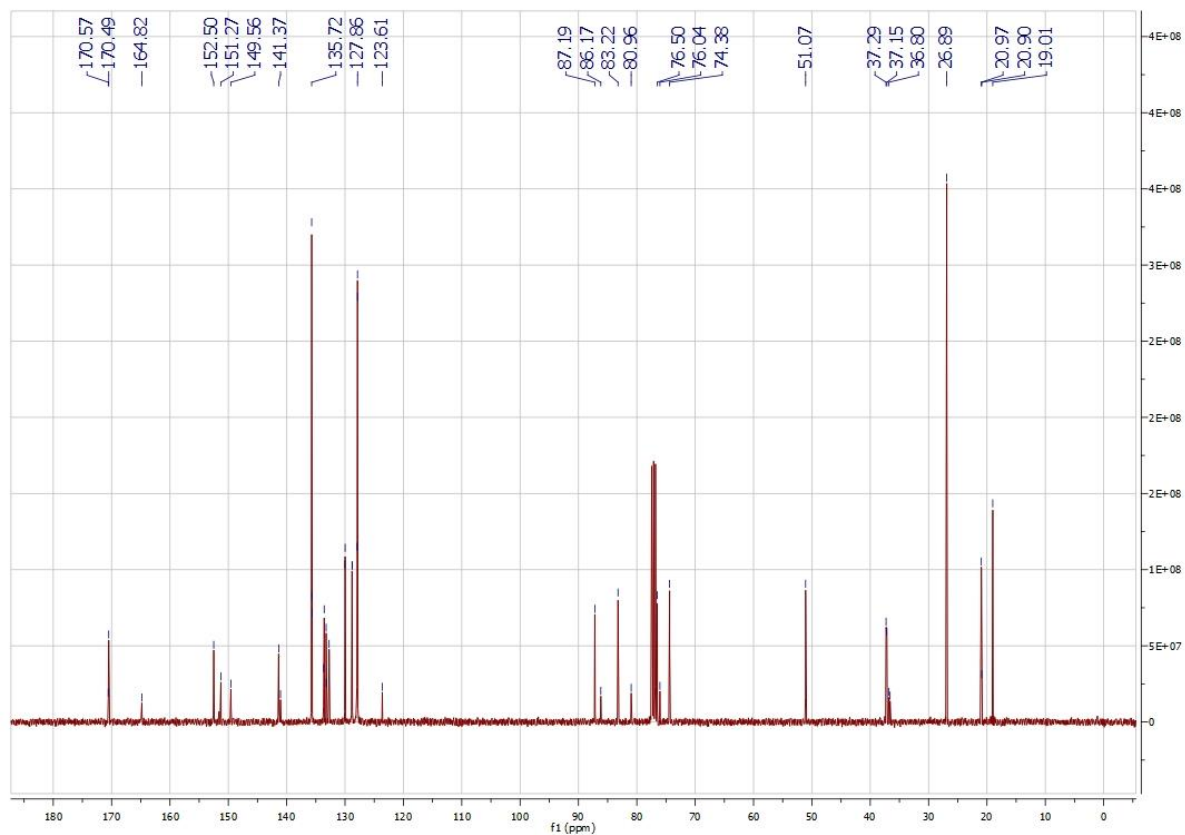
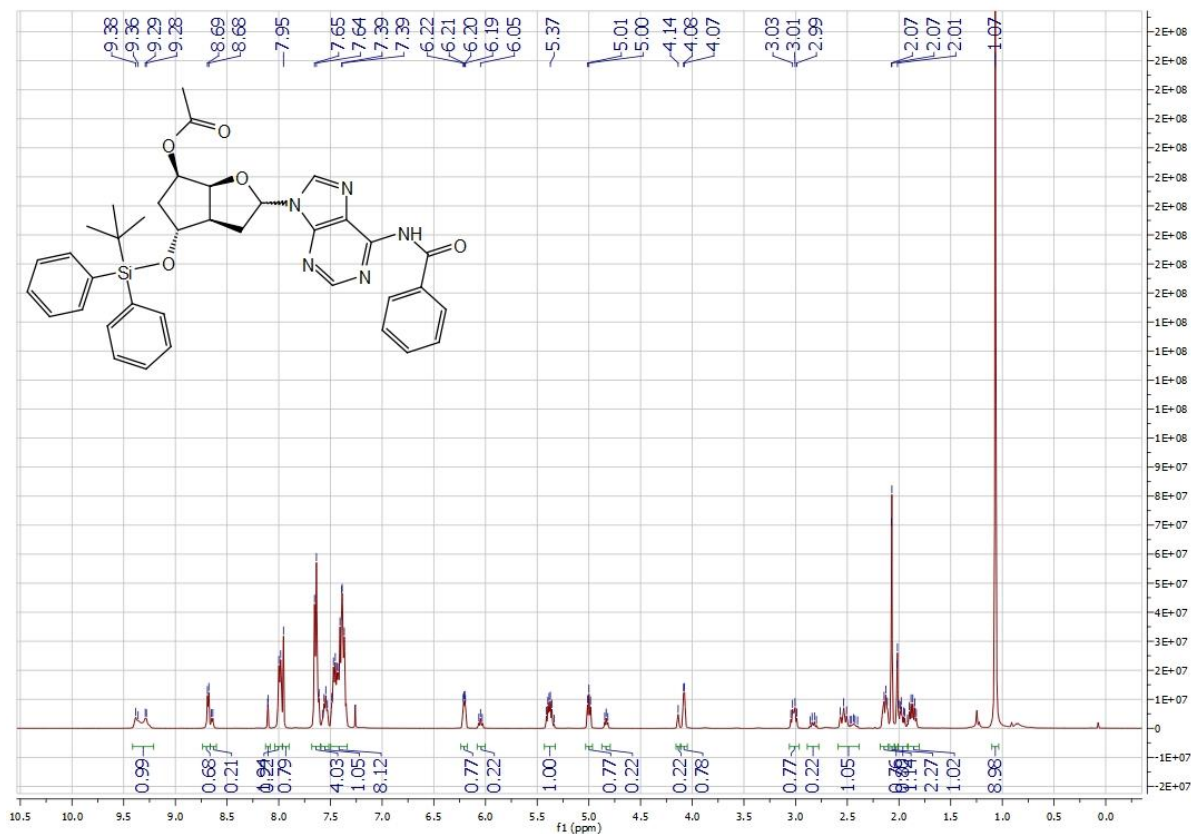




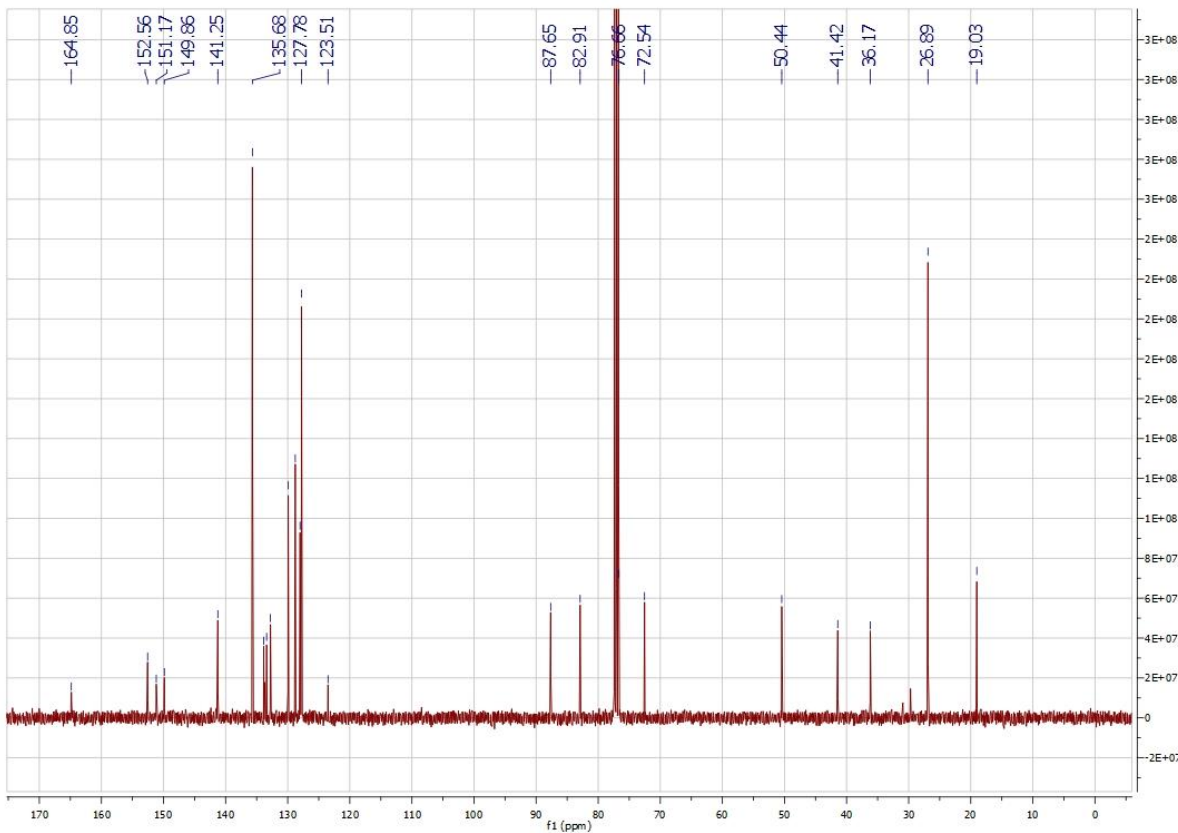
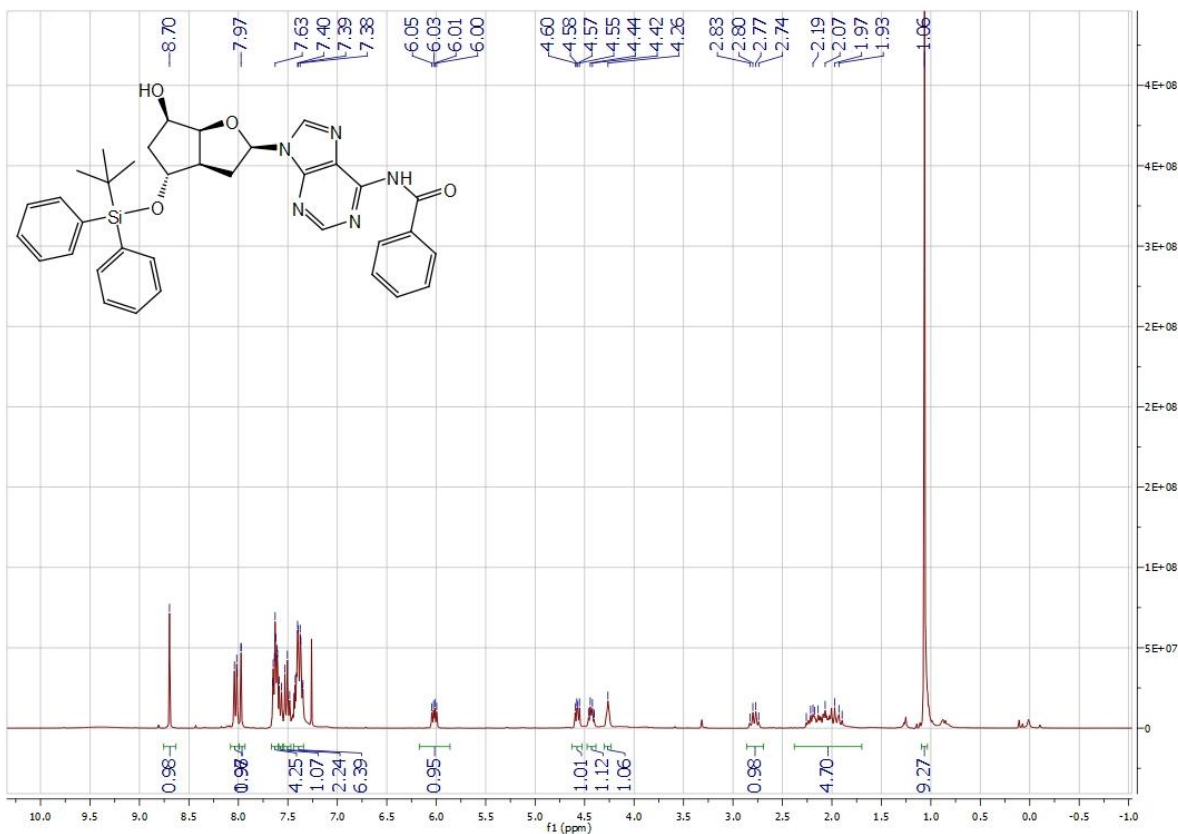
(3a*R*,4*R*,6*R*,6a*S*)-4-((*tert*-butyldiphenylsilyl)oxy)-2-methoxyhexahydro-2*H*-cyclopenta[*b*]furan-6-yl acetate (7) :



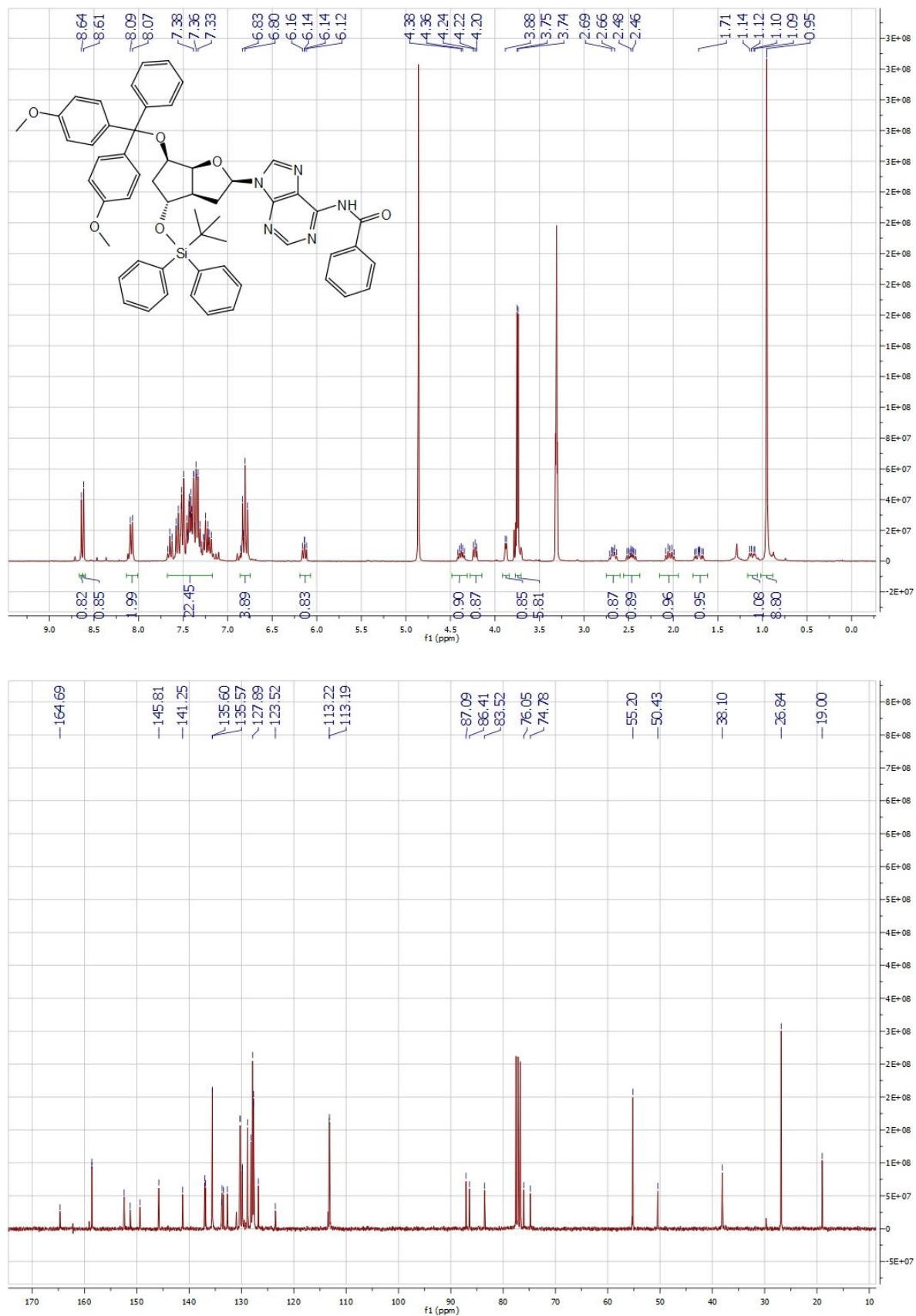
(3'R,5'R,7'R)-N6-Benzoyl-9-{5'-O-acetyl-7'-[*tert*-butyldiphenylsilyl]oxy}-2',3'-Dideoxy-3',5'-ethano- α,β -D-ribofuranosyl adenine (15) :



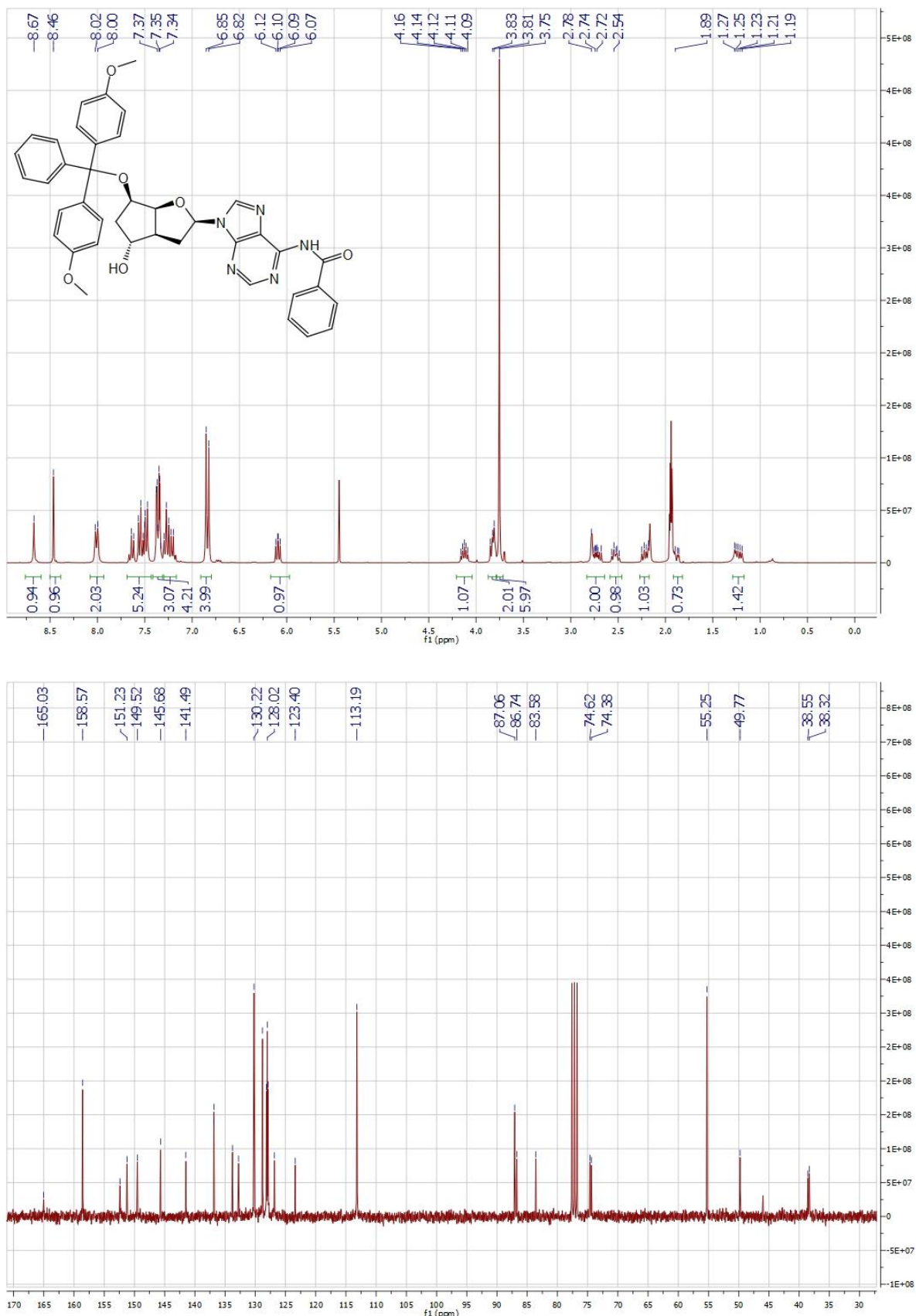
**(3'R,5'R,7'R)-N6-Benzoyl-9-{7'-[tert-butyldiphenylsilyl]oxy}-2',3'-Dideoxy-3',5'-ethano-
 β -D-ribofuranosyl} adenine (16) :**



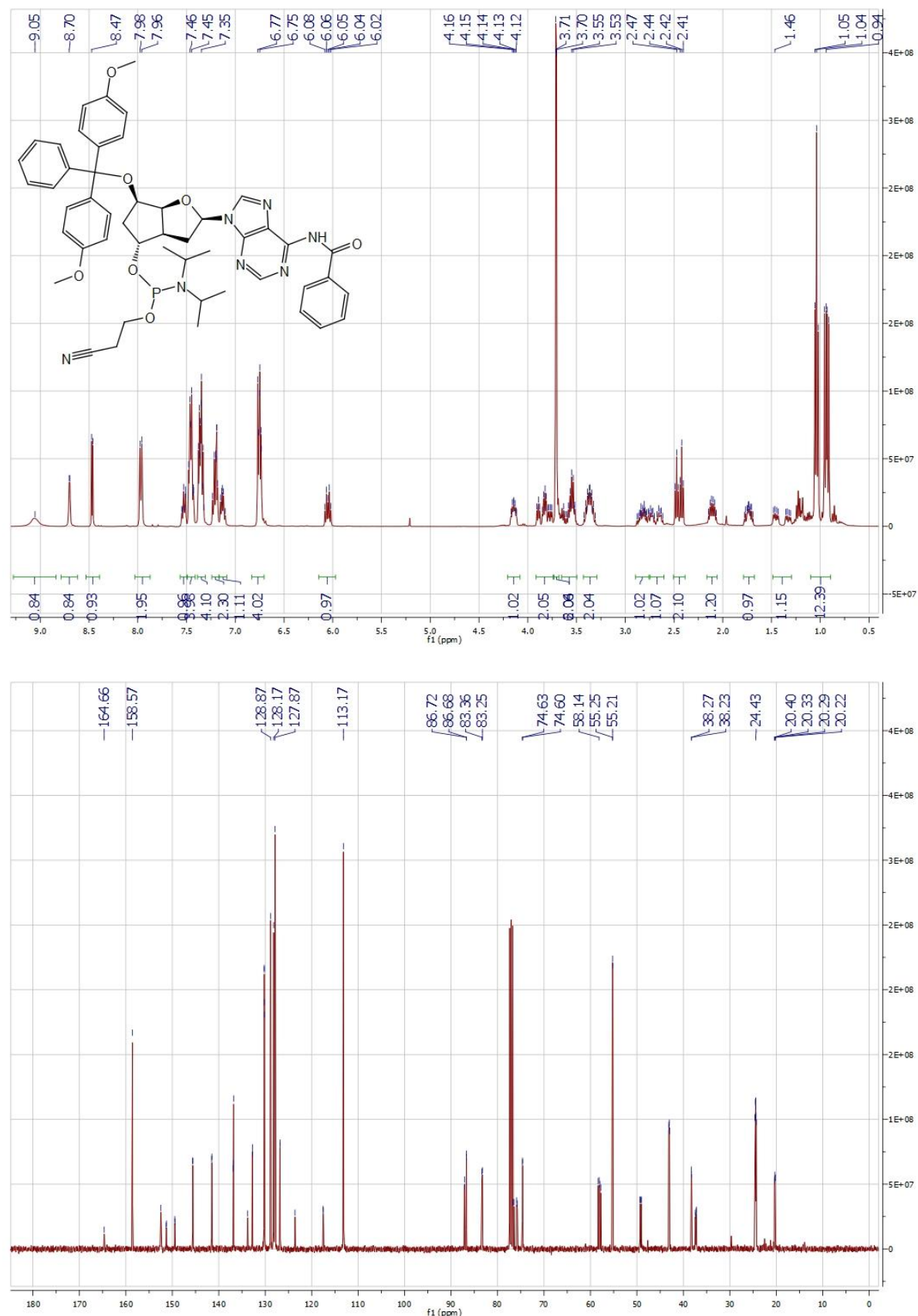
(3'R,5'R,7'R)-N6-Benzoyl-9-{7'-[tert-butyldiphenylsilyl]oxy}-2',3'-Dideoxy-3',5'-ethano-5'-O-[(4,4'-dimethoxytriphenyl)methyl]- β -D-ribofuranosyl adenine (17) :

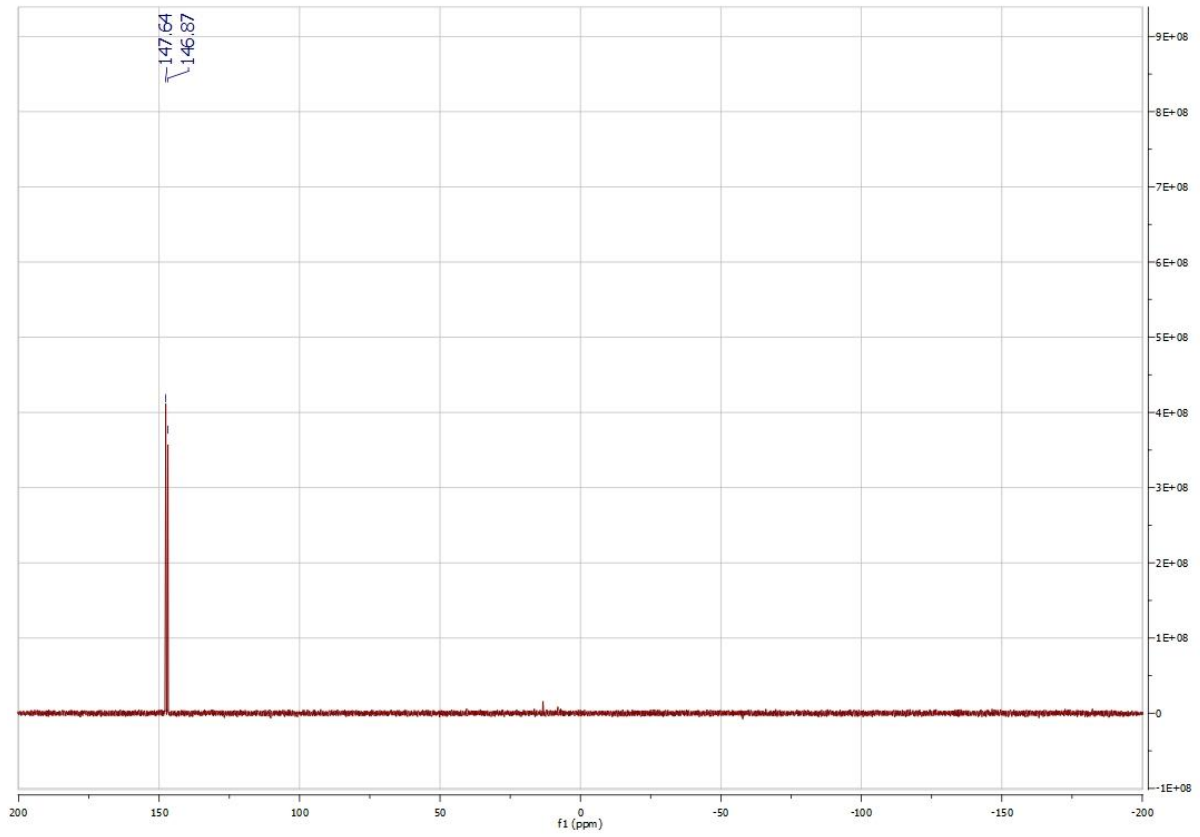


(3'S,5'R,7'R)-N6-Benzoyl-9-{2',3'-Dideoxy-3',5'-ethano-7'-hydroxy-5'-O-[(4,4'-dimethoxytriphenyl)methyl]-β-D-ribofuranosyl} adenine (18) :

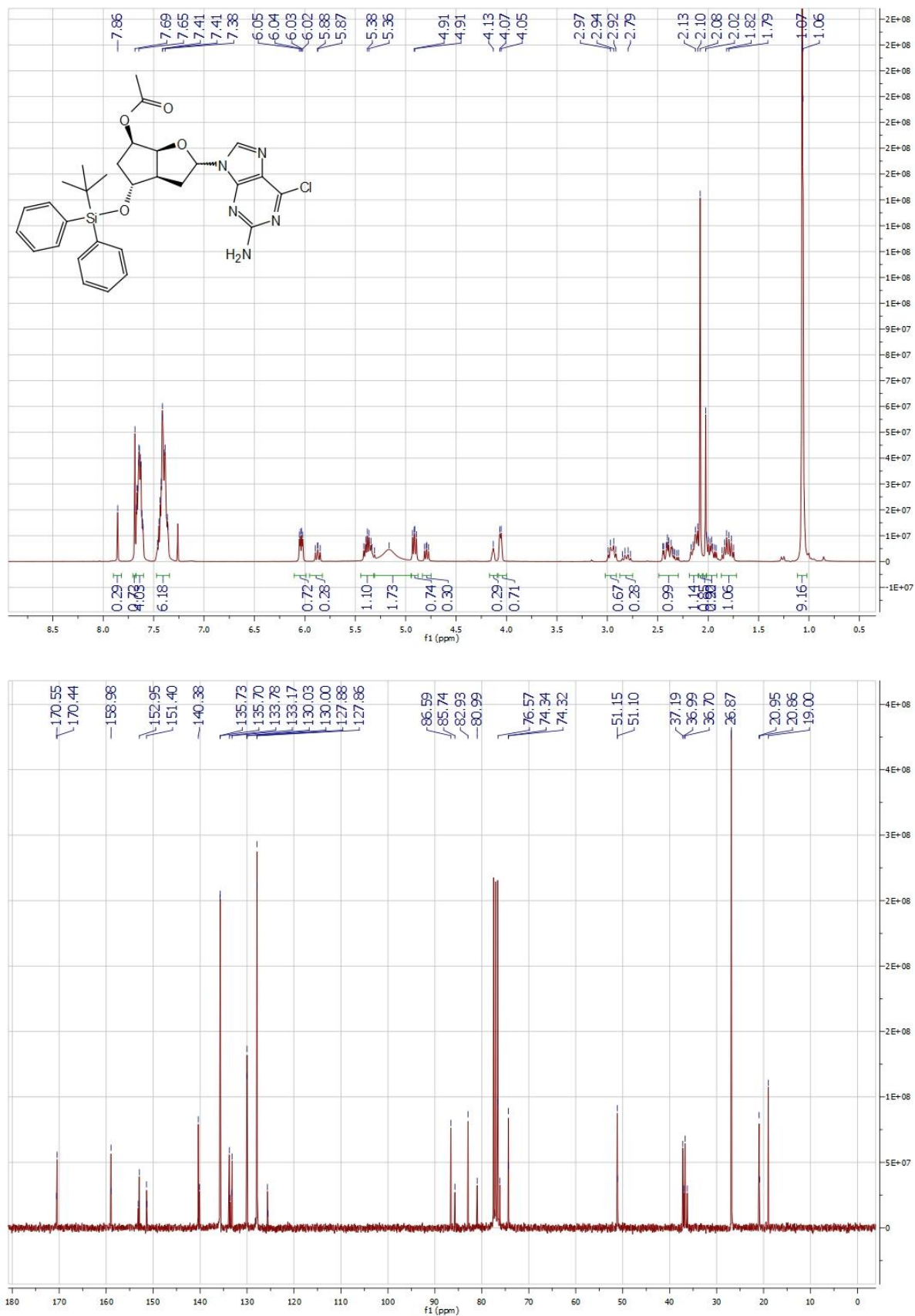


(3'R,5'R,7'R)-N6-Benzoyl-9-{7'-O-[2-cyanoethoxy)-diisopropylaminophosphanyl]-2',3'-Dideoxy-3',5'-ethano-5'-O-[(4,4'-dimethoxytriphenyl)methyl]- β -D-ribofuranosyl} adenine (19) :

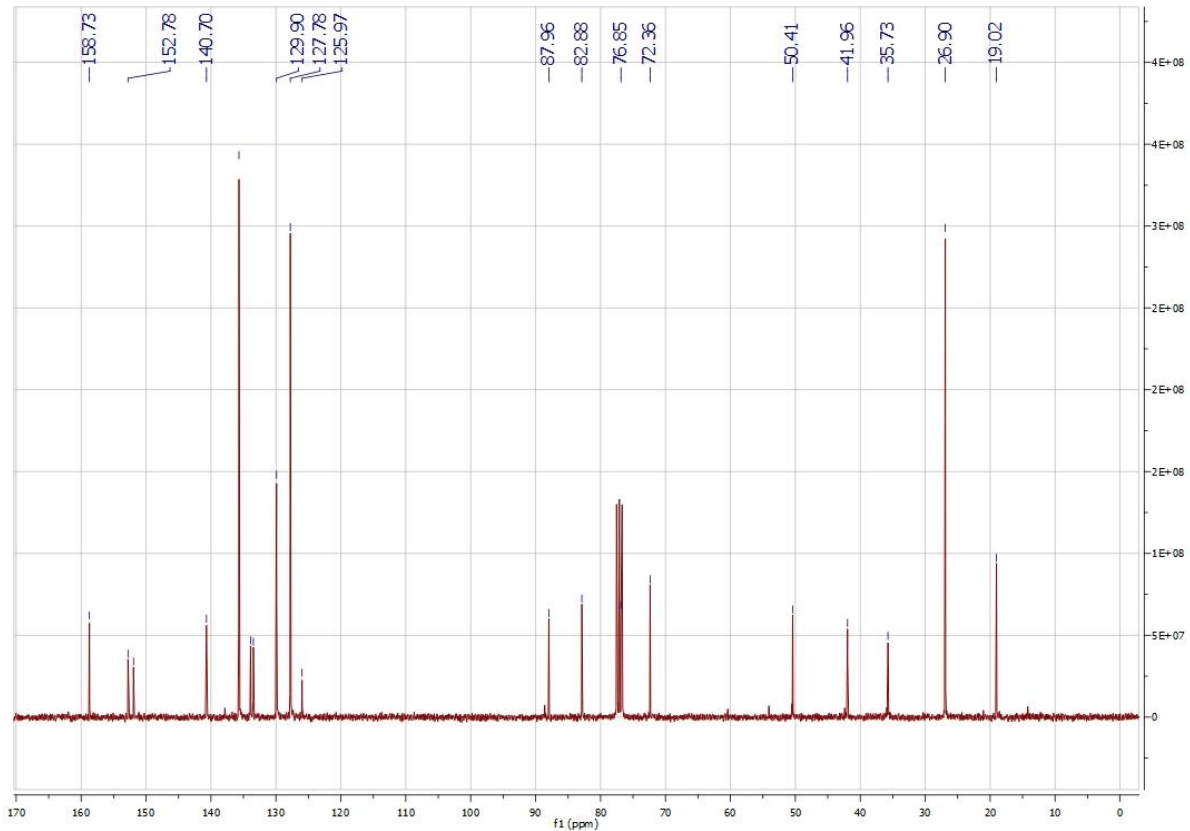
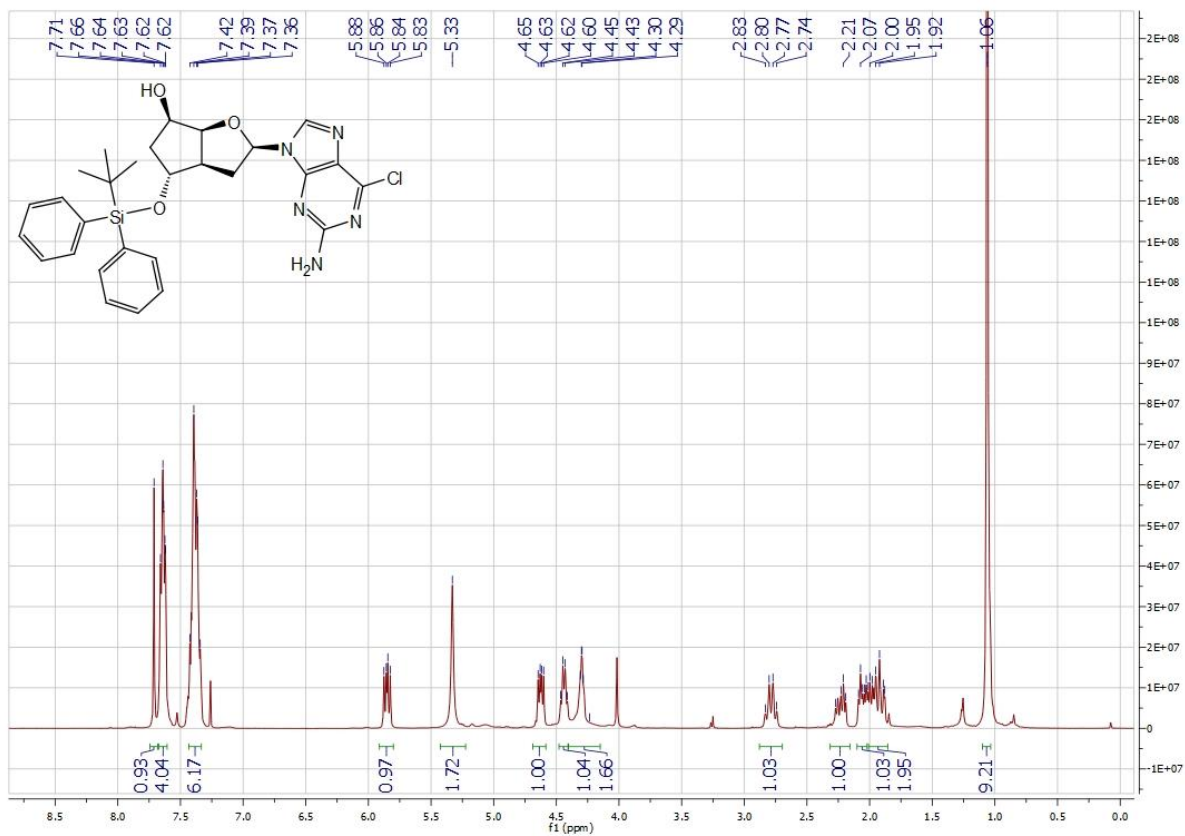




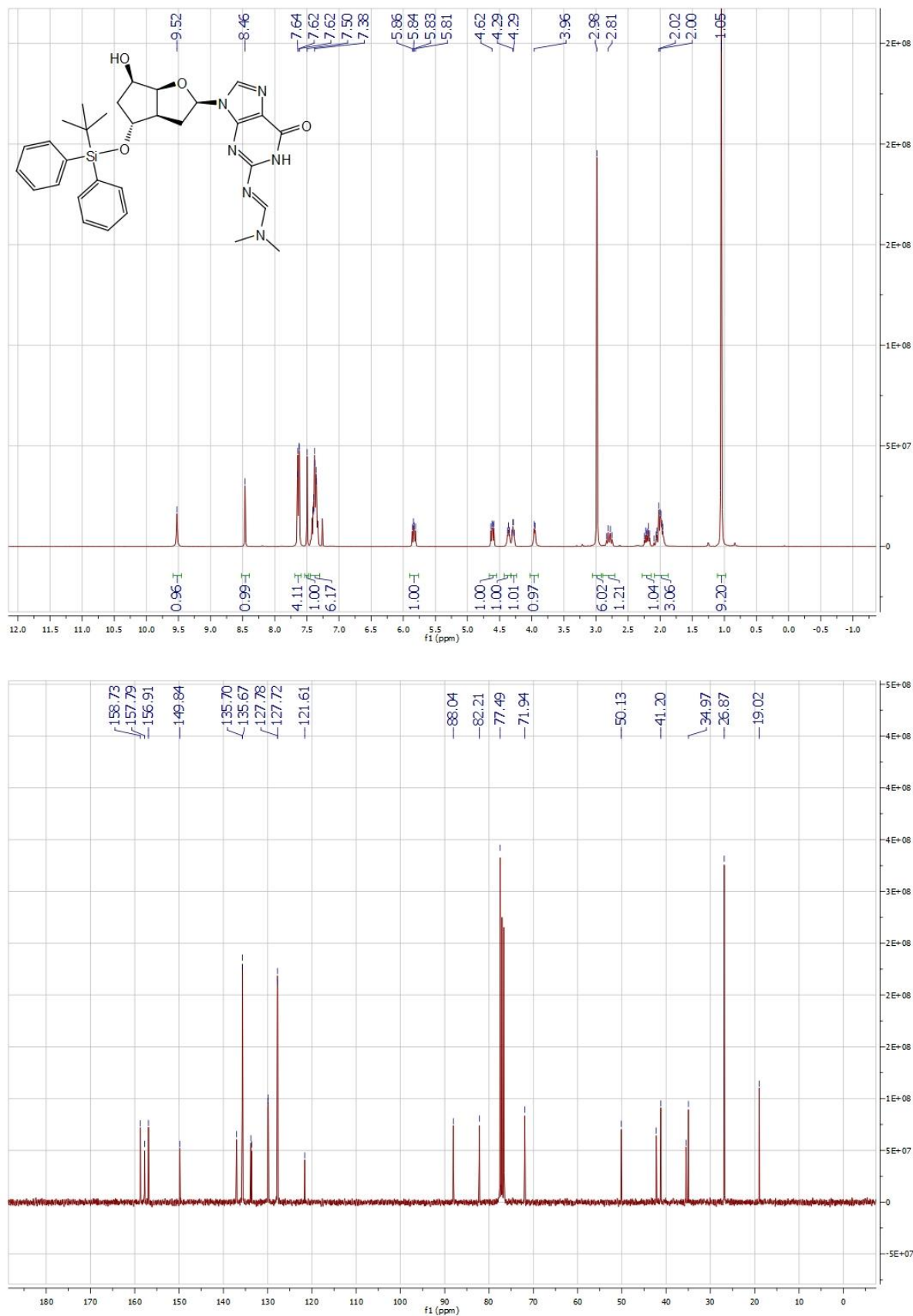
(3'R,5'R,7'R)-2-Amino-6-chloro-9-{5'-O-acetyl-7'-[*tert*-butyldiphenylsilyl]oxy}-2',3'-Dideoxy-3',5'-ethano- α,β -D-ribofuranosyl} purine (20) :



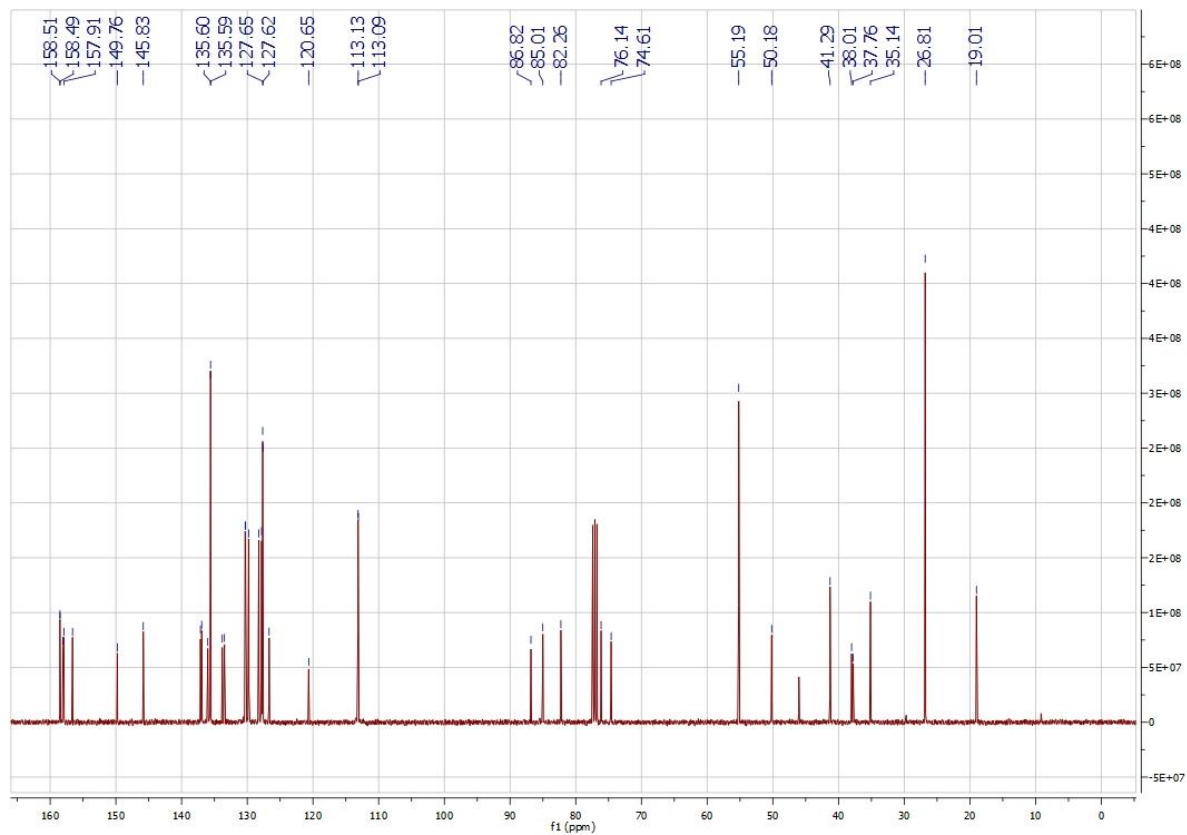
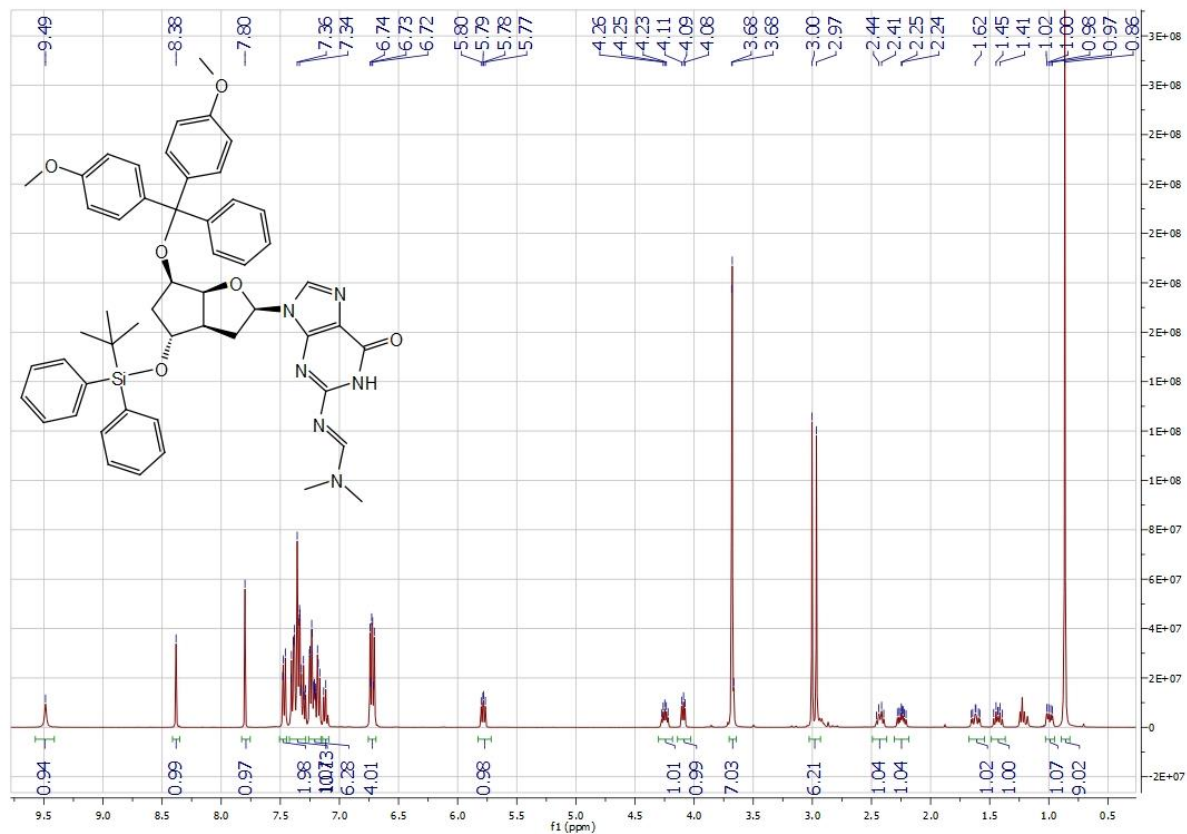
(3'R,5'R,7'R)- 2-Amino-6-chloro-9-{7'-[tert-butyldiphenylsilyl]oxy}-2',3'-Dideoxy-3',5'-ethano- β -D-ribofuranosyl purine (21) :



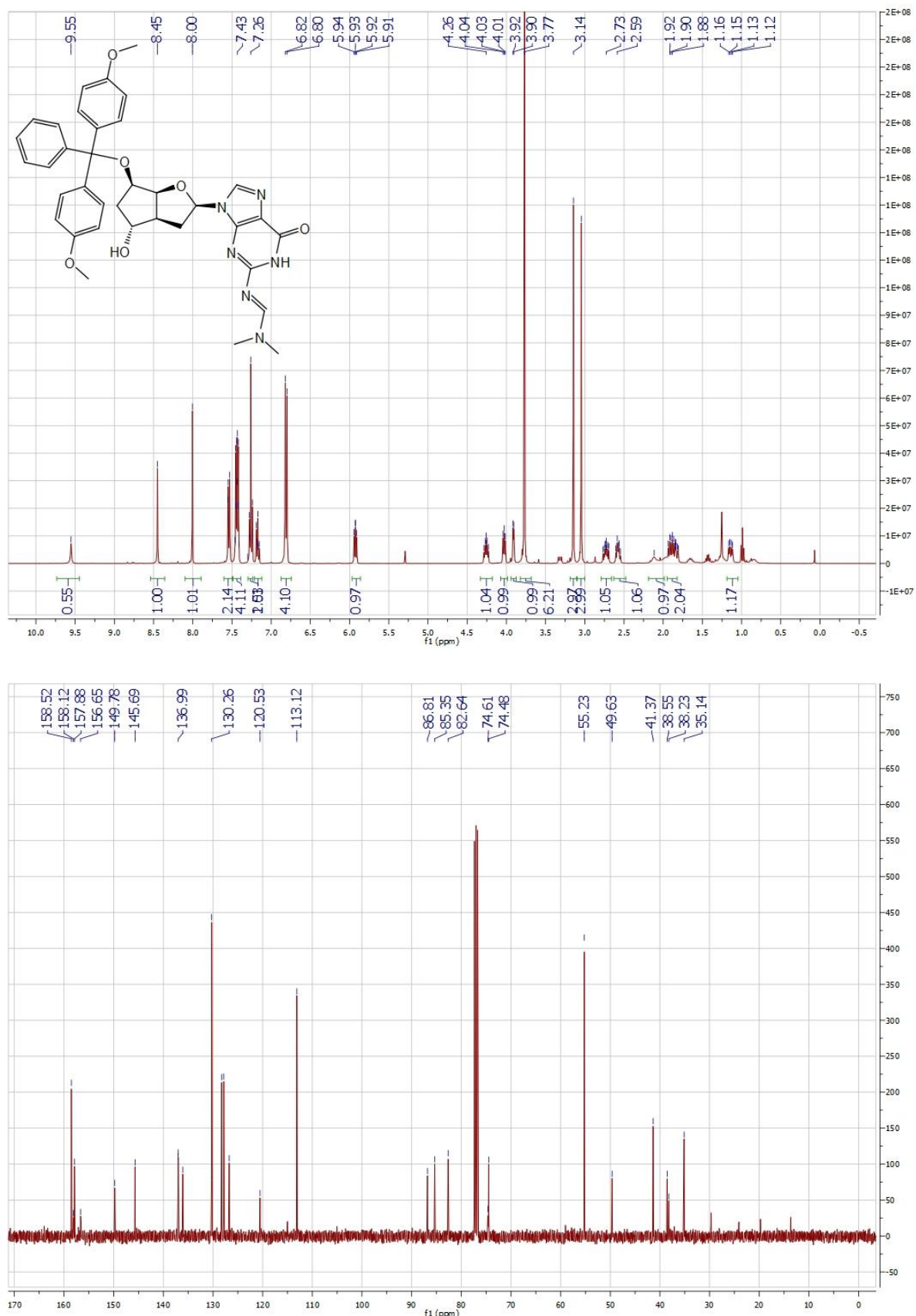
(3'R,5'R,7'R)-N2-(N,N-Dimethylformamidino)-9-{7'-[*tert*-butyldiphenylsilyl]oxy}-2',3'-Dideoxy-3',5'-ethano- β -D-ribofuranosyl guanine (22) :



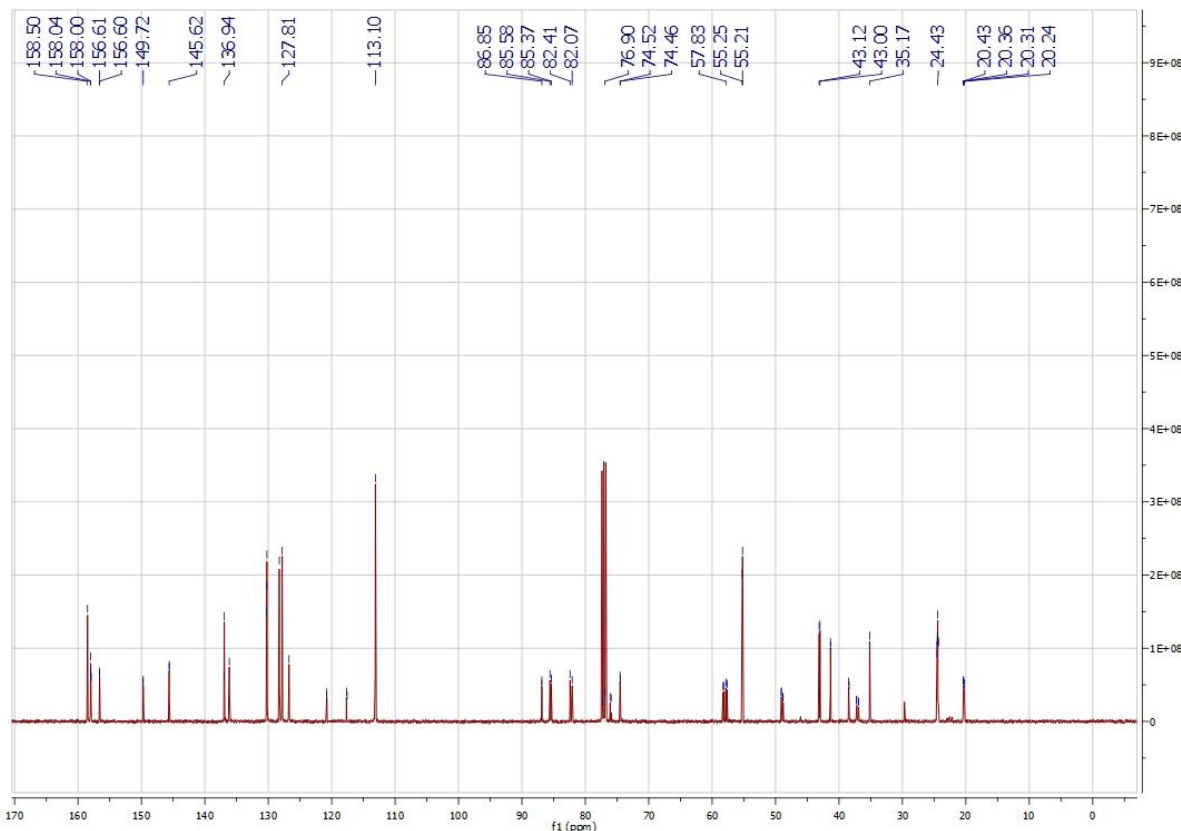
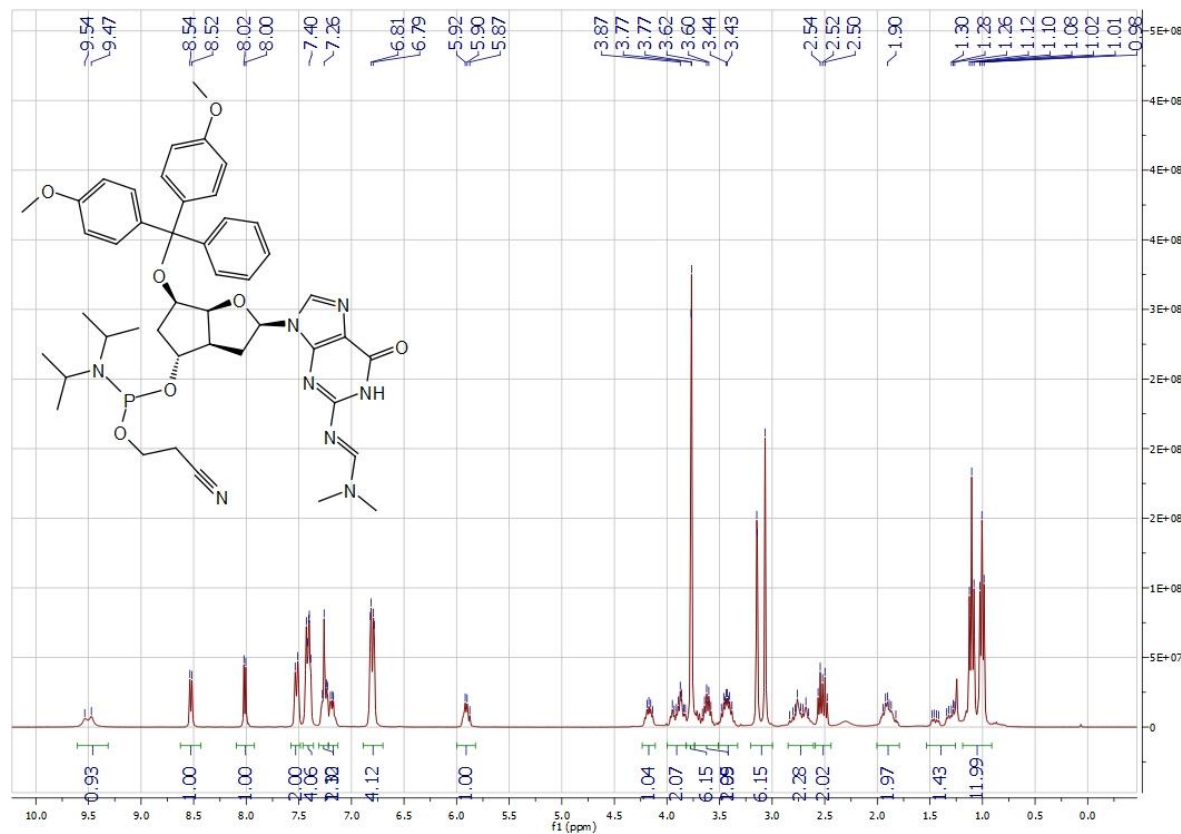
(3'R,5'R,7'R)-N2-(N,N-Dimethylformamidino)-9-{7'-[*tert*-butyldiphenylsilyl]oxy}-2',3'-Dideoxy-3',5'-ethano-5'-O-[(4,4'-dimethoxytriphenyl)methyl]- β -D-ribofuranosyl guanine (23) :



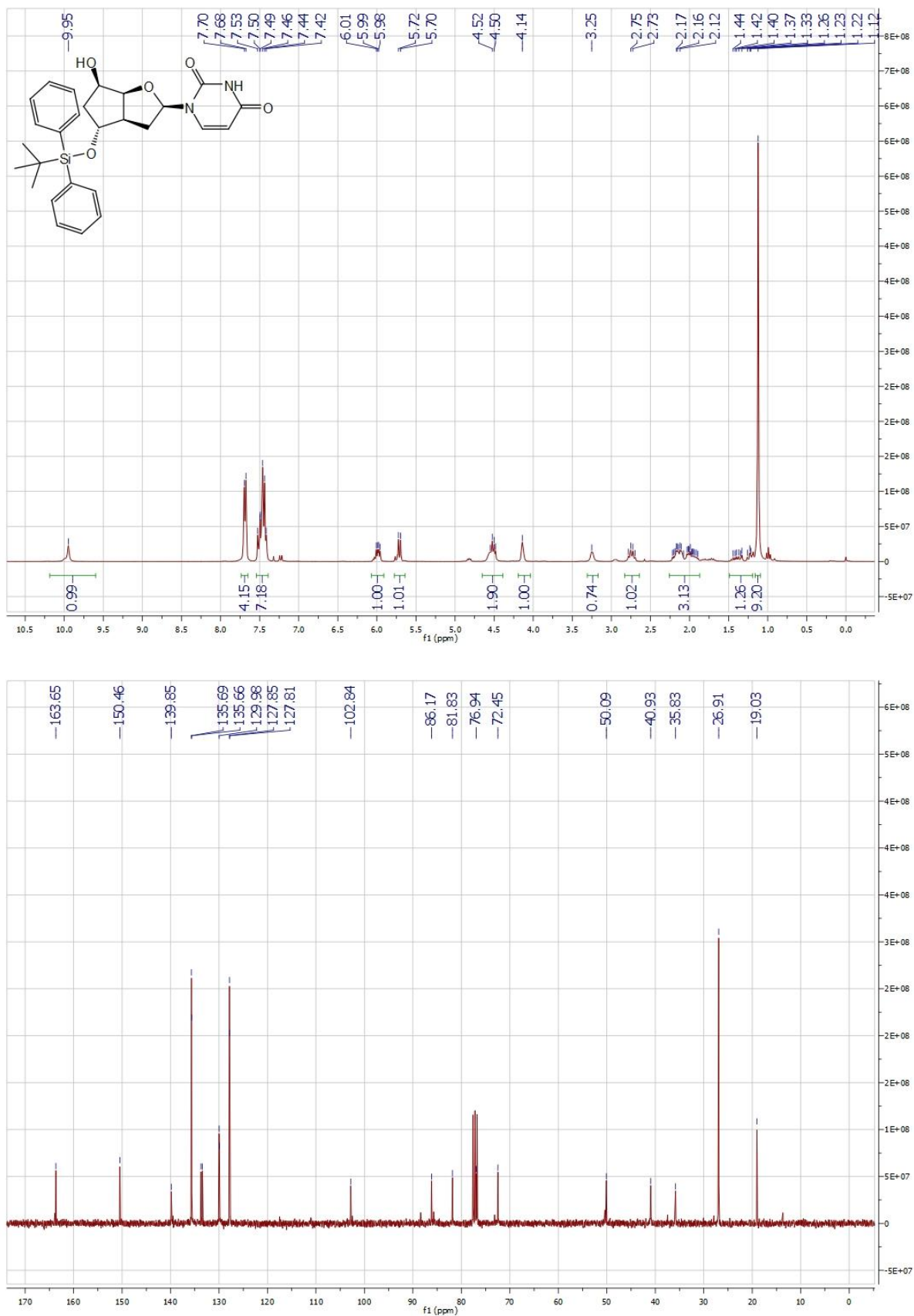
(3'S,5'R,7'R)-N2-(N,N-Dimethylformamidino)-9-{2',3'-Dideoxy-3',5'-ethano-7'-hydroxy-5'-O-[(4,4'-dimethoxytriphenyl)methyl]- β -D-ribofuranosyl} guanine (24) :



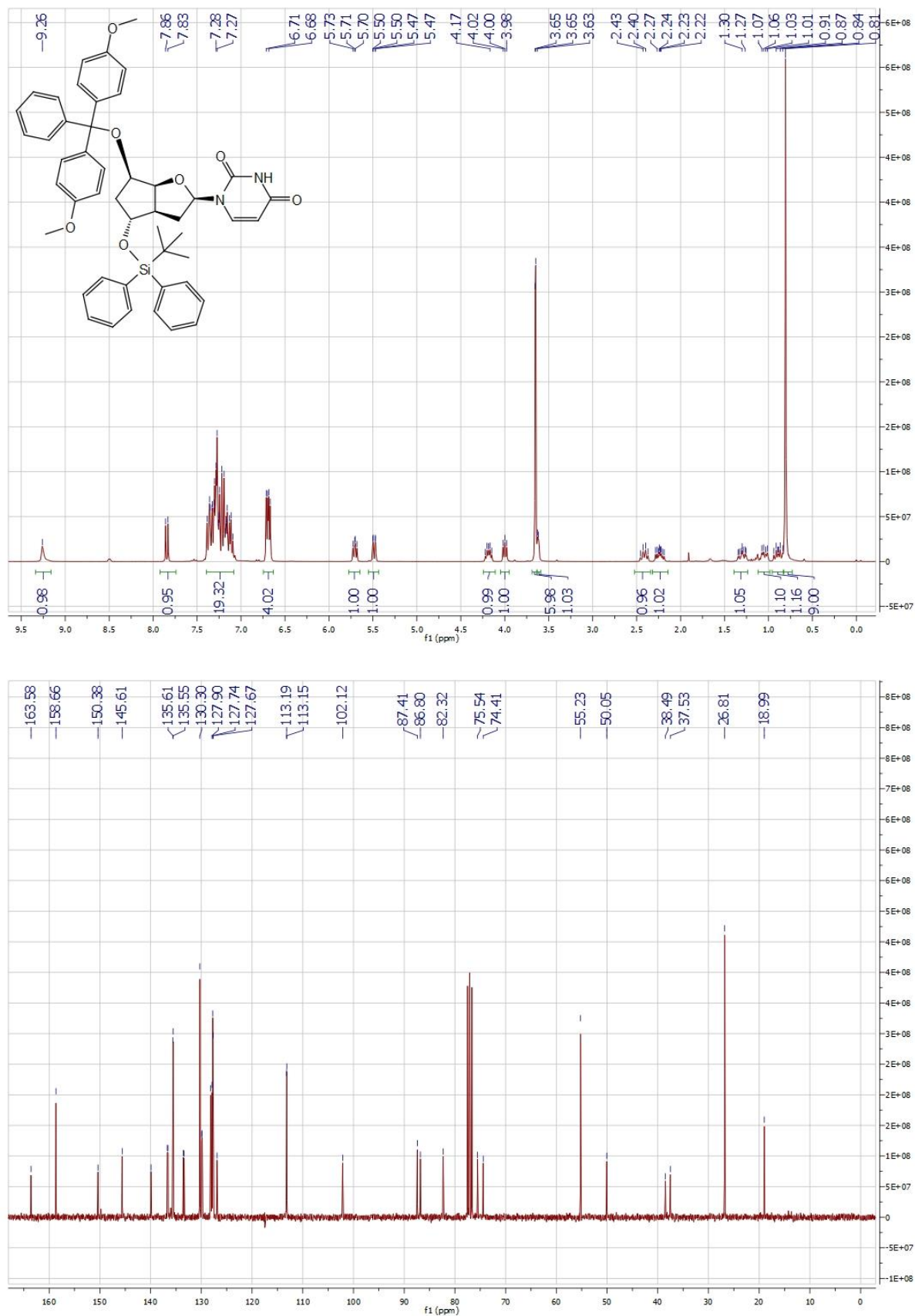
(3'R,5'R,7'R)-N2-(N,N-Dimethylformamidino)-9-{7'-O-[(2-cyanoethoxy)-diisopropylaminophosphanyl]-2',3'-Dideoxy-3',5'-ethano-5'-O-[(4,4'-dimethoxytriphenyl)methyl]-β-D-ribofuranosyl} guanine (25) :



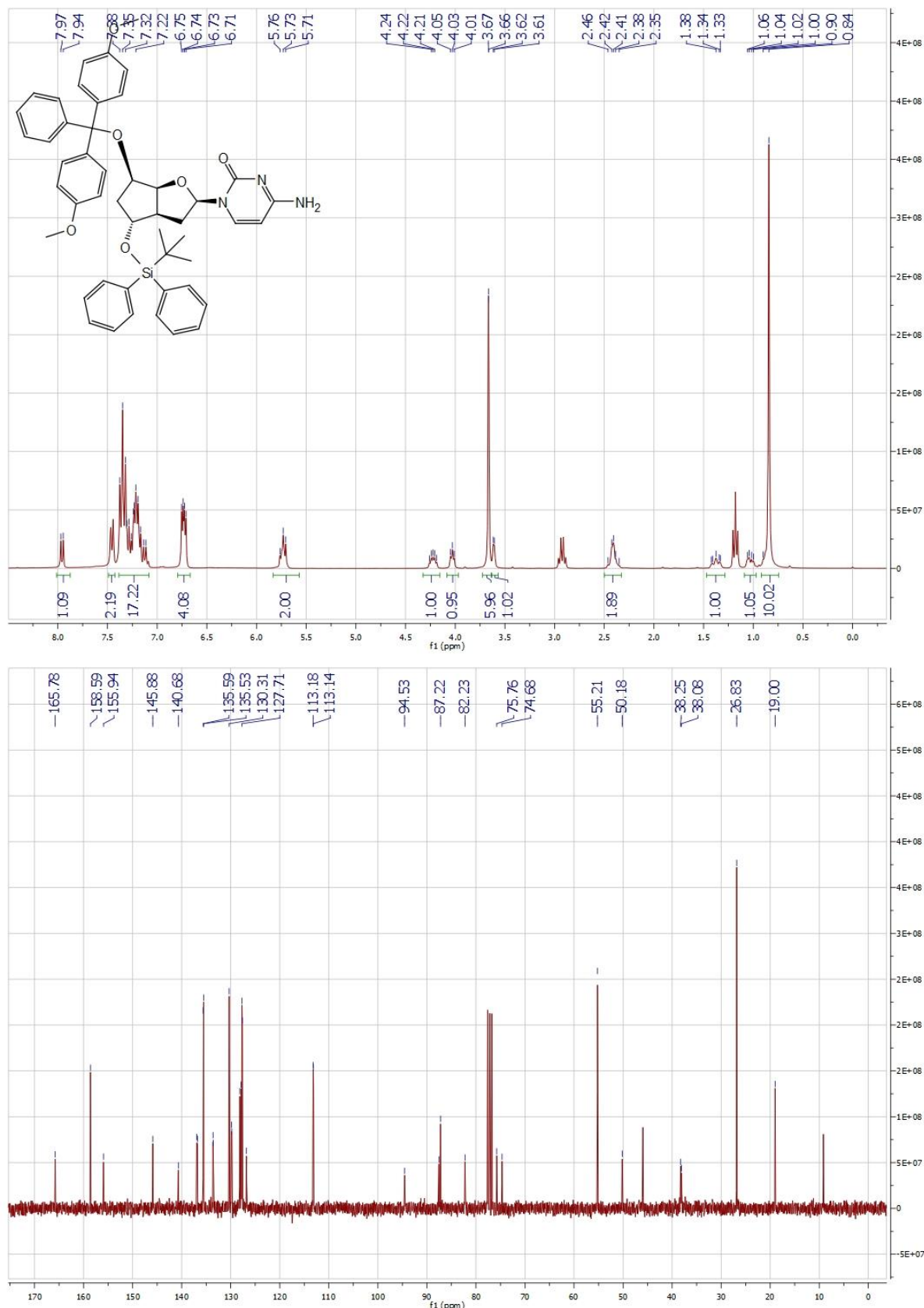
(3'S,5'R,7'R)-1-{7'-[*tert*-butyldiphenylsilyl]oxy}-2',3'-Dideoxy-3',5'-ethano- β -D-ribofuranosyl uracil (26) :



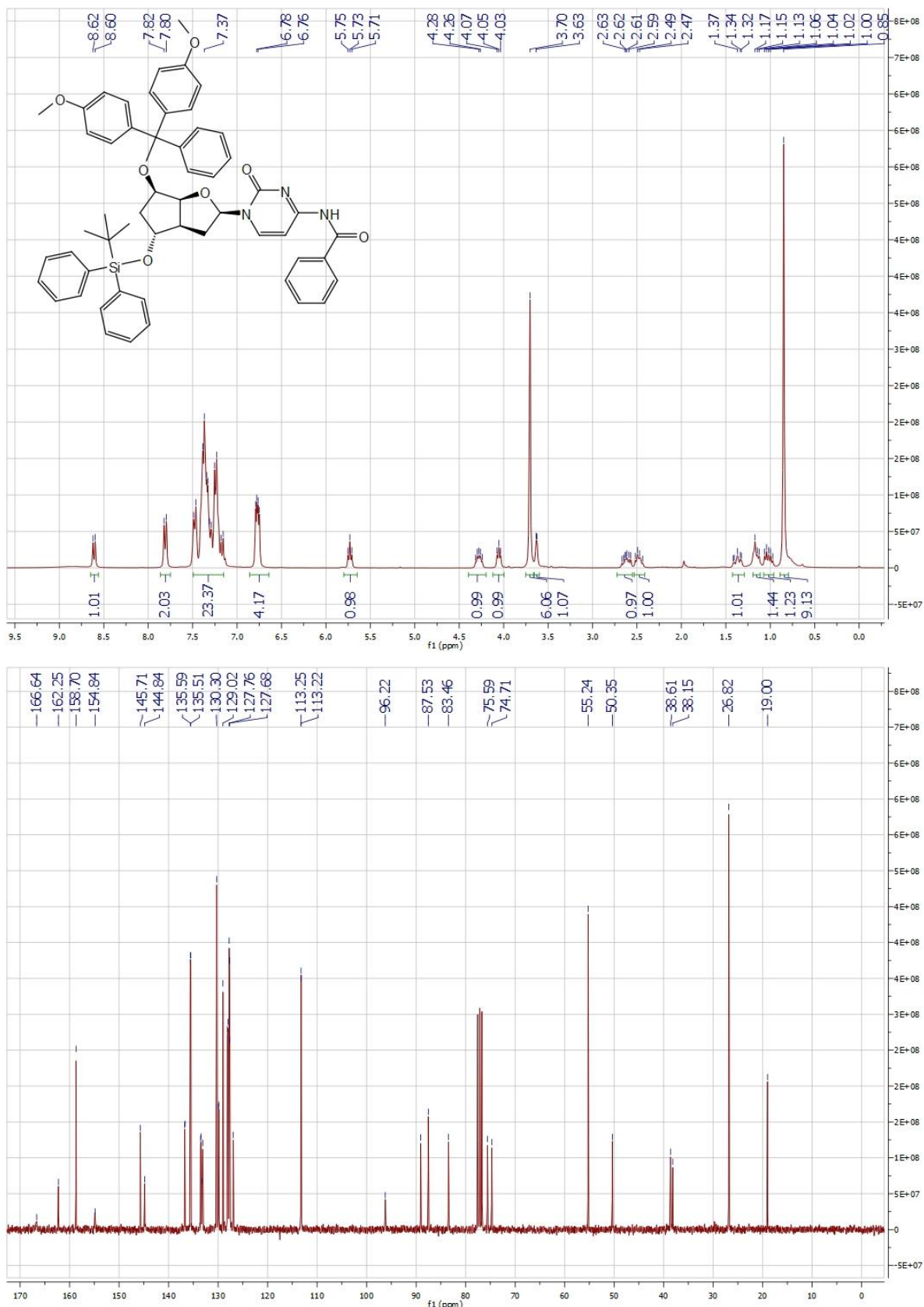
(3'S,5'R,7'R)-1-{7'-[*tert*-butyldiphenylsilyl]oxy}-2',3'-Dideoxy-3',5'-ethano-5'-O-[(4,4'-dimethoxytriphenyl)methyl]- β -D-ribofuranosyl uracil (27) :



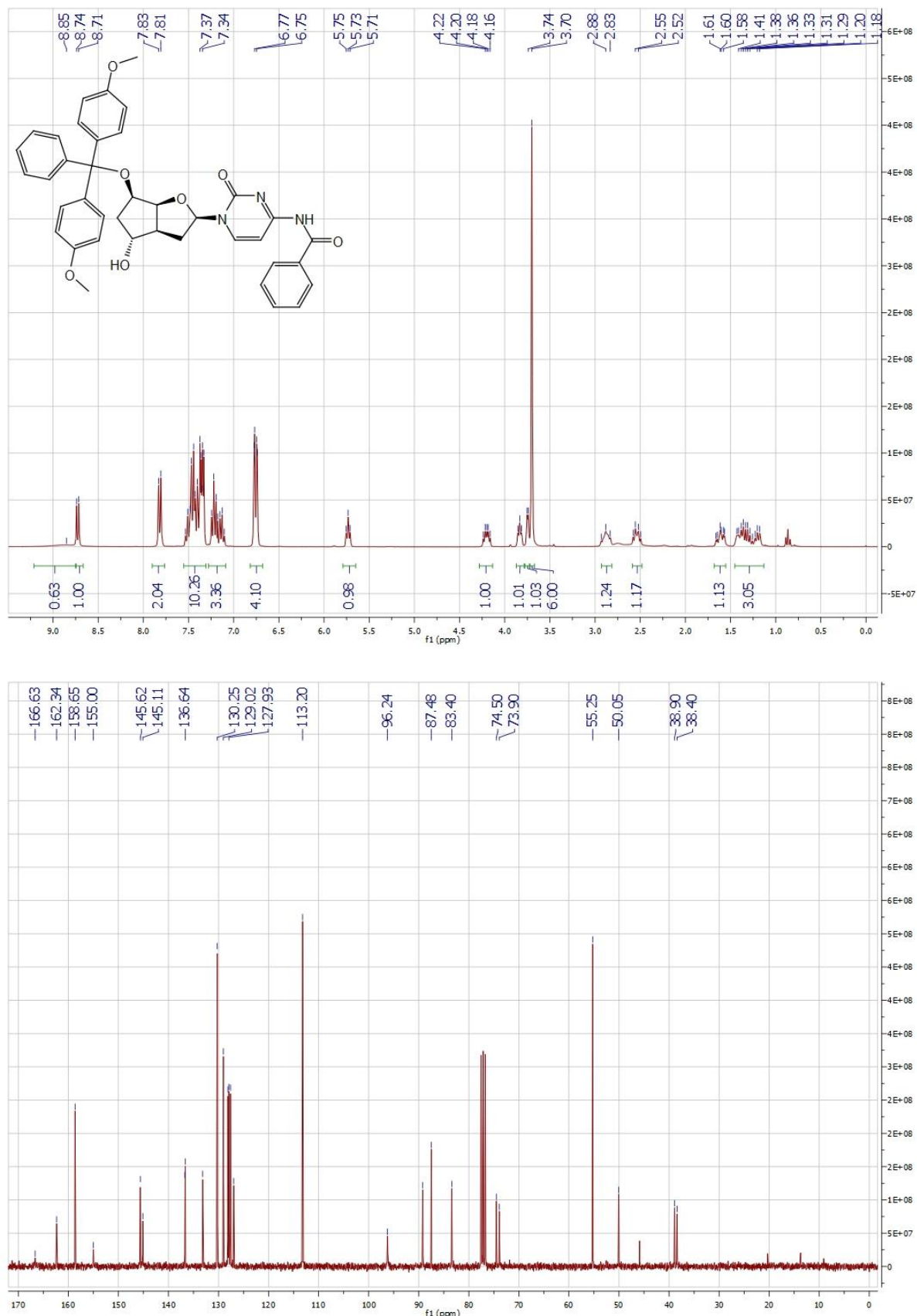
(3'S,5'R,7'R)-1-{7'-[*tert*-butyldiphenylsilyl]oxy}-2',3'-Dideoxy-3',5'-ethano-5'-O-[(4,4'-dimethoxytriphenyl)methyl]- β -D-ribofuranosyl cytosine (28) :



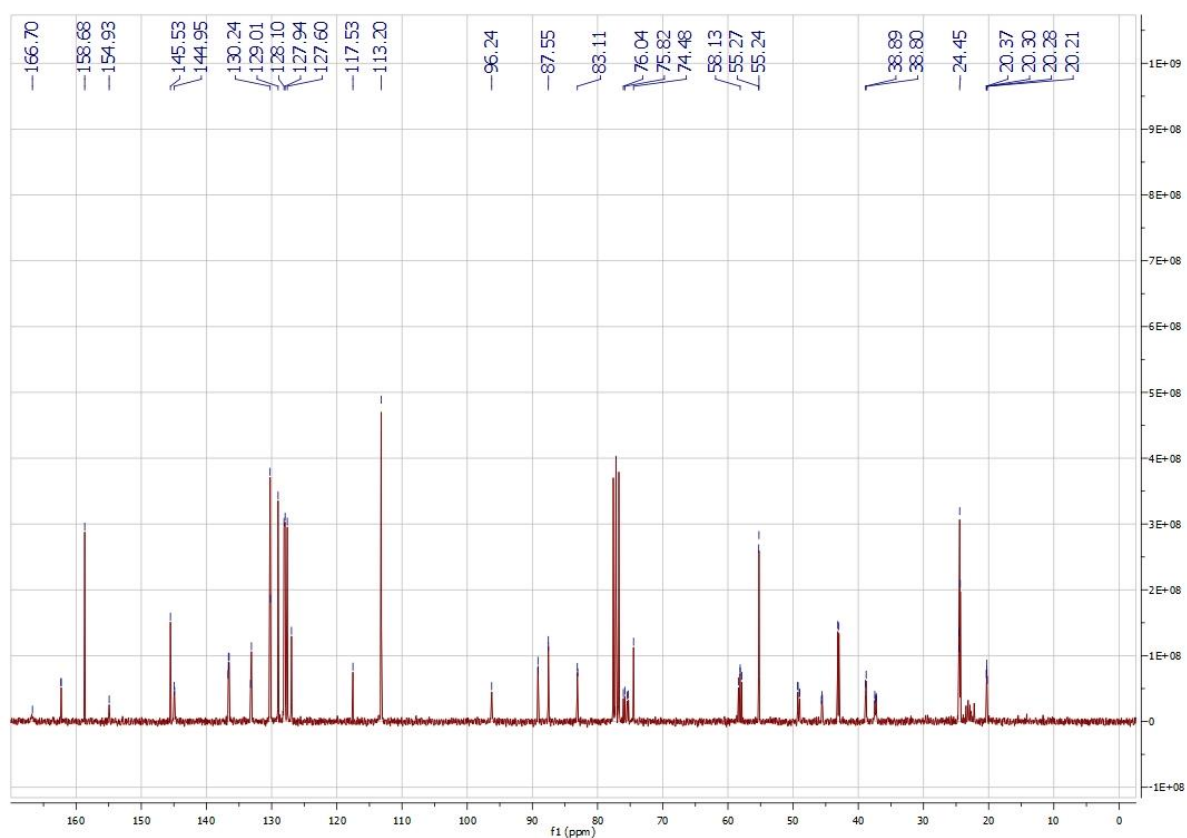
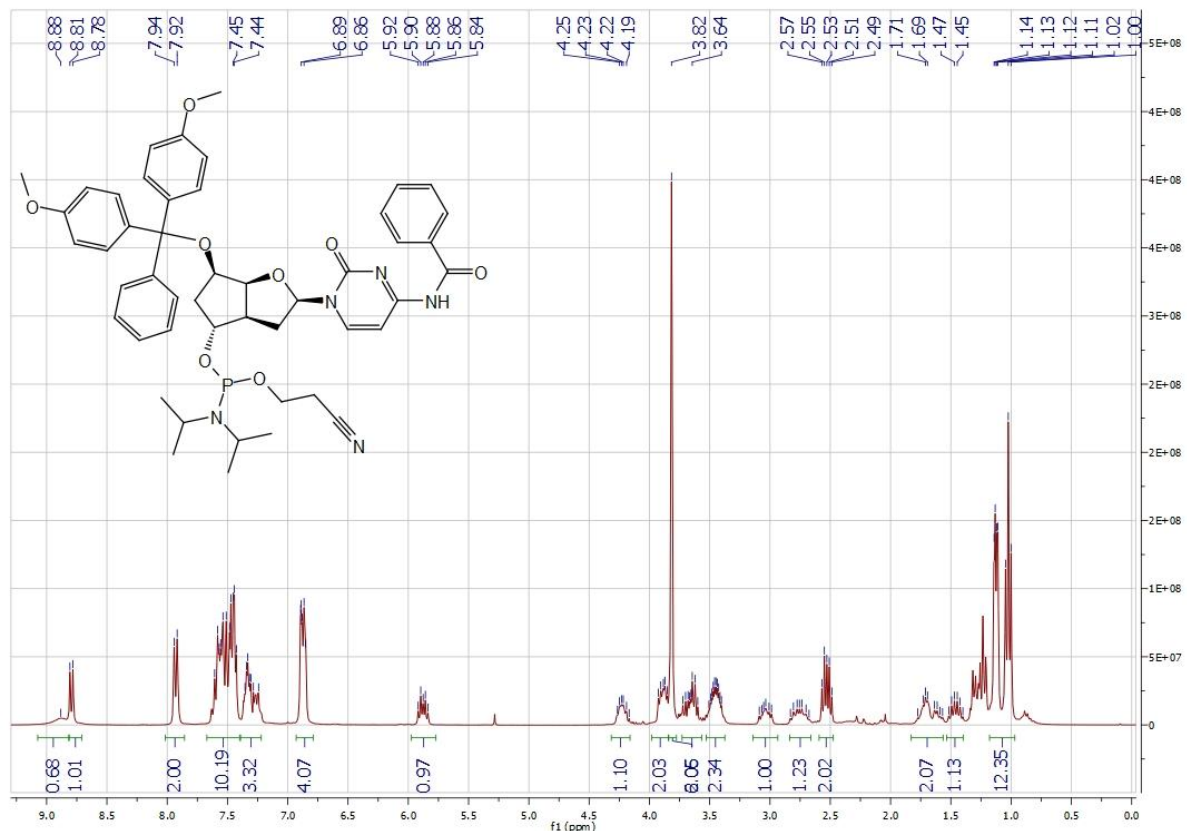
(3'S,5'R,7'R)- N4-Benzoyl-1-{7'-[tert-butylidiphenylsilyl]oxy}-2',3'-Dideoxy-3',5'-ethano-5'-O-[(4,4'-dimethoxytriphenyl)methyl]- β -D-ribofuranosyl} cytosine (29) :

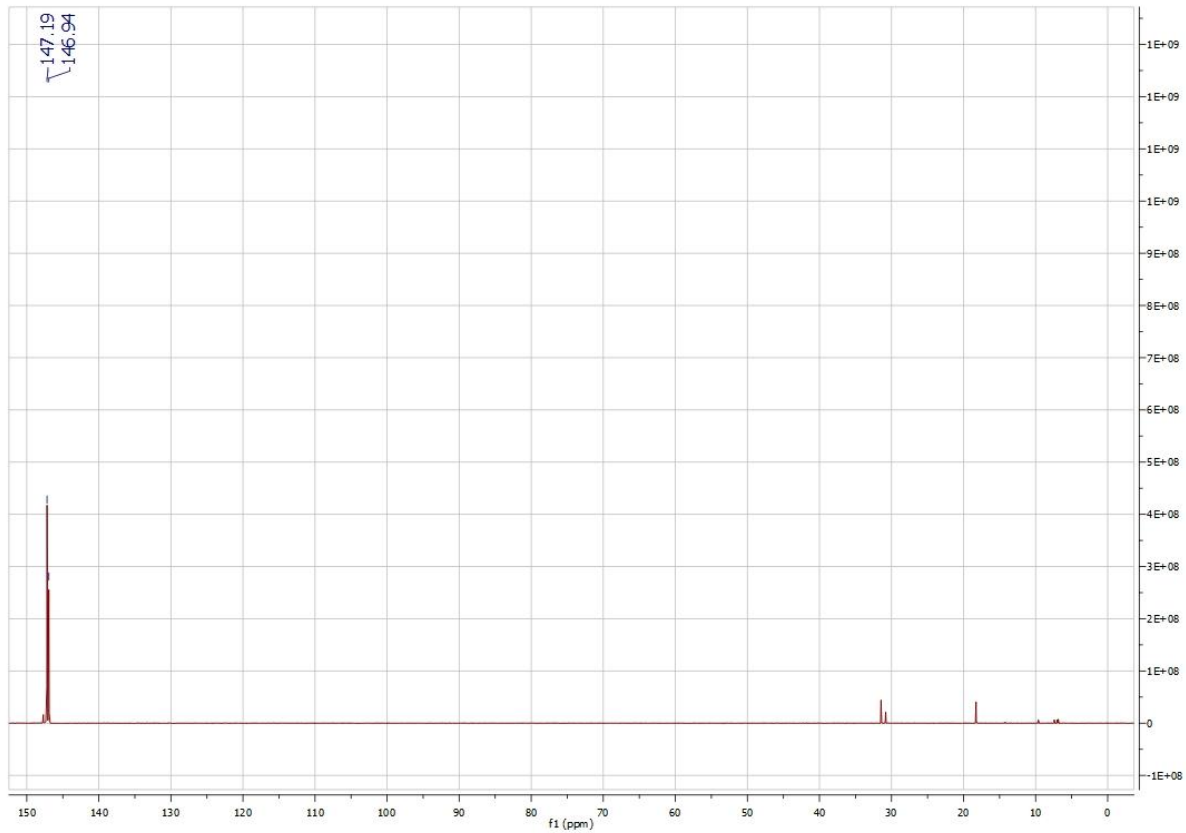


(3'S,5'R,7'R)- N4-Benzoyl-1-{2',3'-Dideoxy-3',5'-ethano-7'-hydroxy-5'-O-[*(4,4'*-dimethoxytriphenyl)methyl]- β -D-ribofuranosyl} cytosine (30) :

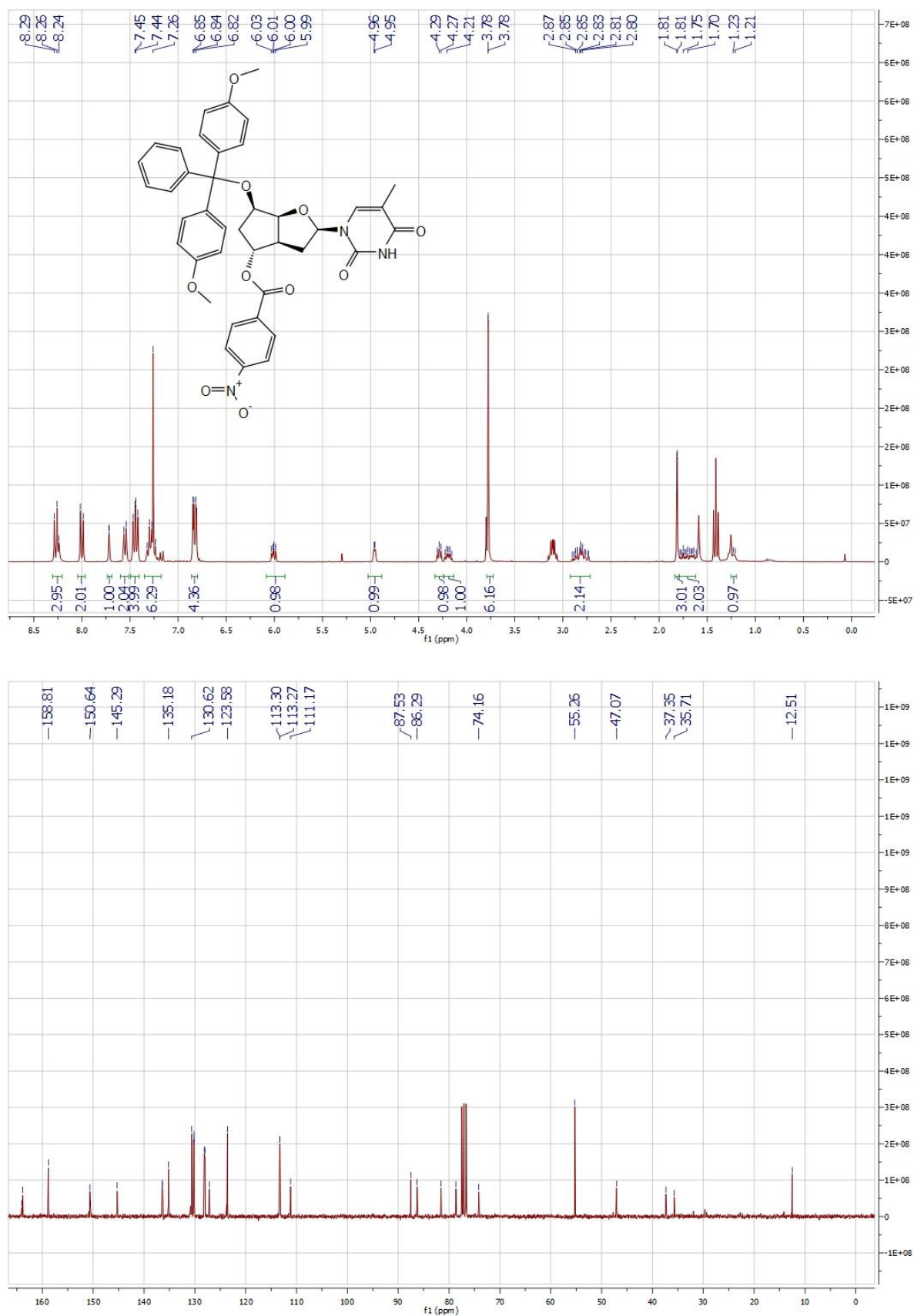


(3'S,5'R,7'R)- N4-Benzoyl-1-{7'-O-[(2-cyanoethoxy)-diisopropylaminophosphanyl]-2',3'-Dideoxy-3',5'-ethano-5'-O-[(4,4'-dimethoxytriphenyl)methyl]- β -D-ribofuranosyl} cytosine (3I) :

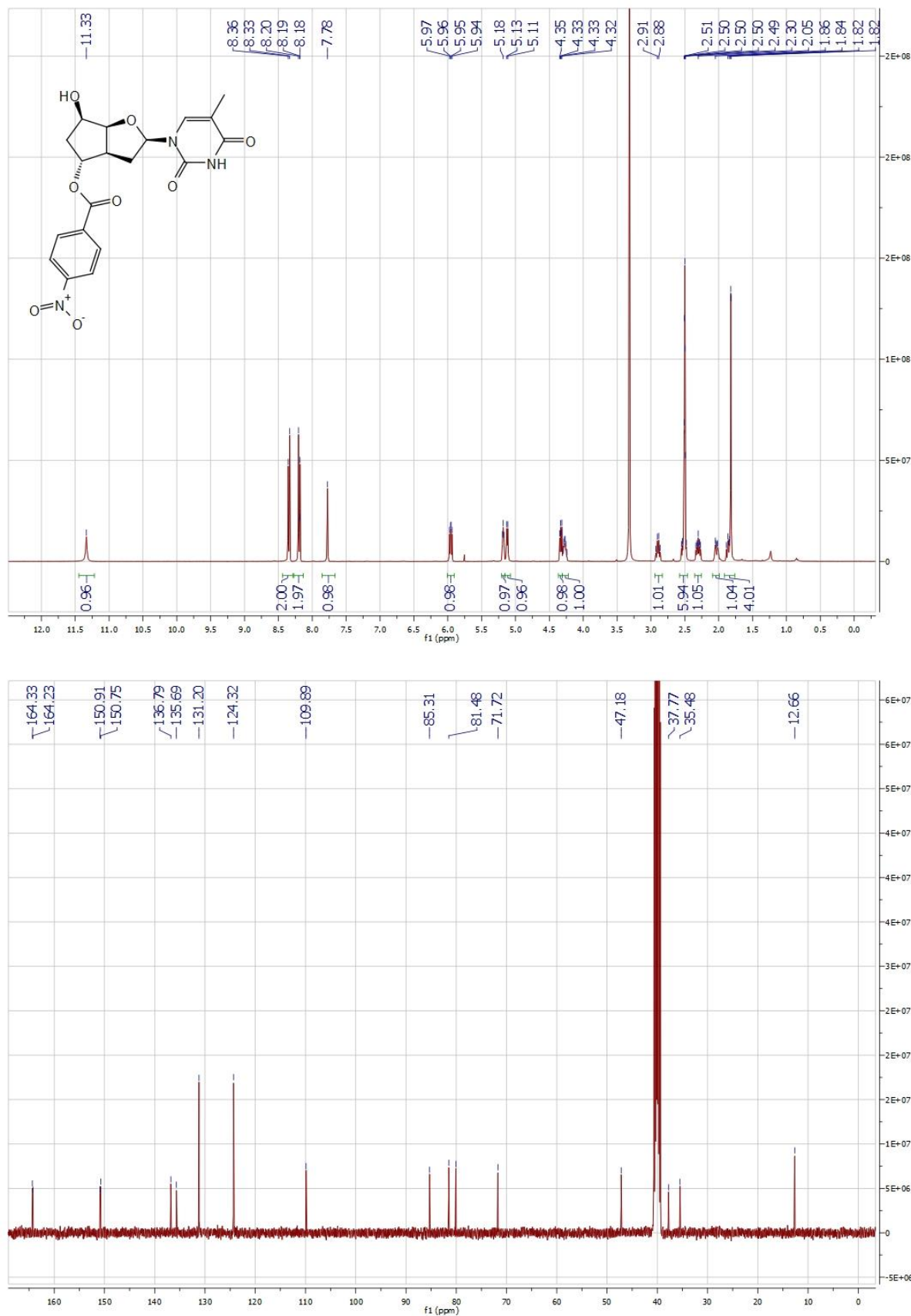




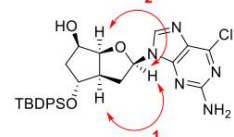
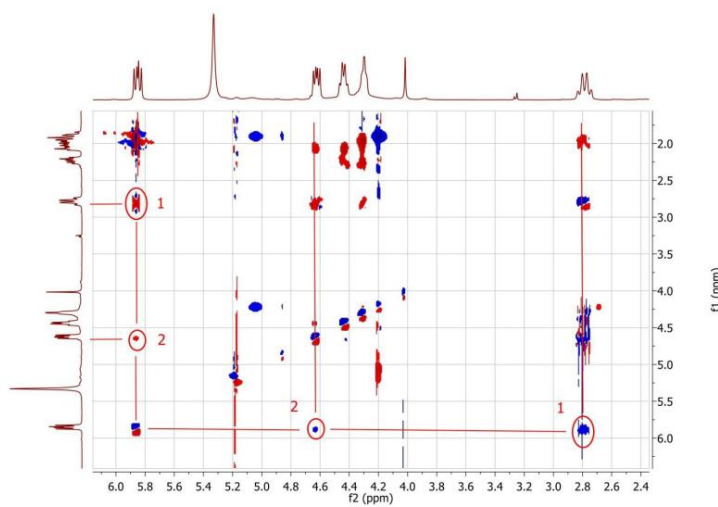
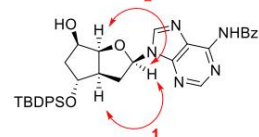
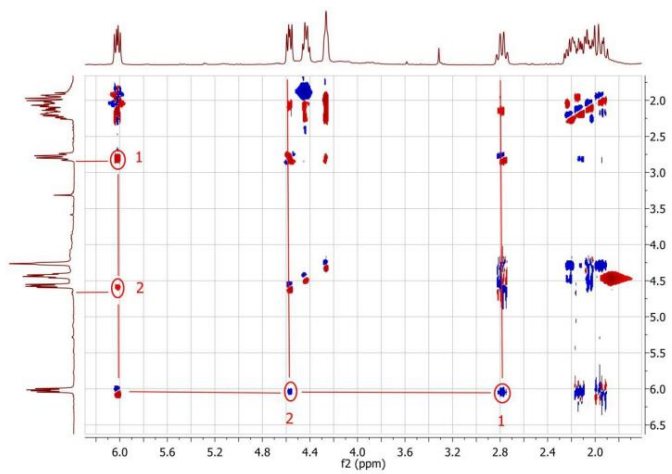
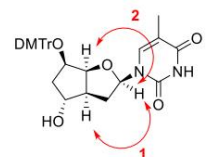
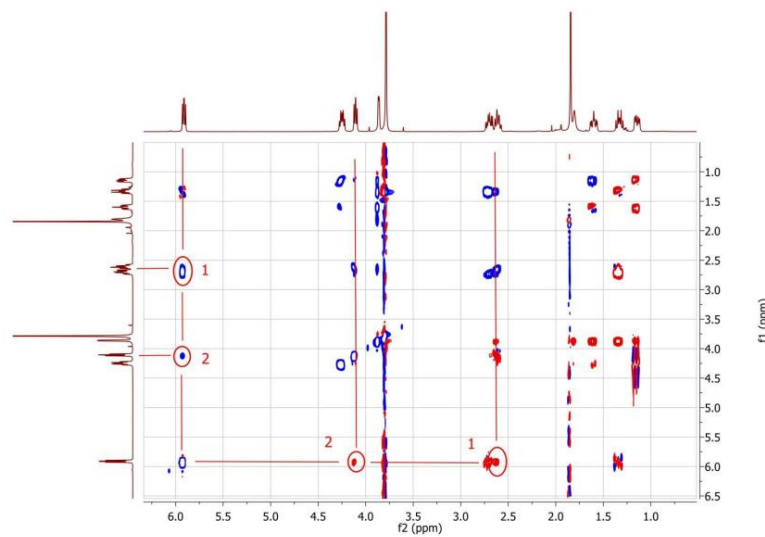
(3'S,5'R,7'R)-1-{2',3'-Dideoxy-3',5'-ethano-7'-O-(4-nitrobenzoate)-5'-O-[(4,4'-dimethoxytriphenyl)methyl]- β -D-ribofuranosyl} thymine (32) :



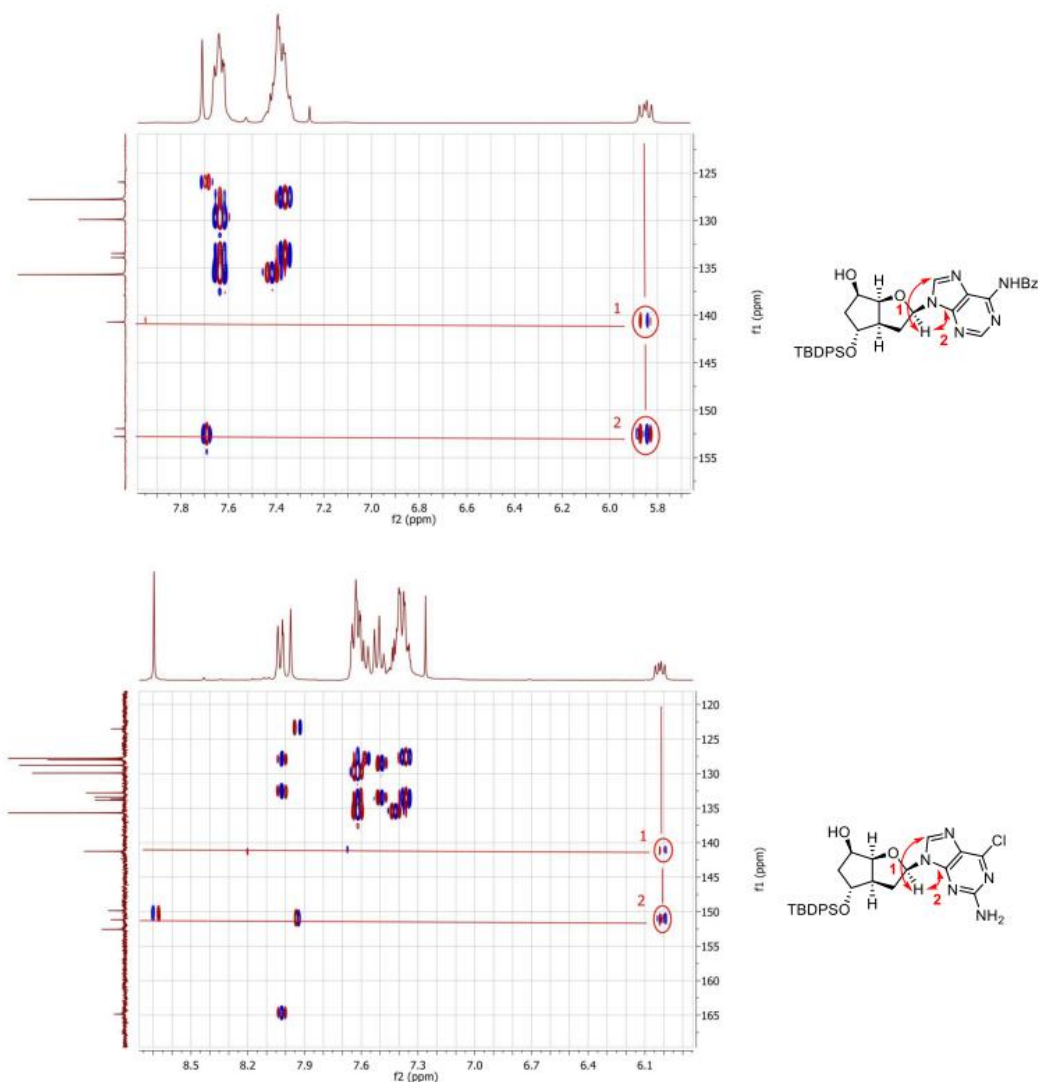
((3'S,5'R,7'R)-1-{2',3'-Dideoxy-3',5'-ethano-7'-O-(4-nitrobenzoate)- β -D-ribofuranosyl} thymine (33):



8. NOESY spectra



9. HMBC spectra



10. Crystal-Structure Determination.

A colorless transparent crystal of $[C_{19}H_{19}N_3O_8]$ (**33**) was mounted in air and used for X-ray structure determination at ambient conditions. All measurements were made on a *Oxford Diffraction SuperNova* area-detector diffractometer¹ using mirror optics monochromated Mo $K\alpha$ radiation ($\lambda = 0.71073 \text{ \AA}$) and Al filtered.² The unit cell constants and an orientation matrix for data collection were obtained from a least-squares refinement of the setting angles of reflections in the range $2.^{\circ} < \theta < 27.^{\circ}$. A total of 530 frames were collected using ω scans, with $2.5+2.5$ seconds exposure time, a rotation angle of 1° per frame, a crystal-detector distance of 65.1 mm, at $T = 173(2)$ K.

Data reduction was performed using the *CrysAlisPro*² program. The intensities were corrected for Lorentz and polarization effects, and an absorption correction based on the multi-scan method using SCALE3 ABSPACK in *CrysAlisPro*² was applied. Data collection and refinement parameters are given in *Table S3*.

The structure was solved by direct methods using *SHELXS-97*³, which revealed the positions of all non-hydrogen atoms of the title compound. The non-hydrogen atoms were refined anisotropically. All H-atoms were placed in geometrically calculated positions and refined using a riding model where each H-atom was assigned a fixed isotropic displacement parameter with a value equal to 1.2 Ueq of its parent atom.

Refinement of the structure was carried out on F^2 using full-matrix least-squares procedures, which minimized the function $\Sigma w(F_o^2 - F_c^2)^2$. The weighting scheme was based on counting statistics and included a factor to downweight the intense reflections. All calculations were performed using the *SHELXL-97*³ program.

Table S4. Crystal data and structure refinement for **33**.

Identification code	shelx	
Empirical formula	C19 H19 N3 O8	
Formula weight	417.37	
Temperature	173(2) K	
Wavelength	0.71073 Å	
Crystal system	Monoclinic	
Space group	P 21	
Unit cell dimensions	a = 7.0712(2) Å	α= 90°.
	b = 6.48123(16) Å	β= 98.062(3)°.
	c = 20.4085(6) Å	γ = 90°.
Volume	926.08(4) Å ³	
Z	2	
Density (calculated)	1.497 Mg/m ³	
Absorption coefficient	0.119 mm ⁻¹	
F(000)	436	
Crystal size	0.5326 x 0.308 x 0.1151 mm ³	
Theta range for data collection	2.016 to 27.110°.	
Index ranges	-8<=h<=8, -7<=k<=8, -24<=l<=24	
Reflections collected	6928	
Independent reflections	3651 [R(int) = 0.0200]	
Completeness to theta = 25.000°	99.8 %	
Absorption correction	Gaussian	
Max. and min. transmission	0.987 and 0.963	
Refinement method	Full-matrix least-squares on F^2	
Data / restraints / parameters	3651 / 1 / 274	
Goodness-of-fit on F^2	1.059	
Final R indices [I>2sigma(I)]	R1 = 0.0344, wR2 = 0.0772	

R indices (all data)	R1 = 0.0387, wR2 = 0.0808
Absolute structure parameter	-0.9(5)
Extinction coefficient	0.009(2)
Largest diff. peak and hole	0.212 and -0.236 e. \AA^{-3}

Table S5. Atomic coordinates ($\times 10^4$) and equivalent isotropic displacement parameters ($\text{\AA}^2 \times 10^3$) for **33**. U(eq) is defined as one third of the trace of the orthogonalized U^{ij} tensor.

	x	y	z	U(eq)
C(1)	299(3)	9337(4)	5451(1)	23(1)
C(2)	-691(3)	9335(4)	4821(1)	23(1)
C(3)	336(3)	9322(4)	4292(1)	22(1)
C(4)	2321(3)	9309(4)	4404(1)	22(1)
C(5)	3277(3)	9325(5)	5046(1)	29(1)
C(6)	2268(4)	9340(5)	5579(1)	28(1)
C(7)	3525(3)	9206(4)	3858(1)	25(1)
C(8)	3594(4)	8752(4)	2714(1)	21(1)
C(9)	2317(3)	9258(4)	2072(1)	22(1)
C(10)	1028(4)	7378(4)	1946(1)	20(1)
C(11)	2315(3)	5541(4)	2174(1)	21(1)
C(12)	3971(3)	6427(4)	2674(1)	21(1)
C(13)	5767(3)	5892(4)	2366(1)	23(1)
C(14)	5052(3)	4087(4)	1933(1)	21(1)
C(15)	6152(3)	4715(4)	857(1)	21(1)
C(16)	6955(3)	4132(4)	330(1)	21(1)
C(17)	6949(4)	5439(4)	-276(1)	28(1)
C(18)	7841(3)	2119(4)	341(1)	21(1)
C(19)	7129(3)	1654(4)	1484(1)	21(1)
N(1)	-777(3)	9330(4)	6018(1)	28(1)
N(2)	6152(3)	3499(3)	1413(1)	21(1)
N(3)	7951(3)	1067(3)	938(1)	22(1)
O(1)	112(3)	9396(5)	6572(1)	54(1)
O(2)	-2519(3)	9246(4)	5910(1)	38(1)
O(3)	5241(2)	9131(4)	3952(1)	41(1)
O(4)	2489(2)	9148(3)	3256(1)	22(1)
O(5)	30(2)	7229(3)	1292(1)	26(1)
O(6)	3196(2)	4719(3)	1633(1)	22(1)
O(7)	7248(3)	594(3)	1980(1)	31(1)
O(8)	8461(3)	1301(3)	-127(1)	29(1)

Table S6. Bond lengths [\AA] and angles [$^\circ$] for **33**.

C(1)-C(2)	1.374(3)
C(1)-C(6)	1.380(3)
C(1)-N(1)	1.472(3)
C(2)-C(3)	1.385(3)
C(2)-H(2)	0.9500
C(3)-C(4)	1.390(3)
C(3)-H(3)	0.9500
C(4)-C(5)	1.388(3)

C(4)-C(7)	1.495(3)
C(5)-C(6)	1.381(3)
C(5)-H(5)	0.9500
C(6)-H(6)	0.9500
C(7)-O(3)	1.203(3)
C(7)-O(4)	1.340(3)
C(8)-O(4)	1.464(3)
C(8)-C(9)	1.519(3)
C(8)-C(12)	1.534(3)
C(8)-H(8)	1.0000
C(9)-C(10)	1.522(4)
C(9)-H(9A)	0.9900
C(9)-H(9B)	0.9900
C(10)-O(5)	1.423(3)
C(10)-C(11)	1.531(3)
C(10)-H(10)	1.0000
C(11)-O(6)	1.442(3)
C(11)-C(12)	1.553(3)
C(11)-H(11)	1.0000
C(12)-C(13)	1.534(3)
C(12)-H(12)	1.0000
C(13)-C(14)	1.510(3)
C(13)-H(13A)	0.9900
C(13)-H(13B)	0.9900
C(14)-O(6)	1.428(3)
C(14)-N(2)	1.452(3)
C(14)-H(14)	1.0000
C(15)-C(16)	1.339(3)
C(15)-N(2)	1.380(3)
C(15)-H(15)	0.9500
C(16)-C(18)	1.446(4)
C(16)-C(17)	1.499(3)
C(17)-H(17A)	0.9800
C(17)-H(17B)	0.9800
C(17)-H(17C)	0.9800
C(18)-O(8)	1.226(3)
C(18)-N(3)	1.390(3)
C(19)-O(7)	1.217(3)
C(19)-N(2)	1.378(3)
C(19)-N(3)	1.380(3)
N(1)-O(1)	1.215(3)
N(1)-O(2)	1.221(3)
N(3)-H(3A)	0.8800
O(5)-H(5A)	0.8400
C(2)-C(1)-C(6)	123.1(2)
C(2)-C(1)-N(1)	118.9(2)
C(6)-C(1)-N(1)	118.0(2)
C(1)-C(2)-C(3)	118.4(2)
C(1)-C(2)-H(2)	120.8
C(3)-C(2)-H(2)	120.8
C(2)-C(3)-C(4)	120.0(2)
C(2)-C(3)-H(3)	120.0
C(4)-C(3)-H(3)	120.0
C(5)-C(4)-C(3)	120.2(2)
C(5)-C(4)-C(7)	116.8(2)
C(3)-C(4)-C(7)	123.0(2)
C(6)-C(5)-C(4)	120.4(2)
C(6)-C(5)-H(5)	119.8
C(4)-C(5)-H(5)	119.8

C(1)-C(6)-C(5)	118.0(2)
C(1)-C(6)-H(6)	121.0
C(5)-C(6)-H(6)	121.0
O(3)-C(7)-O(4)	123.7(2)
O(3)-C(7)-C(4)	123.4(2)
O(4)-C(7)-C(4)	112.90(19)
O(4)-C(8)-C(9)	107.35(19)
O(4)-C(8)-C(12)	109.1(2)
C(9)-C(8)-C(12)	104.7(2)
O(4)-C(8)-H(8)	111.8
C(9)-C(8)-H(8)	111.8
C(12)-C(8)-H(8)	111.8
C(8)-C(9)-C(10)	104.0(2)
C(8)-C(9)-H(9A)	111.0
C(10)-C(9)-H(9A)	111.0
C(8)-C(9)-H(9B)	111.0
C(10)-C(9)-H(9B)	111.0
H(9A)-C(9)-H(9B)	109.0
O(5)-C(10)-C(9)	114.8(2)
O(5)-C(10)-C(11)	115.3(2)
C(9)-C(10)-C(11)	104.78(19)
O(5)-C(10)-H(10)	107.2
C(9)-C(10)-H(10)	107.2
C(11)-C(10)-H(10)	107.2
O(6)-C(11)-C(10)	110.96(19)
O(6)-C(11)-C(12)	105.86(18)
C(10)-C(11)-C(12)	105.87(19)
O(6)-C(11)-H(11)	111.3
C(10)-C(11)-H(11)	111.3
C(12)-C(11)-H(11)	111.3
C(13)-C(12)-C(8)	113.8(2)
C(13)-C(12)-C(11)	103.73(19)
C(8)-C(12)-C(11)	106.09(19)
C(13)-C(12)-H(12)	111.0
C(8)-C(12)-H(12)	111.0
C(11)-C(12)-H(12)	111.0
C(14)-C(13)-C(12)	100.78(19)
C(14)-C(13)-H(13A)	111.6
C(12)-C(13)-H(13A)	111.6
C(14)-C(13)-H(13B)	111.6
C(12)-C(13)-H(13B)	111.6
H(13A)-C(13)-H(13B)	109.4
O(6)-C(14)-N(2)	108.44(17)
O(6)-C(14)-C(13)	103.90(19)
N(2)-C(14)-C(13)	117.5(2)
O(6)-C(14)-H(14)	108.9
N(2)-C(14)-H(14)	108.9
C(13)-C(14)-H(14)	108.9
C(16)-C(15)-N(2)	123.2(2)
C(16)-C(15)-H(15)	118.4
N(2)-C(15)-H(15)	118.4
C(15)-C(16)-C(18)	118.3(2)
C(15)-C(16)-C(17)	123.4(2)
C(18)-C(16)-C(17)	118.2(2)
C(16)-C(17)-H(17A)	109.5
C(16)-C(17)-H(17B)	109.5
H(17A)-C(17)-H(17B)	109.5
C(16)-C(17)-H(17C)	109.5
H(17A)-C(17)-H(17C)	109.5
H(17B)-C(17)-H(17C)	109.5

O(8)-C(18)-N(3)	119.3(2)
O(8)-C(18)-C(16)	125.5(2)
N(3)-C(18)-C(16)	115.2(2)
O(7)-C(19)-N(2)	123.5(2)
O(7)-C(19)-N(3)	121.9(2)
N(2)-C(19)-N(3)	114.6(2)
O(1)-N(1)-O(2)	123.2(2)
O(1)-N(1)-C(1)	118.3(2)
O(2)-N(1)-C(1)	118.5(2)
C(19)-N(2)-C(15)	121.6(2)
C(19)-N(2)-C(14)	117.6(2)
C(15)-N(2)-C(14)	120.8(2)
C(19)-N(3)-C(18)	126.5(2)
C(19)-N(3)-H(3A)	116.7
C(18)-N(3)-H(3A)	116.7
C(7)-O(4)-C(8)	114.64(18)
C(10)-O(5)-H(5A)	109.5
C(14)-O(6)-C(11)	104.36(16)

Symmetry transformations used to generate equivalent atoms:

Table S7. Anisotropic displacement parameters ($\text{\AA}^2 \times 103$) for **33**. The anisotropic

displacement factor exponent takes the form: $-2p_2[h2a^*2U_{11} + \dots + 2 h k a^* b^* U_{12}]$

	U11	U22	U33	U23	U13	U12
C(1)	22(1)	27(1)	21(1)	-5(1)	7(1)	1(1)
C(2)	19(1)	26(1)	25(1)	-4(1)	2(1)	0(1)
C(3)	23(1)	25(1)	18(1)	-4(1)	0(1)	0(1)
C(4)	21(1)	27(1)	19(1)	-6(1)	3(1)	0(1)
C(5)	19(1)	44(2)	23(1)	-6(1)	1(1)	0(1)
C(6)	24(1)	41(2)	19(1)	-7(1)	2(1)	0(1)
C(7)	23(1)	31(1)	19(1)	-6(1)	2(1)	-2(1)
C(8)	22(1)	26(1)	16(1)	-4(1)	6(1)	1(1)
C(9)	26(1)	23(1)	18(1)	-1(1)	4(1)	3(1)
C(10)	19(1)	26(1)	15(1)	-2(1)	4(1)	3(1)
C(11)	22(1)	23(1)	20(1)	-1(1)	10(1)	-1(1)
C(12)	22(1)	26(1)	16(1)	2(1)	4(1)	3(1)
C(13)	20(1)	29(1)	20(1)	-1(1)	3(1)	5(1)
C(14)	22(1)	24(1)	19(1)	3(1)	7(1)	5(1)
C(15)	21(1)	21(1)	21(1)	1(1)	3(1)	2(1)
C(16)	15(1)	28(1)	19(1)	0(1)	1(1)	0(1)
C(17)	27(1)	36(2)	23(1)	7(1)	8(1)	7(1)
C(18)	16(1)	29(1)	17(1)	-2(1)	0(1)	-2(1)
C(19)	18(1)	23(1)	21(1)	0(1)	3(1)	3(1)
N(1)	25(1)	37(1)	24(1)	-5(1)	6(1)	-1(1)
N(2)	23(1)	23(1)	19(1)	0(1)	8(1)	4(1)
N(3)	21(1)	24(1)	23(1)	0(1)	6(1)	9(1)
O(1)	34(1)	110(2)	19(1)	-7(1)	4(1)	-9(2)
O(2)	23(1)	59(1)	32(1)	-9(1)	9(1)	0(1)
O(3)	19(1)	80(2)	23(1)	-7(1)	2(1)	1(1)
O(4)	21(1)	30(1)	16(1)	-5(1)	4(1)	2(1)
O(5)	22(1)	36(1)	19(1)	-7(1)	1(1)	6(1)
O(6)	20(1)	27(1)	20(1)	-5(1)	4(1)	3(1)

O(7)	37(1)	31(1)	27(1)	10(1)	12(1)	12(1)
O(8)	33(1)	37(1)	19(1)	-3(1)	7(1)	7(1)

11. References

- (1) Oxford Diffraction (2010). CrysAlisPro (Version 1.171.34.44). Oxford Diffraction Ltd., Y., Oxfordshire, UK.
- (2) Macchi, P. B., H.B.; Chimpri, A. S.; Hauser, J.; Gal, Z. *J. Appl. Cryst.* **2011**, *44*, 763.
- (3) Sheldrick, G. M. *Acta crystallographica. Section A, Foundations of crystallography* **2008**, *64*, 112.